Time-dependent principal components-based dimension reduction in multi-dimensional foreign exchange option pricing

G.D.J. den Hertog, MSc

3473481

Thesis submitted in partial fulfillment of the requirements for the degree of Master of Science in

Mathematical Sciences - Probability, Statistics and Stochastic modeling

Supervised by

Dr. P.A. Zegeling - UU (project supervisor)
C.S.L. de Graaf MSc - UvA (daily supervisor)
Dr. B.D. Kandhai - UvA (supervisor)
Dr. M.C.J. Bootsma - UU (second examiner)

November 30, 2016

Abstract

I apply a principle components-based dimension reduction technique to foreign exchange (FX) basket option pricing. The underlying FX rates are modeled by the Black-Scholes model extended with Hull-White stochastic interest rates. A full correlation structure between the underlyings is included. The dimension of the model is first reduced by switching to the domestic forward measure. Second, the FX basket option pricing problem is rewritten in terms of the principal components of the forward FX rates. Further dimension reduction is then achieved by substituting all except for a few principal components with large variance by their expected value. I contribute to the existing literature by including the time-dependence of the principle components composition in high-dimensional option pricing. Real market data is used to calibrate the model to several emerging and non-emerging market currencies. In line with expectations, the accuracy of the dimension reduction technique depends on the correlation between the currencies: more accurate results are obtained for higher correlation values.

Keywords: foreign exchange, basket option, multi-dimensional option pricing, dimension reduction, principal component analysis, time-dependent principal components, Black-Scholes, Hull-White, stochastic interest rates.

Acknowledgements

I would like to thank my daily supervisor and PhD candidate Kees de Graaf for numerous discussions, comments and suggestions on this master thesis research. The various iterations to improve both the implementation code and the thesis report were of great contribution. I am grateful to supervisors dr. Drona Kandhai and dr. Paul Zegeling for their sharp view on this research and their contributing comments. Finally I would like to thank dr. Shashi Jain from ING Financial Markets for providing the market data on which the results of my research are based.

Contents

Chapter 1

Introduction

In the 70s and 80s, foreign exchange (FX) options became an important new market innovation. Today the FX market is one of the largest and most liquid over-the-counter (OTC) derivative markets worldwide. According to the 2016 BIS Triennial Central Bank Survey [1], FX markets trading averaged $5.1 trillion per day in April 2016. This is down from $5.4 trillion in April 2013 but up from $4.0 trillion in April 2010 and $3.3 trillion in April 2007. FX swaps ($2.4 trillion per day) and FX spots ($1.7 trillion per day) were the most traded instruments in April 2016.

Nowadays there is an increasing demand for options to hedge the risks of multiple currencies simultaneously. A typical example is a FX basket option, whose underlying is the (weighted) arithmetic or geometric average of multiple FX rates. The two main challenges in basket option pricing are the modeling of the underlying FX rates and the curse of dimensionality. The research in this master thesis addresses both challenges.

Not all models are applicable for modeling multiple FX rates simultaneously. Many models are inconsistent in the sense that they violate the inverse property and triangle property (De Col, Gnoatto & Grasselli, 2013). These properties intuitively state that the stochastic model dynamics of the inverse FX rate and cross FX rates have to be consistent. A large number of models for financial derivatives that are extensively studied in academic literature are not consistent for multi-FX modeling. The Black-Scholes model extended with Hull-White interest rate components is consistent for multi-FX modeling. Therefore in this research this model is used to model multiple FX rates simultaneously.

There are a number of studies on high-dimensional derivative pricing, many

of them focussing on Quasi-Monte Carlo methods. Joy, Boyle and Tan (1996) introduced this method in the field of numerical finance. With this method, deterministic sequences are used for Monte Carlo simulations instead of the random numbers, leading to faster convergence. Others focus on the radial basis function (RBF) approximations to solve the pricing Partial Differential Equation for 1 or 2 dimensions (e.g., Pettersson, Larsson, Marcusson & Persson (2008); Shcherbakov & Larsson, 2016). Finally neural network methods (e.g., Kohler, Krzyzak & Todorovic, 2010) and stochastic mesh methods (e.g., Broadie & Glasserman, 2004) have been used in high-dimensional derivative pricing.

There is little literature on the application of these high dimensional derivative pricing methods to FX basket options. Several studies derive closed-form approximations for valuing arithmetic FX basket options using moment matching (e.g., Hakala & Wystup, 2008; Leippold, 2006). It is assumed that the basket spot exchange rate itself is a log-normal process driven by a Brownian motion[1]. Then, the sum of the log-normal processes of the single FX rates is approximated by a log-normal process itself. The first and second moment of the basket spot are then matched with the first and second moment of the log-normal model for the basket spot, respectively.

A more sophisticated approach of dimension reduction is to look at effective dimensions. In this approach, the original high dimensional derivative pricing problem is rewritten in terms of principal components that are weighted averages of the original variables. The weights are equal to the eigenvector coefficients of the covariance matrix of the original variables, yielding uncorrelated principal components with descending variances. Especially for high correlations and similar variances among the original variables, it is worth to rewrite the original derivative pricing problem in terms of principal components. Subsequently, only the first few principal components with

[1] A stochastic process W is a Brownian motion if:

- $W(0) = 0$;
- the process $W(t) - W(u) \sim N(0, t-u)$, for any $0 \leq u < t$;
- the process $W(t) - W(u)$ is independent of $(W(s))_{s \leq u}$, for any $0 \leq u < t$;
- any sample path of the mapping $t \mapsto W(t)$ is a continuous function.

Brownian motions are often used in the stochastic modeling of interest rates, stock prices, FX rates, etcetera. The denotation Brownian motion is after Robert Brown, while it is sometimes called Wiener process, after Norbert Wiener. For more information on Brownian motions, see e.g., Boshuizen, van der Vaart, van Zanten, Banachewicz, Zareba and Belitser, 2014, section 5.3.

relatively high variance can be included in the pricing problem. The remaining principal components are substituted by their expectation. Most effective dimension-based reduction techniques applied in multi-dimensional derivative pricing are applied to the Quasi-Monte Carlo method. Often the high-dimensional derivative pricing problems are of low effective dimension (Wang & Sloan, 2005), such that functions can be well approximated by their low-order ANOVA (e.g., Imai & Tan, 2006; Sabino, 2007).

In his doctoral thesis, Reisinger (2004) (see also Reisinger & Wissman, 2015; Reisinger & Wittum, 2007) applies a principal components-based dimension reduction to the multi-dimensional Black-Scholes equation with constant drifts and volatilities. Reisinger first transforms the original multi-dimensional Black-Scholes pricing problem in terms of the principal components. Then he substitutes all except for the first few principal components with relatively high variance by their expectation. Ekedahl, Hansander and Lehto (2007) apply this technique to the pricing of a basket option on multiple stocks. For particular market data they show very accurate results, using only 1 or 2 principal components.

The current applications of principal component analysis in multi-dimensional option pricing are limited to the case of the Black-Scholes model with constant drift and volatility terms. In this case the coefficients of the eigenvectors of the covariance matrix are constant over time as the covariance matrix itself is constant over time. As a consequence, the composition of the principal components is independent of time and can be calculated once using the time-independent covariance matrix of the variables. The time-independence of the principal components simplifies the dimension reduction heavily.

In this thesis I contribute to the literature by applying a time-dependent principal components-based dimension reduction to multi-dimensional FX option pricing. The FX rates are modeled by the calibrated Black-Scholes model with Hull-White stochastic interest rates. For this model, the coefficients of the principal components are time-dependent as the coefficients of the eigenvectors of the covariance matrix are time-dependent. It will be shown that the three-dimensional Black-Scholes-Hull-White model can be reduced to a one-dimensional Black-Scholes model with time-dependent volatility. This is accomplished by switching from risk measure and, consequently, by switching to the forward FX rate. The original FX basket pricing problem is then transformed in terms of the time-dependent principal components of the multi-dimensional Black-Scholes-Hull-White model. The dimension of the pricing problem is reduced by substituting all except for the first or first

two principal components with relatively high variance by their time-zero expected value. As the composition of the principal components changes continuously over time, the challenge is to incorporate this in the derivative pricing.

The research question in this master thesis is:

What is the accuracy and performance of time-dependent principal components-based dimension reduction in FX basket option pricing under the multi-dimensional Black-Scholes-Hull-White model?

This report is organized as follows. Chapter 2 gives an introduction to FX markets, quotation rules and FX option pricing. Chapter 3 gives a short overview of the Hull-White model for interest rates and the current standard of modeling FX rates. It extensively addresses the BSHW model and its extension to multi-FX modeling. Chapter 4 first gives a brief introduction to principal component analysis. Then the time-dependent principle components-based dimension reduction technique applied to FX basket option pricing under the multi-FX Black-Scholes-Hull-White model is introduced. Chapter 5 gives a description of the two numerical valuation techniques that are used in this thesis: Monte Carlo simulations and finite differences. Chapter 6 describes the calibration of the multi-dimensional Black-Scholes-Hull-White model to real market data. Moreover it shows numerical results for the valuation of FX basket call options under the calibrated model. The accuracy of the principle components-based dimension reduction technique is assessed using a Monte Carlo reference solution. In chapter 7 I present the conclusion of this research and suggestions for further research.

Chapter 2

FX markets and option pricing

2.1 Quotation

The way FX rates are quoted in the market can be confusing. Although there is no universal quotation rule, the exchange rate between a currency pair (FX_1,FX_2) is often quoted as FX_1FX_2 (e.g., Clark, 2011; Wystup, 2008). This exchange rate is the price of 1 unit of FX_1 in units of FX_2, or a "FX_2 per FX_1 price". FX_1 is called the foreign currency or the base currency, FX_2 is called the domestic currency or quote currency. Clark (2011) presents a useful hierarchical order in which currencies should be used as FX_1:

$$EUR > GBP > AUD > NZD > USD > CAD > CHF > JPY.$$

Consider as an example the following major spot FX rate values from August 15, 2016[1]:

FX rate	Spot value
USDEUR	0.8942
GBPEUR	1.1517
JPYEUR	0.0088310

Table 2.1: Spot FX rate values from August 15, 2016.

For example, the USDEUR exchange rate implies that the price of 1 USD equals 0.8942 euro.

[1]Most FX rates are quoted to five significant figures. This will also be the base of this thesis.

2.2 Spot settlement, expiry and delivery

In general the payments of FX trades are not made on the trade date, but mostly 2 business days later (often called the settlement date or spot date). Similarly, if a FX option is exercised on the option expiration date, the spot FX transaction is often delivered later than the expiration date. Often the delivery date has the same relation to the expiry date as the spot date to today (see e.g., Clark, 2011).

2.3 Options

Although FX swap trades and spot FX trading account for approximately 80% of trading in FX markets [1], several plain vanilla[2] and exotic FX options can be traded, with different exercise and monitoring styles (e.g., Castagna, 2010, Table 1.2, p. 10). The main focus of this thesis is on FX forwards and FX plain vanilla options, with European-style exercise[3]. Both single FX rate options and basket options are considered, which are discussed in the subsections below.

2.3.1 Quotation

For FX trading, the jargon and the option definition slightly differs from options on any other assets like the stock price. First of all, option prices may be quoted in different ways (e.g., Wystup, 2008; Castagna, 2010). For example, plain vanilla option prices are usually quoted in units, while exotic option prices are usually quoted in percentages (in case the payoff of the option is in domestic currency units). Denoting by K the strike price, π_d the option price in domestic currency units and $\pi_{d\%}$ the option price in domestic currency percentages, one has $\pi_{d\%} = \frac{\pi_d}{K} \cdot 100$. The actual premium to pay depends on the notional amount and the currency in which the notional is defined.

Furthermore, the defintion of a FX option can sometimes be ambiguous. In the example below the definition of a European-style FX call option contract is clarified.

Example 1. *A* 6*m EUR call GBP put* 0.9 *has to be interpreted as an option in which the buyer has the right (but not the obligation) at expiry,* 6 *months*

[2]Plain vanilla options are usually used to denote normal call and put options with no extra features. These options are the opposite of the more complex exotic options.

[3]European options are options that can only be exercised at expiry date T.

after initiation, to buy (sell) the notional amount in the EUR (GBP) currency, at strike price 0.9*. The notional amount N in EUR currency units is exchanged against N × K units of the GBP currency.*

In this thesis, the option price will be expressed in domestic currency units, and the notional will be in foreign currency units.

2.3.2 Single FX option

Single FX options admit for hedging of the risk of a single currency pair. Besides the trivial forward option, European-style call/put options and digital call/put options are considered, with payoffs respectively equal to[4]:

$$\begin{aligned} f_1\left(S^{df}(T)\right) &= N_f\left(S^{df}(T) - K\right), \\ f_2\left(S^{df}(T)\right) &= N_f\left(\delta\left(S^{df}(T) - K\right)\right)^+, \\ f_3\left(S^{df}(T)\right) &= N_d 1_{\left\{\delta\left(S^{df}(T)-K\right)\geq 0\right\}}. \end{aligned} \tag{2.1}$$

Here δ equals 1 in case of a call option and -1 in case of a put option. S^{df} denotes the exchange rate between the foreign and domestic currency according to the quotation from section 2.1, N_f (N_d) is the notional amount expressed in foreign (domestic) currency units, T is the maturity in years and K is the strike price.

2.3.3 Basket option

Although most FX options traded in the market have a single underlying FX rate, there is a demand for options that can be used for the hedging of multiple currencies simultaneously. An example is the FX basket option, whose underlying is a weighted average of multiple FX rates. The price of a FX basket option is often lower than the sum of the prices of the separate FX options. Denoting by N_{FX} the number of FX rates in the basket option and by ϕ_i, $i = 1, \ldots, N_{FX}$, the basket weights, the payoffs of the FX basket options are equal to:

$$\begin{aligned} f_1\left(\left(S^{di}(T)\right)_{i\leq N_{FX}}\right) &= N_f\left(\sum_{i=1}^{N_{FX}} \phi_i S^{di}(T) - K\right), \\ f_2\left(\left(S^{di}(T)\right)_{i\leq N_{FX}}\right) &= N_f\left(\delta\left(\sum_{i=1}^{N_{FX}} \phi_i S^{di}(T) - K\right)\right)^+. \end{aligned} \tag{2.2}$$

[4] $x^+ = \max(x, 0)$ for $x \in \mathbb{R}$.

Here f_1 and f_2 are a FX basket forward and FX basket call/put option, respectively. Note that the digital option is not listed, as a digital FX basket option is not traded in the FX markets.

2.4 Option pricing

Denote by $M_d(t)$ the money-market account and by $r_d(t)$ the domestic interest rate at time $t \geq 0$. The dynamics of $M_d(t)$ are given by the stochastic differential equation (SDE)

$$dM_d(t) = r_d(t)M_d(t)dt.$$

The time-t price of the single FX rate option of type $k = 1, 2, 3$ (see (2.1)) is given by

$$\pi_k(t) = \mathbb{E}_{\mathbb{Q}}\left[M_d(t)\frac{f_k\left(S^{df}(T)\right)}{M_d(T)}\big|\mathcal{F}(t)\right], \qquad k = 1, 2, 3, \tag{2.3}$$

and the time-t price of a FX basket option of type $k = 1, 2$ (see (2.2)) is given by

$$\pi_k^{N_{FX}}(t) = \mathbb{E}_{\mathbb{Q}}\left[M_d(t)\frac{f_k\left(\left(S^{di}(T)\right)_{i\leq N_{FX}}\right)}{M_d(T)}\big|\mathcal{F}(t)\right], \qquad k = 1, 2. \tag{2.4}$$

See subsections 2.3.2 and 2.3.3 for definitions of the option payoffs. $\mathbb{Q}$ is the risk-neutral measure, which will be discussed below.

2.4.1 Risk neutrality

One of the main theorems in financial mathematics is called the first fundamental theorem of asset pricing (FTAP). The FTAP states that there are no arbitrage opportunities in a complete market, if and only if there exists a probability measure $\mathbb{Q}$ that is equivalent to the real-world measure $\mathbb{P}$ and under which the discounted risky assets in the market are martingales (e.g., Downarowicz, 2010). Therefore in option pricing, by ensuring that all discounted underlying risky assets are martingales, one can change the underlying measure from the real-world measure $\mathbb{P}$ to the corresponding risk-neutral measure $\mathbb{Q}$. The option price becomes equal to the expectation under $\mathbb{Q}$ of the discounted option payoff. The change of measure from $\mathbb{P}$ to $\mathbb{Q}$ is often guided by a change of the stochastic dynamics of the underlying process. This will be shown multiple times in the next chapters.

2.4.2 The volatility smile and the delta-sticky notation

For European-style vanilla options on a single underlying FX rate, implied volatility can be derived by solving for the volatility parameter in the Black-Scholes pricing formula, using the market price. If all assumptions underlying the Black-Scholes model would hold, the Black-Scholes implied volatility would be the same for different maturities and strike prices of the option. In reality however, this is not true, and a so-called implied volatility surface is observed. The implied volatility surface is a mapping of strike and maturity to implied volatility. Considering implied volatility curves for a specific maturity yields shapes that are often referred to as volatility smiles, skews or frowns, depending on their shape (e.g., Beneder & Elkenbracht-Huizing, 2003). The existence of the volatility smile disagrees with the log-normality assumption of FX rates; incorporating this skew in the model can be done using local volatility, stochastic volatility and/or jumps.

Volatility smiles are not directly observable in the FX OTC derivative market, as opposed to equity markets where volatility smiles are directly observable from, for example, strike-volatility pairs. For FX options a complete volatility smile can nevertheless be constructed using market quotes on the implied volatility of at-the-money (ATM) options, strangles and risk reversals (RR) (e.g., Reiswich & Wystup, 2012). These quotes are different from equity market quotes in the sense that in the FX OTC derivative market, strike price quotes are given in terms of the delta of the option. The purpose of this quotation is that the parties involved in a certain FX transaction agree on a implied volatility level and a certain Black-Scholes delta level before closing the deal.
When the deal is done, the strike is set equal to the level that yields the agreed Black-Scholes delta, using the implied volatility and spot FX rate (e.g., Norgaard, 2011). This agreement is referred to as the delta-sticky notation.

Chapter 3

FX modeling

Garman and Kohlhagen (1993) were one of the first to include domestic and foreign interest rates in the standard Black-Scholes model, for the purpose of FX derivative pricing. Using arbitrage arguments, they derived the following stochastic differential equation dynamics for the FX rate $S(t)$ at time t:

$$dS(t) = (r_d - r_f)S(t)dt + \sigma S(t)dW^{\mathbb{Q}}(t). \tag{3.1}$$

Here r_d and r_f are the domestic and foreign interest rate, respectively, σ is the volatility parameter and $W^{\mathbb{Q}}$ is a Brownian motion under the risk-neutral measure $\mathbb{Q}$. Switching to the forward FX rate yields the following formula for the time-t price of European-style FX options expiring at time T (e.g., Castagna, 2010, formula 2.28):

$$\begin{aligned} \Pi_{GK}(t) &= P_d(t,T)\left[\omega F(t,T)\Phi\left(\omega d_1\right) - \omega K\Phi\left(\omega d_1 - \sigma\sqrt{T-t}\right)\right], \\ d_1 &= \frac{\ln\left(\frac{F(t,T)}{K}\right) + \frac{\sigma^2}{2}(T-t)}{\sigma\sqrt{T-t}}, \end{aligned} \tag{3.2}$$

with $\omega = 1$ for a call and $\omega = -1$ for a put, K the strike price and Φ the cumulative standard normal distribution function. Furthermore $F(t,T) = \frac{P_f(t,T)}{P_d(t,T)}S(t)$ is the forward FX rate, with $P_i(t,T)$ $(i = d, f)$ the zero-coupon bonds for the domestic and foreign currency, respectively.

In the last decades, several model extensions, variations and alternatives to the model (3.1) have been discussed and used in the FX option pricing literature. Furthermore many literature studies focus on including the volatility smile into the model. This chapter discusses the Hull-White model for stochastic interest rates and addresses three of the most used stochastic FX models before extensively discussing the Black-Scholes-Hull-White model for the FX rate.

3.1 The Hull-White model for interest rates

With the introduction of the Hull-White model for interest rates in 1990 (Hull & White, 1990), an exact fit to the term-structure of interest rates became possible. The term-structure of interest rates can be represented by the yield curve, which shows the relation between the continuously compounded spot rate for the time interval $[0, T]$, $R(0, T)$, and maturity T. Alternatively, it can be represented by the discount curve, which shows the relation between the zero-coupon bond price $P(0, T)$ and maturity T. $P(0, T)$ and $R(0, T)$ are related according to $\log(P(0, T)) = -TR(0, T)$.

Under the real-world measure $\mathbb{P}$, the Hull-White model is given by the following dynamics for the instantaneous short rate, defined by $r(t) = \lim_{T \downarrow t} R(t, T)$:

$$dr(t) = \lambda \left(\theta(t) - r(t)\right) dt + \sigma dW^{\mathbb{P}}(t).$$

The short-rate $r(t)$ is pulled towards the time-dependent level $\theta(t)$ at a rate λ, and a random term with variance σ^2 per unit time is added to this process. The mean-reversion function $\theta(t)$ can be chosen to let the model fit the initial term-structure of interest rates. As Hull and White describe in their paper (Hull & White, 1990, p. 576):

> "It is reasonable to conjecture that in some situations the market's expectations about future interest rates involve time-dependent parameters. [...] The time dependence can arise from the cyclical nature of the economy, expectations concerning the future impact of monetary policies, and expected trends in other macroeconomic variables."

The Hull-White model has the affine term-structure [1] and its bond price therefore satisfies the following formula:

$$P(t, T) = e^{A(t,T) + B(t,T) r(t)},$$

with expressions for $A(t, T)$ and $B(t, T)$ given in e.g., Filipovic (2009), Proposition 5.2. The solutions are equal to (e.g., Grzelak & Oosterlee, 2012; Brigo & Mercurio, 2007):

$$B(t, T) = \frac{1}{\lambda} \left(e^{-\lambda(T-t)} - 1\right),$$
$$A(t, T) = \log\left(\frac{P(0, T)}{P(0, t)}\right) - B(t, T) f(0, t) - \frac{\sigma^2}{4\lambda} \left(1 - e^{-2\lambda t}\right) B^2(t, T),$$

[1] For an extensive discussion on affine term-structures, see e.g., Filipovic, 2009, section 5.3.

with the instantaneous forward rate $f(0,t)$ with maturity t prevailing at time 0 defined by $f(0,t) := -\frac{\partial \log P(0,s)}{\partial s}\big|_{s=t}$. Furthermore one has $r(t) := f(t,t)$. The risk-free dynamics of the zero-coupon bond $P(t,T)$ with maturity T are given by [20]

$$dP(t,T) = r(t)P(t,T)dt + P(t,T)\frac{\sigma}{\lambda}\left(e^{-\lambda(T-t)} - 1\right)dW^{\mathbb{P}}(t). \tag{3.3}$$

The mean-reversion function $\theta(t)$ can be calibrated to the initial term-structure $(P(0,T))_{T\geq 0}$, yielding [6]:

$$\theta(t) = \frac{1}{\lambda}\frac{\partial f(0,t)}{\partial t} + f(0,t) + \frac{\sigma^2}{2\lambda^2}\left(1 - e^{-2\lambda t}\right). \tag{3.4}$$

The short rate equals [6]

$$r(t) = r(s)e^{-\lambda(t-s)} + \lambda\int_s^t e^{-\lambda(t-u)}\theta(u)du + \sigma\int_s^t e^{-\lambda(t-u)}dW^{\mathbb{P}}(u).$$

Therefore $r(t)$ conditional on the filtration $(\mathcal{F}_s)_{s\leq t}$[2] is normally distributed with mean and variance given by

$$\begin{aligned}\mathbb{E}\left[r(t)|\mathcal{F}(s)\right] &= r(s)e^{-\lambda(t-s)} + \lambda\int_s^t \theta(u)e^{-\lambda(t-u)}du,\\ \mathrm{Var}\left[r(t)|\mathcal{F}(s)\right] &= \frac{\sigma^2}{2\lambda}\left[1 - e^{-2\lambda(t-s)}\right],\end{aligned}$$

respectively.

3.2 Local volatility and stochastic volatility models

Some of the most used FX models in the literature are the local volatility Black-Scholes-Hull-White model, and the Schöbel-Zhu-Hull-White model and the Heston-Hull-White model, which are stochastic volatility models. With stochastic volatility models it is possible to incorporate the volatility smile. The three above mentioned models are briefly discussed in the subsections below.

[2] In the remaining of this thesis, $\mathcal{F}$ denotes the natural filtration of stochastic process. For background information on filtrations and σ-fields, see e.g., Boshuizen, van der Vaart, van Zanten, Banachewicz, Zareba and Belitser, 2014, section 5.3.

3.2.1 The local volatility Black-Scholes-Hull-White model

Several literature studies on FX modeling have been devoted to a three-factor model where the spot FX rate is modeled by the Black-Scholes model with local volatility and the interest rates are modeled by Hull-White models (e.g., Dang, Christara, Jackson & Lakhany, 2010; Deelstra & Rayée, 2011). In this model volatility is a function of both time and the spot FX rate itself. The model dynamics are given by

$$\begin{aligned}
dS(t) &= (r_d(t) - r_f(t))S(t)dt + \gamma(t, S(t))S(t)dW_S^{\mathbb{Q}}(t), \\
dr_d(t) &= (\theta_d(t) - k_d(t)r_d(t))dt + \sigma_d dW_d^{\mathbb{Q}}(t), \\
dr_f(t) &= [\theta_f(t) - k_F(t)r_f(t) - \rho_{fS}\sigma_f\gamma(t, S(t))]\, dt + \sigma_f dW_f^{\mathbb{Q}}(t), \\
d\left[W_d^{\mathbb{Q}}, W_S^{\mathbb{Q}}\right](t) &= \rho_{dS}dt, \\
d\left[W_f^{\mathbb{Q}}, W_S^{\mathbb{Q}}\right](t) &= \rho_{fS}dt, \\
d\left[W_d^{\mathbb{Q}}, W_f^{\mathbb{Q}}\right](t) &= \rho_{df}dt,
\end{aligned} \tag{3.5}$$

with $\mathbb{Q}$ the domestic spot risk-neutral measure, corresponding to taking the domestic money market account as numéraire, and $\gamma(t, S(t))$ the local volatility function. The parameters ρ_{dS}, ρ_{fS} and ρ_{df} denote the correlation values between the Brownian motions. Furthermore, changing the measure from the foreign spot risk-neutral measure to the domestic spot risk neutral measure yields the "quanto" drift adjustment $-\rho_{fS}\sigma_f\gamma(t, S(t))$. Deelstra and Rayée derive expressions for the local volatility function by differentiating European call price expressions with respect to the strike and maturity. Dang et al. use a constant elasticity of variance (CEV)-type local volatility process.

3.2.2 The Schöbel-Zhu-Hull-White model

Van Haastrecht, Lord, Pelsser and Schrager (2009) extended the Schöbel and Zhu stochastic volatility model by including Hull-White stochastic interest rates. They call the resulting model the Schöbel-Zhu Hull-White (SZHW)

model, with a FX generalization that reads:

$$\begin{aligned}
dS(t) &= (r_d(t) - r_f(t))S(t)dt + \nu(t)S(t)dW_S^{\mathbb{Q}}(t), \\
dr_d(t) &= (\theta_d(t) - a_d r_d(t))dt + \sigma_d dW_d^{\mathbb{Q}}(t), \\
dr_f(t) &= [\theta_f(t) - a_f r_f(t) - \rho_{fS}\nu(t)\sigma_f]\,dt + \sigma_f dW_f^{\mathbb{Q}}(t), \\
d\nu(t) &= \kappa(\psi - \nu(t))dt + \tau dW_\nu^{\mathbb{Q}}(t), \\
d\left[W_d^{\mathbb{Q}}, W_S^{\mathbb{Q}}\right](t) &= \rho_{dS}dt, \\
d\left[W_f^{\mathbb{Q}}, W_S^{\mathbb{Q}}\right](t) &= \rho_{fS}dt, \\
d\left[W_\nu^{\mathbb{Q}}, W_S\right](t) &= \rho_{\nu S}dt, \\
d\left[W_d^{\mathbb{Q}}, W_f^{\mathbb{Q}}\right](t) &= \rho_{df}dt, \\
d\left[W_d^{\mathbb{Q}}, W_\nu^{\mathbb{Q}}\right](t) &= \rho_{d\nu}dt, \\
d\left[W_f^{\mathbb{Q}}, W_\nu^{\mathbb{Q}}\right](t) &= \rho_{f\nu}dt.
\end{aligned} \tag{3.6}$$

Here $\nu(t)$ denotes the stochastic volatility process at time t.

3.2.3 The Heston-Hull-White model

The widely used Heston stochastic volatility model can also be extended with Hull-White interest rate models. The model dynamics are the following (e.g., Grzelak & Oosterlee, 2012):

$$\begin{aligned}
dS(t) &= (r_d(t) - r_f(t))S(t)dt + \sqrt{\nu(t)}S(t)dW_S^{\mathbb{Q}}(t), \\
d\nu(t) &= \kappa(\bar{\nu} - \nu(t))dt + \gamma\sqrt{\nu(t)}W_\nu^{\mathbb{Q}}(t), \\
dr_d(t) &= \lambda_d(\theta_d(t) - r_d(t))dt + \sigma_d dW_d^{\mathbb{Q}}(t), \\
dr_f(t) &= \lambda_f\left[\theta_f(t) - r_f(t) - \rho_{fS}\sqrt{\nu(t)}\sigma_f\right]dt + \sigma_f dW_f^{\mathbb{Q}}(t), \\
d\left[W_d^{\mathbb{Q}}, W_S^{\mathbb{Q}}\right](t) &= \rho_{dS}dt, \\
d\left[W_f^{\mathbb{Q}}, W_S^{\mathbb{Q}}\right](t) &= \rho_{fS}dt, \\
d\left[W_\nu^{\mathbb{Q}}, W_S^{\mathbb{Q}}\right](t) &= \rho_{\nu S}dt, \\
d\left[W_d^{\mathbb{Q}}, W_f^{\mathbb{Q}}\right](t) &= \rho_{df}dt, \\
d\left[W_d^{\mathbb{Q}}, W_\nu^{\mathbb{Q}}\right](t) &= \rho_{d\nu}dt, \\
d\left[W_f^{\mathbb{Q}}, W_\nu^{\mathbb{Q}}\right](t) &= \rho_{f\nu}dt.
\end{aligned} \tag{3.7}$$

See Grzelak, Oosterlee and Van Weeren (2012) for a comparison of the Schöbel-Zhu-Hull-White (SZHW), Heston-Hull-White (HHW) and the stochastic volatility Heston model in their performance with respect to calibration

and hybrid product pricing. See also Simaitis, de Graaf, Hari and Kandhai (2016) for an application of the Heston-Hull-White model in counterparty credit risk.

3.2.4 The Black-Scholes-Hull-White model

Several studies (e.g., Grzelak & Oosterlee, 2012; Simaitis, 2014) consider the three-dimensional Black-Scholes-Hull-White model (henceforth BSHW model) for the FX rate $S^{df}(t)$ under the domestic spot risk-neutral measure $\mathbb{Q}$. Its dynamics are given by

$$\begin{aligned} dS^{df}(t) &= (r_d(t) - r_f(t))\, S^{df}(t)dt + \sigma S^{df}(t)dW^{\mathbb{Q}}_{S^{df}}(t), \\ dr_d(t) &= \lambda_d\left(\theta_d(t) - r_d(t)\right)dt + \sigma_d dW^{\mathbb{Q}}_d(t), \\ dr_f(t) &= \left(\lambda_f\left(\theta_f(t) - r_f(t)\right) - \rho_{S^{df}r_f}\sigma\sigma_f\right)dt + \sigma_f dW^{\mathbb{Q}}_f(t). \end{aligned} \tag{3.8}$$

The full correlation structure between the Brownian motions is represented by

$$\begin{aligned} d\left[W^{\mathbb{Q}}_{S^{df}}, W^{\mathbb{Q}}_d\right](t) &= \rho_{S^{df}r_d}dt, \\ d\left[W^{\mathbb{Q}}_{S^{df}}, W^{\mathbb{Q}}_f\right](t) &= \rho_{S^{df}r_f}dt, \\ d\left[W^{\mathbb{Q}}_d, W^{\mathbb{Q}}_f\right](t) &= \rho_{r_d r_f}dt. \end{aligned}$$

The "$-\rho_{S^{df}r_f}\sigma\sigma_f$"-term in the drift of the foreign interest rate is the quanto drift adjustment resulting from changing the measure from the foreign spot risk-neutral measure to the domestic spot risk neutral measure.

The BSHW model under the $\mathbb{Q}_T$-measure

For the three-dimensional BSHW model given by (3.8) there are no analytical formulas available for the prices of European-style options with a single FX rate underlying. However by switching from the domestic spot risk-neutral measure $\mathbb{Q}$ to the domestic forward risk-neutral measure, analytical formulas for FX European options can be derived (e.g., [20], [43]). The domestic forward risk-neutral measure corresponds to taking the domestic zero-coupon bond $P_d(t,T)$ as numéraire. Let $\mathbb{Q}_T$ denote the T-forward risk-neutral measure. Under $\mathbb{Q}_T$, the forward exchange rate given by

$$F^{df}(t) = S^{df}(t)\frac{P_f(t,T)}{P_d(t,T)} \tag{3.9}$$

has to be a martingale (Shreve, 2004)[3]. From (3.9) it is clear that $F^{df}(T) = S^{df}(T)$, i.e. the spot FX rate and forward FX rate are equal at maturity T. As the payoff of European-style single FX options only depends on the FX rate at maturity, it is therefore sufficient to determine the model dynamics of the forward exchange rate $F^{df}(t)$ under the $\mathbb{Q}_T$-measure. These dynamics are given by (see appendix A for a complete derivation)

$$\begin{aligned} &dF^{df}(t) \\ &= \sigma F^{df}(t) dW_{S^{df}}^{\mathbb{Q}_T}(t) + \sigma_f A_f(t,T) F^{df}(t) dW_f^{\mathbb{Q}_T}(t) - \sigma_d A_d(t,T) F^{df}(t) dW_d^{\mathbb{Q}_T}(t), \end{aligned} \tag{3.10}$$

with

$$A_i(t,T) = \frac{e^{-\lambda_i(T-t)-1}}{\lambda_i}, \qquad i = d, f, \tag{3.11}$$

and $W_i^{\mathbb{Q}_T}(t)$ a Brownian motion under the $\mathbb{Q}_T$ measure, for $i = S^{df}, d, f$. From the above $\mathbb{Q}_T$-dynamics it is clear that the stochastic processes $r_d(t)$ and $r_f(t)$ are not incorporated in the model dynamics of the forward FX rate. The European-style single FX option pricing problem under the 3-dimensional BSHW model is therefore reduced to a ordinary pricing problem under the one-dimensional Black-Scholes model with zero drift and time-dependent volatility. Moreover by the change to the domestic forward risk-neutral measure, the discounting with the stochastic domestic interest rate can be taken out of the expectation. The European-style single FX option pricing problem (2.3) transforms to

$$\Pi_k(t) = P_d(t,T) \mathbb{E}_{\mathbb{Q}_T} \left[f_k \left(F^{df}(T) \right) \middle| \mathcal{F}(t) \right]$$

under the $\mathbb{Q}_T$-measure, with $k = 1, 2, 3$. The sum of three correlated, normally distributed random variables remains normal with mean equal to the sum of the individual means and variance equal to the cross-covariance terms. Therefore (3.10) can be represented as (e.g., Grzelak & Oosterlee, 2012, Remark 1)

$$\begin{aligned} dF^{df}(t) := \big[&\sigma^2 + \sigma_f^2 A_f^2(t,T) + \sigma_d^2 A_d^2(t,T) + 2\rho_{S^{df} r_f} \sigma \sigma_f A_f(t,T) \\ &- 2\rho_{S^{df} r_d} \sigma \sigma_d A_d(t,T) - 2\rho_{r_d r_f} \sigma_d \sigma_f A_d(t,T) A_f(t,T) \big] F^{df}(t) dW^{\mathbb{Q}_T}(t). \end{aligned} \tag{3.12}$$

[3]For $t \in [0,T]$. This addition will be omitted at similar martingale statements in the remaining of this thesis.

From (3.12) it is clear that under the $\mathbb{Q}_T$-measure one has

$$F^{df}(T) = F^{df}(0)e^{-\frac{1}{2}(\sigma^*(0,T))^2 T + \sigma^*(0,T)\sqrt{T}Z}, \tag{3.13}$$

with $Z \sim N(0,1)$[4] and $\sigma^*(0,T)$ the implied volatility given by (e.g., Lee, 2005)

$$\begin{aligned}
&(\sigma^*(0,T))^2 \\
&= \frac{1}{T}\int_0^T \left(\sigma^2 + \sigma_f^2 A_f^2(t,T) + \sigma_d^2 A_d^2(t,T) + 2\rho_{S^{df}r_f}\sigma\sigma_f A_f(t,T)\right. \\
&\left. -2\rho_{S^{df}r_d}\sigma\sigma_d A_d(t,T) - 2\rho_{r_d r_f}\sigma_d\sigma_f A_d(t,T)A_f(t,T)\right) dt \\
&= \frac{1}{T}\int_0^T \left(\sigma^2 + \frac{\sigma_f^2}{\lambda_f^2}\left[e^{-2\lambda_f(T-t)} - 2e^{-\lambda_f(T-t)} + 1\right] + \frac{\sigma_d^2}{\lambda_d^2}\left[e^{-2\lambda_d(T-t)}\right.\right. \\
&\left. -2e^{-\lambda_d(T-t)} + 1\right] + 2\rho_{S^{df}r_f}\sigma\frac{\sigma_f}{\lambda_f}\left[e^{-\lambda_f(T-t)} - 1\right] - 2\rho_{S^{df}r_d}\sigma\frac{\sigma_d}{\lambda_d} \\
&\left.\times\left[e^{-\lambda_d(T-t)} - 1\right] - 2\rho_{r_d r_f}\frac{\sigma_d\sigma_f}{\lambda_d\lambda_f}\left[e^{-\lambda_d(T-t)} - 1\right]\left[e^{-\lambda_f(T-t)} - 1\right]\right) dt \\
&= \frac{1}{T}\left(\sigma^2 t + \frac{\sigma_f^2}{\lambda_f^2}\left[\frac{1}{2\lambda_f}e^{-2\lambda_f(T-t)} - \frac{2}{\lambda_f}e^{-\lambda_f(T-t)} + t\right]\right. \\
&+\frac{\sigma_d^2}{\lambda_d^2}\left[\frac{1}{2\lambda_d}e^{-2\lambda_d(T-t)} - \frac{2}{\lambda_d}e^{-\lambda_d(T-t)} + t\right] \\
&+2\rho_{S^{df}r_f}\frac{\sigma\sigma_f}{\lambda_f}\left[\frac{1}{\lambda_f}e^{-\lambda_f(T-t)} - t\right] - 2\rho_{S^{df}r_d}\sigma\frac{\sigma_d}{\lambda_d}\left[\frac{1}{\lambda_d}e^{-\lambda_d(T-t)} - t\right] \\
&\left.-2\rho_{r_d r_f}\frac{\sigma_d\sigma_f}{\lambda_d\lambda_f}\left[\frac{1}{\lambda_d+\lambda_f}e^{-(\lambda_d+\lambda_f)(T-t)} - \frac{1}{\lambda_d}e^{-\lambda_d(T-t)} - \frac{1}{\lambda_f}e^{-\lambda_f(T-t)} + t\right]\Big|_{t=0}^{t=T}\right) \\
&= \frac{1}{T}\left(\sigma^2 T + \frac{\sigma_f^2}{\lambda_f^2}\frac{4e^{-\lambda_f T} - e^{-2\lambda_f T} - 3 + 2\lambda_f T}{2\lambda_f}\right. \\
&+\frac{\sigma_d^2}{\lambda_d^2}\frac{4e^{-\lambda_d T} - e^{-2\lambda_d T} - 3 + 2\lambda_d T}{2\lambda_d} \\
&+2\rho_{S^{df}r_f}\frac{\sigma\sigma_f}{\lambda_f}\frac{1 - e^{-\lambda_f T} - T\lambda_f}{\lambda_f} - 2\rho_{S^{df}r_d}\frac{\sigma\sigma_d}{\lambda_d}\frac{1 - e^{-\lambda_d T} - T\lambda_d}{\lambda_d} \\
&\left.-2\rho_{r_d r_f}\frac{\sigma_d\sigma_f}{\lambda_d\lambda_f}\left[\frac{1 - e^{-(\lambda_d+\lambda_f)T}}{\lambda_d+\lambda_f} - \frac{1 - e^{-\lambda_d T}}{\lambda_d} - \frac{1 - e^{-\lambda_f T}}{\lambda_f} + T\right]\right).
\end{aligned}$$

Consider as an example a European-style call option on a single FX rate (the calculation of the price of other European-style options goes similarly). The

[4] $N(0,1)$ denotes the standard normal distribution.

time-zero price equals

$$\begin{aligned}\Pi_2(0) &= P_d(0,T)\mathbb{E}_{\mathbb{Q}_T}\left(\left(F^{df}(T)-K\right)^+ \big| \mathcal{F}(0)\right) \\ &= P_d(0,T)\int_{-\infty}^{\infty}\left(F^{df}(0)e^{-\frac{1}{2}(\sigma^*(0,T))^2T+\sigma^*(0,T)\sqrt{T}z}-K\right)^+ f_z(z)dz,\end{aligned} \tag{3.14}$$

with f_z the density function of the standard normal distribution. It holds that $F^{df}(0)e^{-\frac{1}{2}(\sigma^*(0,T))^2T+\sigma^*(0,T)\sqrt{T}z}-K \geq 0$ if and only if

$$z \geq \frac{\ln\left(\frac{K}{F^{df}(0)}\right)+\frac{1}{2}\left(\sigma^*(0,T)\right)^2T}{\sigma^*(0,T)\sqrt{T}} := z_0.$$

Then one has that

$$\begin{aligned}&\Pi_2(0) \\ &= P_d(0,T)\int_{z_0}^{\infty}\left(F^{df}(0)e^{-\frac{1}{2}(\sigma^*(0,T))^2T+\sigma^*(0,T)\sqrt{T}z}-K\right)^+ f_z(z)dz \\ &= P_d(0,T)\left(\int_{z_0}^{\infty}F^{df}(0)e^{-\frac{1}{2}(\sigma^*(0,T))^2T+\sigma^*(0,T)\sqrt{T}z}f_z(z)dz-\int_{z_0}^{\infty}Kf_z(z)dz\right) \\ &= P_d(0,T)\left(\int_{z_0}^{\infty}F^{df}(0)\frac{1}{\sqrt{2\pi}}e^{-\frac{1}{2}\left(z-\sigma^*(0,T)\sqrt{T}\right)^2}dz-K\left(1-\Phi(z_0)\right)\right) \\ &= P_d(0,T)\left(F^{df}(0)\int_{z_0-\sigma^*(0,T)\sqrt{T}}^{\infty}f_y(y)dy-K\left(1-\Phi(z_0)\right)\right) \\ &= P_d(0,T)\left(F^{df}(0)\left(1-\Phi\left(z_0-\sigma^*(0,T)\sqrt{T}\right)\right)-K\left(1-\Phi(z_0)\right)\right).\end{aligned} \tag{3.15}$$

For $\sigma_d = \sigma_f = 0$ one has $r_d(t) = r_d(0)$ and $r_f(t) = r_f(0)$. Letting $r_f(0) = 0$, the single FX rate call option price should equal the Black-Scholes call option price. This is immediate from (3.15).

Using similar calculations as in (3.15) one has for the time-zero price of a digital call option:

$$\begin{aligned}\Pi_3(0) &= P_d(0,T)\int_{-\infty}^{\infty}1_{\left\{F^{df}(0)e^{-\frac{1}{2}(\sigma^*(0,T))^2T+\sigma^*(0,T)\sqrt{T}z}\geq K\right\}}f_z(z)dz \\ &= P_d(0,T)\int_{z_0}^{\infty}f_z(z)dz \\ &= P_d(0,T)\left(1-\Phi\left(z_0\right)\right).\end{aligned} \tag{3.16}$$

3.3 Multi-FX modeling

In the previous sections, stochastic dynamic models for a single FX rate were considered. These models allow for valuation of derivatives with a single underlying FX rate. The financial sector however is in need of valuation of multi-FX rate based instruments, like FX basket options. FX basket options can be cheaper alternatives for hedging a portfolio with different FX exposures.

3.3.1 Consistent multi-FX modeling

De Col, Gnoatto and Grassell (2013) list two intuitive properties for a multi-FX model to be consistent, namely:

- **Inversion property**: the inverted process $\frac{1}{S^{di}(t)}$ has the same risk modeling dynamics as the original process $S^{di}(t)$, but under the i-th foreign risk neutral measure.
- **Triangle property**: the inferred cross rate $S^{ji} = \frac{S^{di}}{S^{dj}}$ has the same risk modeling dynamics as the original processes S^{di} and S^{dj}, but under the j-th foreign risk neutral measure.

Doust (2012) and De Col et al. both show that although the widely-used SABR and Heston stochastic volatility models are able to reproduce the market's volatility smiles and skews for single FX rates, they cannot be extended to model multiple FX rates in a consistent way. In both models, the FX rates do not satisfy the triangle property. This means that when two FX rates with a common domestic currency are both modeled by one of the models (i.e. SABR or Heston dynamics), the inferred FX rate associated with the three currencies has different model dynamics.

Consistency in the BSHW model

The disadvantage of the BSHW model is that, in contrast with models like the SABR model or the Heston model extended with stochastic interest rates, the model does not incorporate the volatility smile/skew effect by means of local volatility or stochastic volatility. The advantage compared to other models is that the model satisfies the inversion property and triangle property.

Theorem 1. *The BSHW model* (3.8) *satisfies the inversion property under the foreign risk neutral measure $\mathbb{Z}$, i.e. the inverted rate $\frac{1}{S^{df}(t)}$ has the BSHW dynamics under the foreign risk neutral measure $\mathbb{Z}$.*

Proof. Applying Itô's lemma to (3.8), the process $\frac{1}{S^{df}(t)}$ has the $\mathbb{Q}$-dynamics given by

$$d\frac{1}{S^{df}(t)} = \left(r_f(t) - r_d(t) + \sigma^2\right)\frac{1}{S^{df}(t)}dt - \sigma\frac{1}{S^{df}(t)}dW^{\mathbb{Q}}_{S^{df}}(t), \tag{3.17}$$

with the processes $r_f(t)$ and $r_d(t)$ still following the processes as given in (3.8). The drift term $r_f(t) - r_d(t) + \sigma^2$ is not equal to $r_f(t) - r_d(t)$, this asymmetry is introduced by the convexity of the function $f(x) = \frac{1}{x}$. The solution to this problem (Siegel's Exchange Rate Paradox, see Shreve, 2004) is to change the measure from the domestic spot risk-neutral measure $\mathbb{Q}$ to the foreign spot risk-neutral measure $\mathbb{Z}$. From chapter 9 in Shreve we know that the following processes should be martingales under the foreign risk neutral measure:

$$C_1(t) = \frac{1}{S^{df}(t)}\frac{M_d(t)}{M_f(t)},$$
$$C_2(t) = \frac{1}{S^{df}(t)}\frac{P_d(t,T)}{M_f(t)}.$$

Here $C_1(t)$ is the discounted value of the domestic money market account in foreign currency and $C_2(t)$ is the domestic zero-coupon bond in foreign currency. One has that

$$\begin{aligned} dM_d(t) &= M_d(t)r_d(t)dt, \\ dM_f(t) &= M_f(t)r_f(t)dt, \\ d\frac{1}{M_f(t)} &= -\frac{1}{M_f(t)}r_f(t)dt, \\ dP_d(t,T) &= r_d(t)P_d(t,T)dt + P_d(t,T)\sigma_d A_d(t,T)dW^{\mathbb{Q}}_d(t), \end{aligned} \tag{3.18}$$

where the last equation follows from the Hull and White dynamics for the zero-coupon bond under the domestic spot risk-neutral measure (3.3). Applying Itô to (3.18) yields

$$d\frac{M_d(t)}{M_f(t)} = \left(r_d(t) - r_f(t)\right)\frac{M_d(t)}{M_f(t)}dt, \tag{3.19}$$

and thus, combining (3.17) and (3.19),

$$dC_1(t) = \sigma^2 C_1(t)dt - \sigma C_1(t)dW^{\mathbb{Q}}_{S^{df}}(t).$$

Now using Girsanov's first fundamental theorem (Girsanov, 1960), one has that the process

$$W^{\mathbb{Z}}_{S^{df}}(t) := W^{\mathbb{Q}}_{S^{df}}(t) - \int_0^t \sigma ds \tag{3.20}$$

is a Brownian motion under the foreign spot risk-neutral measure $\mathbb{Z}$, making the process $C_1(t)$ a martingale under $\mathbb{Z}$. Applying (3.20) to (3.17) yields the $\mathbb{Z}$-dynamics for the process $\frac{1}{S^{df}(t)}$:

$$d\frac{1}{S^{df}(t)} = (r_f(t) - r_d(t))\frac{1}{S^{df}(t)}dt - \sigma\frac{1}{S^{df}(t)}dW^{\mathbb{Z}}_{S^{df}}(t). \tag{3.21}$$

Applying Itô to (3.18) once more yields

$$d\frac{P_d(t,T)}{M_f(t)} = (r_d(t) - r_f(t))\frac{P_d(t,T)}{M_f(t)}dt + \sigma_d A_d(t,T)\frac{P_d(t,T)}{M_f(t)}dW^{\mathbb{Q}}_d(t). \tag{3.22}$$

From (3.21) and (3.22) one has

$$\begin{aligned} dC_2(t) = &-\rho_{S^{df}r_d}\sigma\sigma_d A_d(t,T)C_2(t)dt - \sigma C_2(t)dW^{\mathbb{Z}}_{S^{df}}(t) \\ &+ \sigma_d A_d(t,T)C_2(t)dW^{\mathbb{Q}}_d(t). \end{aligned}$$

Now using Girsanov's first fundamental theorem (Girsanov, 1960), one has that the process

$$W^{\mathbb{Z}}_d(t) := W^{\mathbb{Q}}_d(t) - \int_0^t \rho_{S^{df}r_d}\sigma ds \tag{3.23}$$

is a Brownian motion under the foreign spot risk-neutral measure $\mathbb{Z}$, making the process $C_2(t)$ a martingale under $\mathbb{Z}$. Now using (3.21) and (3.23) one has the following $\mathbb{Z}$-dynamics:

$$\begin{aligned} d\frac{1}{S^{df}(t)} &= (r_f(t) - r_d(t))\frac{1}{S^{df}(t)}dt - \sigma\frac{1}{S^{df}(t)}dW^{\mathbb{Z}}_{S^{df}}(t), \\ dr_d(t) &= \lambda_d\left(\theta_d(t) - r_d(t) - \sigma\sigma_d\rho_{S^{df}r_d}\right)dt + \sigma_d dW^{\mathbb{Z}}_d(t), \\ dr_f(t) &= \lambda_f\left(\theta_f(t) - r_f(t)\right)dt + \sigma_f dW^{\mathbb{Z}}_f(t). \end{aligned} \tag{3.24}$$

These dynamics are equal to the BSHW model dynamics under the measure $\mathbb{Z}$[5]. □

Theorem 2. *The BSHW model* (3.8) *satisfies the triangle property under the foreign risk neutral measure $\mathbb{Z}_2$, i.e. the rate $\frac{S^{d1}(t)}{S^{d2}(t)}$ has the BSHW dynamics under the foreign risk neutral measure $\mathbb{Z}_2$. Here the measure $\mathbb{Z}_2$ corresponds to taking the money market account $M_{f,2}$ as numéraire.*

[5]Note that if the stochastic process W is a Brownian motion, $-W$ is a Brownian motion as well. This can be applied to the first equation in (3.24).

Proof. Denote by $\sigma_1, r_{f,1}$ and $\sigma_2, r_{f,2}$ the volatility parameter and short rate for the FX rates S^{d1} and S^{d2}, respectively. Using Itô's lemma, the process $\frac{S^{d1}(t)}{S^{d2}(t)}$ has the $\mathbb{Q}$-dynamics given by

$$\begin{aligned} d\frac{S^{d1}(t)}{S^{d2}(t)} &= \left(r_{f,2}(t) - r_{f,1}(t) + \sigma_2^2 - \rho_{S^{d1}S^{d2}}\sigma_1\sigma_2\right)\frac{S^{d1}(t)}{S^{d2}(t)}dt \\ &\quad + \frac{S^{d1}(t)}{S^{d2}(t)}\left(\sigma_1 dW^{\mathbb{Q}}_{S^{d1}}(t) - \sigma_2 dW^{\mathbb{Q}}_{S^{d2}}(t)\right), \end{aligned} \tag{3.25}$$

with the Hull-White processes $r_{f,1}(t)$, $r_{f,2}(t)$ and $r_d(t)$. Consider now a change of measure from the domestic spot risk-neutral measure $\mathbb{Q}$ to the foreign spot risk-neutral measure $\mathbb{Z}_2$. From chapter 9 in Shreve (2004) we know that the following processes should be martingales under the foreign risk neutral measure $\mathbb{Z}_2$:

$$\begin{aligned} C_1(t) &= \frac{S^{d1}(t)}{S^{d2}(t)}\frac{M_{f,1}(t)}{M_{f,2}(t)}, \\ C_2(t) &= \frac{S^{d1}(t)}{S^{d2}(t)}\frac{P_{f,1}(t,T)}{M_{f,2}(t)}. \end{aligned}$$

Similarly to (3.19) one has

$$d\frac{M_{f,1}(t)}{M_{f,2}(t)} = \left(r_{f,1}(t) - r_{f,2}(t)\right)\frac{M_{f,1}(t)}{M_{f,2}(t)}dt. \tag{3.26}$$

Applying Itô to (3.25) and (3.26) results in the following dynamics:

$$dC_1(t) = \left(\sigma_2^2 - \rho_{S^{d1}S^{d2}}\sigma_1\sigma_2\right)C_1(t)dt + C_1(t)\left(\sigma_1 dW^{\mathbb{Q}}_{S^{d1}}(t) - \sigma_2 dW^{\mathbb{Q}}_{S^{d2}}(t)\right). \tag{3.27}$$

Now using Girsanov's first fundamental theorem (Girsanov, 1960), one has that the processes

$$\begin{aligned} W^{\mathbb{Z}_2}_{S^{d1}}(t) &:= W^{\mathbb{Q}}_{S^{d1}}(t) - \int_0^t \rho_{S^{d1}S^{d2}}\sigma_2 ds, \\ W^{\mathbb{Z}_2}_{S^{d2}}(t) &:= W^{\mathbb{Q}}_{S^{d2}}(t) - \int_0^t \sigma_2 ds, \end{aligned} \tag{3.28}$$

are Brownian motions under the foreign spot risk-neutral measure $\mathbb{Z}_2$, making the process $C_1(t)$ a martingale under the foreign spot risk-neutral measure $\mathbb{Z}_2$. From (3.25) and (3.28) it follows that the process $\frac{S^{d1}(t)}{S^{d2}(t)}$ has the $\mathbb{Z}_2$-dynamics

given by

$$d\frac{S^{d1}(t)}{S^{d2}(t)} = \left(r_{f,2}(t) - r_{f,1}(t)\right)\frac{S^{d1}(t)}{S^{d2}(t)}dt + \frac{S^{d1}(t)}{S^{d2}(t)}\left(\sigma_1 dW^{\mathbb{Z}_2}_{S^{d1}}(t) - \sigma_2 dW^{\mathbb{Z}_2}_{S^{d2}}(t)\right). \tag{3.29}$$

Using that the zero-coupon bond $P_{f,1}(t,T)$ has the following dynamics under the foreign spot risk-neutral measure $\mathbb{Z}_1$,

$$dP_{f,1}(t,T) = r_{f,1}(t)P_{f,1}(t,T)dt + P_{f,1}(t,T)\sigma_{f,1}A_{f,1}(t,T)dW^{\mathbb{Z}_1}_{f,1},$$

and that we have

$$d\frac{1}{M_{f,2}(t)} = -\frac{1}{M_{f,2}(t)}r_{f,2}(t)dt,$$

one has, using Itô:

$$d\frac{P_{f,1}(t,T)}{M_{f,2}(t)} = \left(r_{f,1}(t) - r_{f,2}(t)\right)\frac{P_{f,1}(t,T)}{M_{f,2}(t)}dt + \sigma_{f,1}A_{f,1}(t,T)\frac{P_{f,1}(t,T)}{M_{f,2}(t)}dW^{\mathbb{Z}_1}_{f,1}. \tag{3.30}$$

And thus one has, using (3.29) and (3.30),

$$\begin{aligned} &dC_2(t) \\ &= \sigma_{f,1}A_{f,1}(t,T)\left(\rho_{S^{d1}r_{f,1}}\sigma_1 - \rho_{S^{d2}r_{f,1}}\sigma_2\right)C_2(t)dt + \sigma_1 C_2(t)dW^{\mathbb{Z}_2}_{S^{d1}}(t) \\ &\quad - \sigma_2 C_2(t)dW^{\mathbb{Z}_2}_{S^{d2}}(t) + \sigma_{f,1}A_{f,1}(t,T)C_2(t)dW^{\mathbb{Z}_1}_{f,1}(t). \end{aligned} \tag{3.31}$$

Now using Girsanov's first fundamental theorem (Girsanov, 1960), one has that the process

$$W^{\mathbb{Z}_2}_{f,1}(t) := W^{\mathbb{Z}_1}_{f,1}(t) + \int_0^t \left(\rho_{S^{d1}r_{f,1}}\sigma_1 - \rho_{S^{d2}r_{f,1}}\sigma_2\right)ds \tag{3.32}$$

is a Brownian motion under the foreign spot risk-neutral measure $\mathbb{Z}_2$, making the process $C_2(t)$ a martingale under $\mathbb{Z}_2$. Using (3.29) and (3.32), the resulting $\mathbb{Z}_2$-dynamics for the inferred cross rate and the interest rates are given by

$$\begin{aligned} d\frac{S^{d1}(t)}{S^{d2}(t)} &= \left(r_{f,2}(t) - r_{f,1}(t)\right)\frac{S^{d1}(t)}{S^{d2}(t)}dt + \frac{S^{d1}(t)}{S^{d2}(t)}\left(\sigma_1 dW^{\mathbb{Z}_2}_{S^{d1}}(t) - \sigma_2 dW^{\mathbb{Z}_2}_{S^{d2}}(t)\right), \\ dr_{f,2}(t) &= \lambda_{f,2}\left(\theta_{f,2}(t) - r_{f,2}(t)\right)dt + \sigma_{f,2}dW^{\mathbb{Z}_2}_{f,2}(t), \\ dr_{f,1}(t) &= \lambda_{f,1}\left(\theta_{f,1}(t) - r_{f,1}(t) - \rho_{S^{d1}r_{f,1}}\sigma_1\sigma_{f,1}(t) + \rho_{S^{d2}r_{f,1}}\sigma_2\sigma_{f,1}(t)\right)dt \\ &\quad + \sigma_{f,1}dW^{\mathbb{Z}_2}_{f,1}(t). \end{aligned} \tag{3.33}$$

The sum of two correlated, normally distributed random variables remains normal with mean equal to the sum of the individual means and variance equal to the sum of the cross-covariance terms. Therefore the $\mathbb{Z}_2$-dynamics of the process $\frac{S^{d1}(t)}{S^{d2}(t)}$ in (3.33) can be represented as (e.g., Grzelak & Oosterlee, 2012, Remark 1)

$$\begin{aligned} d\frac{S^{d1}(t)}{S^{d2}(t)} &= \left(r_{f,2}(t) - r_{f,1}(t)\right) \frac{S^{d1}(t)}{S^{d2}(t)} dt \\ &\quad + \left(\sigma_1^2 + \sigma_2^2 - 2\rho_{S^{d1}S^{d2}}\sigma_1\sigma_2\right)^{\frac{1}{2}} \frac{S^{d1}(t)}{S^{d2}(t)} dW^{\mathbb{Z}_2}(t), \end{aligned} \tag{3.34}$$

with $W^{\mathbb{Z}_2}(t)$ a Brownian motion under $\mathbb{Z}_2$. □

Remark 1. *From result* 3.34 *a triangle relation in volatility, in order to ensure risk-neutrality, can be deducted. The volatility parameter of the inferred cross FX rate depends on the volatilities of the original FX rates and their correlation coefficient. Denoting by* S^{d1}, S^{d2} *and* $S^{21} = \frac{S^{d1}}{S^{d2}}$ *the two original FX rates with the same domestic currency and the inferred cross FX rate, respectively, the triangle property for FX volatility under the BSHW model is given by*

$$\sigma_{21}^2 = \sigma_1^2 + \sigma_2^2 - 2\rho_{S^{d1}S^{d2}}\sigma_1\sigma_2.$$

Here σ_{21} *denotes the volatility parameter for the cross rate* S^{21}.

The above theorems show that the BSHW model is consistent in the modeling of multiple FX rates simultaneously. The extension to multiple FX rates will be covered in the next chapter.

3.3.2 The multi-FX BSHW model under the $\mathbb{Q}$-measure

Extending the BSHW model (3.8) to multiple FX rates with the same domestic currency yields the multi-FX BSHW model (henceforth M-BSHW model), given by the risk-neutral dynamics

$$\begin{aligned} dS^{di}(t) &= \left(r_d(t) - r_{f,i}(t)\right) S^{di}(t)dt + \sigma_i S^{di}(t) dW^{\mathbb{Q}}_{S^{di}}(t), \qquad i = 1, \ldots, N_{FX}, \\ dr_d(t) &= \lambda_d \left(\theta_d(t) - r_d(t)\right) dt + \sigma_d dW^{\mathbb{Q}}_d(t), \\ dr_{f,i}(t) &= \left[\lambda_{f,i}\left(\theta_{f,i}(t) - r_{f,i}(t)\right) - \rho_{S^{di}r_{f,i}}\sigma_i\sigma_{f,i}\right] dt + \sigma_{f,i} dW^{\mathbb{Q}}_{f,i}(t), \\ &\quad i = 1, \ldots, N_{FX}, \end{aligned} \tag{3.35}$$

with N_{FX} the number of FX rates. The M-BSHW model is $(2N_{FX}+1)$-dimensional, as the domestic currency is equal for all FX rates. Consider the FX basket option pricing problem 2.4 under the above M-BSHW model. In section 3.2.4 it was shown that the European-style single FX option pricing problem can be heavily simplified by changing the numéraire from the domestic money market account to the domestic zero-coupon bond. The measure corresponding to the new numéraire was denoted by $\mathbb{Q}_T$, the T-forward measure. Secondly, the FX rate in the pricing problem was substituted by the forward FX rate as both rates are equal at maturity T. As the forward FX rate dynamics are one-dimensional and independent of the stochastic interest rates, a huge computational advantage is attained. For the FX basket option pricing problem (2.4) under the M-BSHW model (3.35), this approach can be applied as well.

3.3.3 The multi-FX BSHW model under the $\mathbb{Q}_{\mathbb{T}}$-measure

Under the measure $\mathbb{Q}_T$, all non-dividend paying traded assets (in domestic currency) discounted by the domestic zero-coupon bond should be martingales. For the M-BSHW model (3.35) therefore the following processes should be martingales under $\mathbb{Q}_T$:

$$\psi_i(t) = S^{di}(t)\frac{M_{f,i}(t)}{P_d(t,T)}, \qquad i = 1,\dots,N_{FX},$$
$$F^{di}(t) = S^{di}(t)\frac{P_{f,i}(t,T)}{P_d(t,T)}, \qquad i = 1,\dots,N_{FX}.$$

Using the same calculations as in section 3.2.4, the model dynamics of the i-th FX rate F^{di} under the measure $\mathbb{Q}_T$ are given by

$$\begin{aligned} &dF^{di}(t) = \\ &\sigma_i F^{di}(t) dW_{S^{di}}^{\mathbb{Q}_T}(t) + \sigma_{f,i} A_{f,i}(t,T) F^{di}(t) dW_{f,i}^{\mathbb{Q}_T}(t) - \sigma_d A_d(t,T) F^{di}(t) dW_d^{\mathbb{Q}_T}(t) \end{aligned} \tag{3.36}$$

for $i \leq N_{FX}$. This can equivalently be represented as (e.g., Grzelak & Oosterlee, 2012)

$$\begin{aligned} &dF^{di}(t) = \\ &\left[\sigma_i^2 + \sigma_{f,i}^2 A_{f,i}^2(t,T) + \sigma_d^2 A_d^2(t,T) + 2\rho_{S^{di}r_{f,i}}\sigma_i\sigma_{f,i}A_{f,i}(t,T)\right. \\ &\left.-2\rho_{S^{di}r_d}\sigma_i\sigma_d A_d(t,T) - 2\rho_{r_d r_{f,i}}\sigma_d\sigma_{f,i}A_d(t,T)A_{f,i}(t,T)\right]^{\frac{1}{2}} F^{di}(t) dW_i^{\mathbb{Q}_T}(t), \end{aligned} \tag{3.37}$$

with $W_i^{\mathbb{Q}_T}$, $i \leq N_{FX}$, Brownian motions under the $\mathbb{Q}_T$-measure. For quadratic covariation processes $\left[F^{di}, F^{dj}\right](t)$ all the specific covariation processes should be taken into account. From (3.36) one has for $i, j \leq N_{FX}$

$$\begin{aligned}
&d\left[\log\left(F^{di}\right), \log\left(F^{dj}\right)\right](t) \\
&= \big[\sigma_i\sigma_j\rho_{S^{di}S^{dj}} + \sigma_i\sigma_{f,j}A_{f,j}(t,T)\rho_{S^{di}r_{f,j}} - \sigma_i\sigma_d A_d(t,T)\rho_{S^{di}r_d} \\
&+\sigma_{f,i}A_{f,i}(t,T)\sigma_j\rho_{S^{dj}r_{f,i}} + \sigma_{f,i}\sigma_{f,j}A_{f,i}(t,T)A_{f,j}(t,T)\rho_{r_{f,i}r_{f,j}} \\
&-\sigma_{f,i}A_{f,i}(t,T)\sigma_d A_d(t,T)\rho_{r_{f,i}r_d} - \sigma_d A_d(t,T)\sigma_j\rho_{S^{dj}r_d} \\
&-\sigma_d A_d(t,T)\sigma_{f,j}A_{f,j}(t,T)\rho_{r_d r_{f,j}} + \sigma_d^2 A_d^2(t,T)\big]\,dt \\
&:= \omega_{ij}(t,T)dt.
\end{aligned} \tag{3.38}$$

Combining (3.37) and (3.38) and applying Itô yields

$$d\log\left(F^{di}(t)\right) = -\frac{1}{2}\omega_{ii}(t,T)dt + \sqrt{\omega_{ii}(t,T)}dW_i^{\mathbb{Q}_T}(t), \qquad i \leq N_{FX}. \tag{3.39}$$

Using that $F^{di}(T) = S^{di}(T)$ for $i \leq N_{FX}$ and changing the numéraire to the domestic zero-coupon bond in the pricing problem (2.4) yields the following time-t price of the European-style FX basket option under the M-BSHW model:

$$\Pi_k^{N_{FX}}(t) = P_d(t,T)\mathbb{E}_{\mathbb{Q}_\mathbb{T}}\left[f_k\left(\left(F^{di}(T)\right)_{i\leq N_{FX}}\right)\big|\mathcal{F}(t)\right], \qquad k = 1, 2. \tag{3.40}$$

From the above pricing formula it is clear that an analytical expression is available for the time-t price of a FX basket forward option. From (3.36) it is clear that the forward FX rate $F^{di}(t)$ is a martingale, therefore this particular price becomes:

$$\begin{aligned}
\Pi_1^{N_{FX}}(t) &= P_d(t,T)\mathbb{E}_{\mathbb{Q}_\mathbb{T}}\left[\sum_{i\leq N_{FX}}\phi_i S^{di}(T) - K\big|\mathcal{F}(t)\right] \\
&= P_d(t,T)\mathbb{E}_{\mathbb{Q}_\mathbb{T}}\left[\sum_{i\leq N_{FX}}\phi_i F^{di}(T) - K\big|\mathcal{F}(t)\right] \\
&= P_d(t,T)\left[\sum_{i\leq N_{FX}}\phi_i\mathbb{E}_{\mathbb{Q}_\mathbb{T}}\left[F^{di}(T)\big|\mathcal{F}(t)\right] - K\right] \\
&= P_d(t,T)\sum_{i\leq N_{FX}}\phi_i F^{di}(t) - P_d(t,T)K \\
&= P_d(t,T)\sum_{i\leq N_{FX}}\phi_i S^{di}(t)\frac{P_{f,i}(t,T)}{P_d(t,T)} - P_d(t,T)K \\
&= \sum_{i\leq N_{FX}}\phi_i S^{di}(t)P_{f,i}(t,T) - P_d(t,T)K.
\end{aligned} \tag{3.41}$$

In case the strike K equals the forward basket rate,

$$K = \sum_{i \leq N_{FX}} \phi_i S^{di}(0) \frac{P_{f,i}(0,T)}{P_d(0,T)},$$

the time-zero price of the FX basket forward equals 0. Using (3.41) one has

$$\begin{aligned}
\Pi_1^{N_{FX}}(0) &= \sum_{i \leq N_{FX}} \phi_i S^{di}(0) P_{f,i}(0,T) - P_d(0,T) K \\
&= \sum_{i \leq N_{FX}} \phi_i S^{di}(0) P_{f,i}(0,T) - P_d(0,T) \sum_{i \leq N_{FX}} \phi_i S^{di}(0) \frac{P_{f,i}(0,T)}{P_d(0,T)} \\
&= \sum_{i \leq N_{FX}} \phi_i S^{di}(0) P_{f,i}(0,T) - \sum_{i \leq N_{FX}} \phi_i S^{di}(0) P_{f,i}(0,T) \\
&= 0. \qquad (3.42)
\end{aligned}$$

Chapter 4

Dimension reduction for the M-BSHW model

4.1 Principal component analysis

A possible dimension reduction method for a certain dataset can be found in principal component analysis (PCA). The aim of principal component analysis is to "reduce the dimensionality of a data set consisting of a large number of interrelated variables, while retaining as much as possible of the variation present in the data set." (Jolliffe, 2002, p.1). This is done by transforming the original set of $u \geq 1$ possibly correlated variables $\mathbf{X} = (X_1, \ldots, X_u)^\top$ to a new set of uncorrelated principal components $\mathbf{Z} = (Z_1, \ldots, Z_u)^\top$[1]. The Z_i, $i \in \{1, \ldots, u\}$, are ordered such that Z_1 exhibits the most variation present in all the original variables and such that Z_u exhibits the least variation.

Principal component analysis applies linear transformations to the original variables $\mathbf{X}$. The aim is to find vectors $\boldsymbol{\beta}_i = (\beta_{i1}, \ldots, \beta_{iu})^\top$ $(i \leq u)$ such that the transformed variable $Z_1 := \boldsymbol{\beta}_1^\top \mathbf{X}$ has maximum variance, and such that the transformed variable $Z_i := \boldsymbol{\beta}_i^\top \mathbf{X}$ has maximum variance subject to being uncorrelated with $Z_j := \boldsymbol{\beta}_j^\top \mathbf{X}$ for $j < i$. The u derived variables $Z_1, \ldots, Z_u$ are the so-called principal components: linear transformations of the original set of variables that are uncorrelated and have decreasing variance.

To derive the first principal component, Z_1, the vector $\boldsymbol{\beta}_1$ that maximizes $\text{var}\left[\boldsymbol{\beta}_1^\top \mathbf{X}\right] = \boldsymbol{\beta}_1^\top \Sigma \boldsymbol{\beta}_1$ has to be derived. Here Σ is the covariance matrix of the original set of variables $\mathbf{X}$. A widely imposed normalization constant is $\boldsymbol{\beta}_1^\top \boldsymbol{\beta}_1 = 1$ (see e.g., Jolliffe, 2012). The method of Lagrange multipliers

[1]The symbol $\top$ denotes the transpose of a vector or matrix.

yields that $\boldsymbol{\beta}_1$ is the eigenvector corresponding to the largest eigenvalue of Σ, and $\text{var}\left[\boldsymbol{\beta}_1^\top \mathbf{X}\right] = \boldsymbol{\beta}_1^\top \Sigma \boldsymbol{\beta}_1 = \lambda_1$, the largest eigenvalue. Furthermore for $i \leq u$, $\text{var}\left[\boldsymbol{\beta}_i^\top \mathbf{X}\right] = \boldsymbol{\beta}_i^\top \Sigma \boldsymbol{\beta}_i = \lambda_i$ with λ_i the i-th largest eigenvalue of Σ and $\boldsymbol{\beta}_i$ the corresponding eigenvector. Now let $\mathbf{Q}$ denote the matrix with the eigenvectors of the covariance matrix Σ as columns, i.e. $\mathbf{Q} = (\boldsymbol{\beta}_1, \ldots, \boldsymbol{\beta}_u)$. The vector with principal components $\mathbf{Z}$ is then given by

$$\mathbf{Z} = \mathbf{Q}^\top \mathbf{X}. \tag{4.1}$$

As variance maximization is preserved under time translation, one can add a time-component $\mathbf{B}(t)$ to the PCA transformation (4.1):

$$\mathbf{Z} = \mathbf{Q}^\top \left[\mathbf{X} + \mathbf{B}(t)\right]. \tag{4.2}$$

This transformation will appear to be very useful for derivative pricing as the time-component can be used to eliminate the drift term from the partial differential equation. This will be discussed in more detail in subsequent sections.

4.2 Time-dependent principal components-based dimension reduction for the M-BSHW model

In this section, a principal components-based transformation is applied to the M-BSHW model for log forward FX rates (3.39) in order to reduce the complexity of the pricing of European-style FX basket options (see the pricing problem formulation (2.4)). As the covariance matrix of the M-BSHW model is time-dependent, the main challenge is to incorporate the time-dependent transformation into the FX basket option pricing problem.

One can use the Feynman-Kac formula[2] to derive the PDE for the time-t value $\Pi_k^{N_{FX}}(t)$ of the European-style FX basket option of type $k \in \{1, 2\}$ (see (2.4)). Using the dynamics (3.39) and covariances (3.38) for the M-BSHW model for log forward FX rates, the pricing PDE is given by

$$\frac{\partial \Pi_k^{N_{FX}}}{\partial t} - \sum_{i=1}^{N_{FX}} \frac{1}{2}\omega_{ii}(t,T)\frac{\partial \Pi_k^{N_{FX}}}{\partial Y^{di}} + \frac{1}{2}\sum_{i=1}^{N_{FX}}\sum_{j=1}^{N_{FX}} \omega_{ij}(t,T)\frac{\partial^2 \Pi_k^{N_{FX}}}{\partial Y^{di}\partial Y^{dj}} = 0, \tag{4.3}$$

with terminal condition

$$\Pi_k^{N_{FX}}(T) = f_k\left(\left(e^{Y^{di}(T)}\right)_{i \leq N_{FX}}\right). \tag{4.4}$$

[2]See e.g., Björk, 2009, Proposition 5.8.

Here $Y^{di} = \log\left(F^{di}\right)$, $i \leq N_{FX}$. From (3.38) it is clear that the covariance matrix for the N_{FX} log FX rates $\left(Y^{di}\right)_{i \leq N_{FX}}$ is given by

$$\mathbf{\Sigma}(t) := \left(\omega_{ij}(t,T)\right)_{i,j \in \{1,\ldots,N\}}. \tag{4.5}$$

The matrix $\mathbf{Q}(t)$ with the eigenvectors of the covariance matrix and the vector $\mathbf{\Lambda}(t)$ with corresponding eigenvalues are therefore time-dependent as well. The principal components $\mathbf{Z}(t) = (Z_1(t), \ldots, Z_{N_{FX}}(t))^\top$ of the N_{FX} log FX rates under the M-BSHW model (3.39) are given by

$$\mathbf{Z}(t) = \mathbf{Q}^\top(t)\mathbf{Y}(t), \tag{4.6}$$

with $\mathbf{Y}(t) = \left(\log\left(F^{d1}(t)\right), \ldots, \log\left(F^{dN_{FX}}(t)\right)\right)^\top$.

$$\begin{aligned}\mathbf{Q}(t) &:= (\mathbf{q}_1(t), \ldots, \mathbf{q}_{N_{FX}}(t)) \\ &:= (q_{ij}(t))_{i,j \leq N_{FX}}\end{aligned}$$

is the matrix with the eigenvectors of $\mathbf{\Sigma}(t)$ as columns, ordered by the corresponding eigenvalues. Adding a time-translation term in order to remove the drift term from 4.3 yields the principal-components based transformation for the log FX rates:

$$\mathbf{Z}(t) = \mathbf{Q}^\top(t)\left[\mathbf{Y}(t) - \mathbf{B}(t)\right]. \tag{4.7}$$

The vector $\mathbf{B}(t) = (B_1(t), \ldots, B_{N_{FX}}(t))^\top$ is given by

$$B_i(t) = -\int_0^t \frac{1}{2}\omega_{ii}(u,T)du, \qquad i \leq N_{FX}. \tag{4.8}$$

The variance of principal component i ($i \leq N_{FX}$) at time t is given by

$$\mathrm{Var}\left[Z_i(t)\right] = \mathbf{q}_i^\top \mathbf{\Sigma}(t)\mathbf{q}_i = \lambda_i(t). \tag{4.9}$$

By definition, one has $\lambda_1(t) \geq \lambda_2(t) \geq \cdots \geq \lambda_{N_{FX}}(t)$ for all $t \in [0,T]$. Using the variable transformation 4.7, the FX basket option pricing problem under the M-BSHW model is transformed as follows.

Theorem 3. *Under the time-dependent principal components-based transformation* 4.7 *the FX basket option pricing problem* 2.4 *under the M-BSHW model transforms to*

$$\begin{aligned}\frac{\partial V_k^{N_{FX}}}{\partial \tau} = \frac{1}{2}\sum_{i=1}^{N_{FX}} \lambda_i(T-\tau)\frac{\partial^2 V_k^{N_{FX}}}{\partial\left(Z_i\right)^2} - \sum_{l=1}^{N_{FX}} \frac{\partial V_k^{N_{FX}}}{\partial Z_l}\sum_{m=1}^{N_{FX}} \frac{\partial q_{ml}(T-\tau)}{\partial \tau} \\ \times \left[\sum_{j=1}^{N_{FX}} q_{mj}(T-\tau)Z_j(T-\tau)\right],\end{aligned} \tag{4.10}$$

with terminal condition (4.4) *transforming to the initial condition*

$$V_k^{N^{FX}}(\mathbf{Z},0) = f_k\left(\left(e^{\sum_{j=1}^{N_{FX}} q_{ij}(T)Z_j(T)+B_i(T)}\right)_{i\leq N_{FX}}\right), \qquad k=1,2. \quad (4.11)$$

Here $V_k^{N_{FX}}(\mathbf{Z},\tau)$ *is the value process corresponding to the transformed variables* (4.7)*, and* $\lambda_i(t)$ *according to* 4.9*.*

Proof. From $\Pi_k^{N_{FX}}(\mathbf{Y},t) = \Phi_k^{N_{FX}}(\mathbf{Z},t) = \Phi_k^{N_{FX}}\left(\mathbf{Q}^\top[\mathbf{Y}-\mathbf{B}],t\right)$ one has, using the well-known chain rule:

$$\begin{aligned}
\frac{\partial \Pi_k^{N_{FX}}}{\partial Y^{di}(t)} &= \sum_{l=1}^{N_{FX}} \frac{\partial \Phi_k^{N_{FX}}}{\partial Z_l(t)} q_{il}(t), \qquad i \leq N_{FX},\\
\frac{\partial^2 \Pi_k^{N_{FX}}}{\partial Y^{di}(t)\partial Y^{dj}(t)} &= \sum_{l=1}^{N_{FX}} \frac{\partial^2 \Phi_k^{N_{FX}}}{\partial Z_l^2(t)} q_{il}(t)q_{jl}(t), \qquad i,j \leq N_{FX},\\
\frac{\partial \Pi_k^{N_{FX}}}{\partial t} &= \sum_{l=1}^{N_{FX}}\sum_{m=1}^{N_{FX}} \frac{\partial \Phi_k^{N_{FX}}}{\partial Z_l} q_{ml}(t)\frac{1}{2}\omega_{mm}(t,T)\\
&\quad + \sum_{l=1}^{N_{FX}} \frac{\partial \Phi_k^{N_{FX}}}{\partial Z_l} \sum_{m=1}^{N_{FX}} \frac{\partial q_{ml}(t)}{\partial t}\left[Y_m(t) - B_{mm}(t)\right] + \frac{\partial \Phi_k^{N_{FX}}}{\partial t}\\
&= \sum_{l=1}^{N_{FX}}\sum_{m=1}^{N_{FX}} \frac{\partial \Phi_k^{N_{FX}}}{\partial Z_l} q_{ml}(t)\frac{1}{2}\omega_{mm}(t,T)\\
&\quad + \sum_{l=1}^{N_{FX}} \frac{\partial \Phi_k^{N_{FX}}}{\partial Z_l} \sum_{m=1}^{N_{FX}} \frac{\partial q_{ml}(t)}{\partial t}\left[\sum_{j=1}^{N_{FX}} q_{mj}(t)Z_j(t)\right] + \frac{\partial \Phi_k^{N_{FX}}}{\partial t}.
\end{aligned} \quad (4.12)$$

Substituting 4.12 into the original FX basket option pricing problem 4.3 yields

$$\begin{aligned}
&\frac{\partial \Phi_k^{N_{FX}}}{\partial t} + \frac{1}{2}\sum_{l=1}^{N_{FX}}\sum_{i=1}^{N_{FX}}\sum_{j=1}^{N_{FX}} \frac{\partial^2 \Phi_k^{N_{FX}}}{\partial Z_l^2} q_{il}(t)q_{jl}(t)\omega_{ij}(t,T)\\
&\qquad + \sum_{l=1}^{N_{FX}} \frac{\partial \Phi_k^{N_{FX}}}{\partial Z_l} \sum_{m=1}^{N_{FX}} \frac{\partial q_{ml}(t)}{\partial t}\left[\sum_{j=1}^{N_{FX}} q_{mj}(t)Z_j(t)\right] = 0.
\end{aligned} \quad (4.13)$$

Reversing time and substituting $\Phi_k^{N_{FX}}(\mathbf{Z},t) = V_k^{N_{FX}}(\mathbf{Z},\tau)$ with

$\tau = T - t$ in (4.13) yields

$$-\frac{\partial V_k^{N_{FX}}}{\partial \tau} + \frac{1}{2}\sum_{l=1}^{N_{FX}}\sum_{i=1}^{N_{FX}}\sum_{j=1}^{N_{FX}} \frac{\partial^2 V_k^{N_{FX}}}{\partial Z_l^2} q_{il}(T-\tau)q_{jl}(T-\tau)\omega_{ij}(T-\tau,T) - \sum_{l=1}^{N_{FX}} \frac{\partial V_k^{N_{FX}}}{\partial Z_l} \sum_{m=1}^{N_{FX}} \frac{\partial q_{ml}(T-\tau)}{\partial \tau} \left[\sum_{j=1}^{N_{FX}} q_{mj}(T-\tau)Z_j(T-\tau)\right] = 0. \tag{4.14}$$

From $\mathbf{q}_i^\top(t)\mathbf{\Sigma}(t)\mathbf{q}_i(t) = \lambda_i(t)$ for all $t \in [0,T]$ one has

$$\lambda_l(t) = \sum_{i=1}^{N_{FX}}\sum_{j=1}^{N_{FX}} q_{il}(t)q_{jl}(t)\omega_{ij}(t,T), \qquad t \in [0,T]. \tag{4.15}$$

Using (4.15) the PDE (4.14) transforms into

$$\frac{\partial V_k^{N_{FX}}}{\partial \tau} = \frac{1}{2}\sum_{l=1}^{N_{FX}} \lambda_l(T-\tau)\frac{\partial^2 V_k^{N_{FX}}}{\partial Z_l^2} - \sum_{l=1}^{N_{FX}} \frac{\partial V_k^{N_{FX}}}{\partial Z_l} \sum_{m=1}^{N_{FX}} \frac{\partial q_{ml}(T-\tau)}{\partial \tau} \times \left[\sum_{j=1}^{N_{FX}} q_{mj}(T-\tau)Z_j(T-\tau)\right]. \tag{4.16}$$

The initial condition (4.11) follows straightforward by applying the transformation 4.7 to the terminal condition 4.4. □

4.2.1 Dimension reduction in the M-BSHW model

By definition, the principal components (4.7) have descending variance for all $t \in [0,T]$:

$$\lambda_1(t) \geq \lambda_2(t) \geq \cdots \geq \lambda_{N_{FX}}(t). \tag{4.17}$$

Moreover the variance $\lambda_i(t)$ of principal component $i \leq N_{FX}$ approaches zero for larger i. The degree in which the variances descend to zero depends on the volatilities of the FX rates and the Hull-White interest rate components. Furthermore it depends on the correlations between the FX rates, between the FX rates and the Hull-White interest rates and between the Hull-White interest rates. For high correlations and similar volatilities for the original variables, the variances of the principal components will rapidly descend to zero. For low correlations and nonsimilar volatilities more principal components will have significant variance.

The dimension of the transformed FX basket option pricing problem (4.10) with initial condition (4.11) under the M-BSHW model can be reduced as follows. The sum in (4.10) and (4.11) can be truncated to a certain ordered index set $\alpha \subset \{1, \ldots, N_{FX}\}$ of principal components. The principal components belonging to the set $\{1, \ldots, N_{FX}\} \setminus \alpha$ are then substituted by their time-zero expectation[3]. Then the reduced version of the pricing problem (4.10) with initial condition (4.11) is[4]

$$\begin{aligned}
\frac{\partial V_k^{N_{FX}}}{\partial \tau} &= \frac{1}{2} \sum_{i \in \alpha} \lambda_i (T-\tau) \frac{\partial^2 V_k^{N_{FX}}}{\partial \left(Z_i\right)^2} - \sum_{l \in \alpha} \frac{\partial V_k^{N_{FX}}}{\partial Z_l} \sum_{m=1}^{N_{FX}} \frac{\partial q_{ml}(T-\tau)}{\partial \tau} \\
&\quad \times \left[\sum_{j \in \alpha} q_{mj}(T-\tau) Z_j(T-\tau) + \sum_{j \notin \alpha} q_{mj}(T-\tau) \mathbb{E}\left[Z_j(T-\tau)\right] \right], \\
V_k^{N_{FX}}(\mathbf{Z}_\alpha, 0) &= f_k \left(\left(e^{\sum_{j \in \alpha} q_{ij}(T) Z_j(T) + \sum_{j \notin \alpha} q_{ij}(T) \mathbb{E}[Z_j(T)] + B_i(T)} \right)_{i \leq N_{FX}} \right), \\
&\quad k = 1, 2.
\end{aligned} \tag{4.18}$$

Here $\mathbf{Z}_\alpha = (Z_i)_{i \in \alpha}^\top$ and $V_k^{N_{FX}}(\mathbf{Z}_\alpha, \tau)$ is the associated value process. From (3.39) and (4.8) it is immediate that the stochastic process $Y_j(t) - B_j(t)$ for $j \leq N_{FX}$ is a martingale, and therefore

$$\begin{aligned}
\mathbb{E}\left[Y_j(T) - B_j(T) | \mathcal{F}(0)\right] &= Y_j(0) - B_j(0) \\
&= \log\left(S^{dj}(0)\right) + \log\left(P_j(0,T)\right) - \log\left(P_d(0,T)\right)
\end{aligned} \tag{4.19}$$

for $j \leq N_{FX}$.

In the remaining of this thesis the solution to the reduced FX basket option pricing problem (4.18) will in general be referred to as the PCA1 solution, in case $\alpha = \{1\}$, or the PCA2(i,j) solution, in case $\alpha = \{i, j\}$ for $i < j \leq N_{FX}$. These solutions correspond to solving the FX basket option pricing problem reduced to the first principal component or the i-th and j-th principal component, respectively, according to (4.18).

[3]The expectation with respect to the natural filtration $\mathcal{F}$ is taken.

[4]The problem arising with the PDE in (4.18) is that when applying finite differences (see section 5.2), a large grid is needed. This is because one has to deal with the time-dependence of the expectation of the principal components. It is therefore much more efficient to consider an adapted version of the principal components $\mathbf{Z}$ (4.7): $\mathbf{Z}' = \mathbf{Z} - \mathbb{E}[\mathbf{Z}]$. As $\mathbb{E}[\mathbf{Z}] = \mathbf{Q}^\top \mathbb{E}[\mathbf{Y}]$, the change from $\mathbf{Z}$ to $\mathbf{Z}'$ implies a change of the function $\mathbf{B}$.

Principal component selection

The choice which approximative principal components to include in the index set α in (4.18) and which ones to substitute by their expectation is not trivial. The percentage of total variation explained by the first n principal components, ordered in descending variance, is often defined as (e.g., Jolliffe, 2002)

$$\frac{\sum_{i \leq n} \lambda_i(t)}{\sum_j \lambda_j(t)}, \qquad t \in [0, T]. \tag{4.20}$$

For high correlations and similar volatilities for the original variables, often the first two principal components already explain a large percentage of total variation. Using Taylor expansions and finite differences, Reisinger (2004) formulates an asymptotic expansion for the value process $V_k^{N_{FX}}(\mathbf{Z}, \tau)$, for $k = 1, 2$ and $\tau \in [0, T]$:

$$\begin{aligned} & V_k^{N_{FX}}(\mathbf{Z}, \tau) \\ & = V_k^{N_{FX}}\left(\mathbf{Z}_{\{1\}}, \tau\right) + \sum_{j=2}^{d} \left(V_k^{N_{FX}}\left(\mathbf{Z}_{\{1,j\}}, \tau\right) - V_k^{N_{FX}}\left(\mathbf{Z}_{\{1\}}, \tau\right)\right) + \mathcal{O}\left(j\right). \end{aligned} \tag{4.21}$$

The intuitive explanation behind formula (4.21) is that the PCA1 solution $V_k^{N_{FX}}\left(\mathbf{Z}_{\{1\}}, \tau\right)$ is corrected for additional variance seperately captured by the other principal components.

Chapter 5

Numerical valuation techniques

5.1 Monte Carlo simulation

5.1.1 Monte Carlo for the BSHW model under the $\mathbb{Q}$-measure

Under the model (3.8) the time-zero price of European-style single FX options (2.3) can be approximated using Monte Carlo. The Euler scheme for the BSHW model under the domestic risk-neutral measure $\mathbb{Q}$ equals

$$\begin{aligned} Y^{df}(t+\Delta t) &= Y^{df}(t) + \left[r_d(t) - r_f(t) - \frac{1}{2}\sigma^2\right]\Delta t + \sigma\sqrt{\Delta t}Z_1, \\ r_d(t+\Delta t) &= r_d(t) + \lambda_d\left(\theta_d(t) - r_d(t)\right)\Delta t + \sigma_d\sqrt{\Delta t}Z_2, \\ r_f(t+\Delta t) &= r_f(t) + \left(\lambda_f\left(\theta_f(t) - r_f(t)\right) - \rho_{S^{df}r_f}\sigma\sigma_f\right)\Delta t + \sigma_f\sqrt{\Delta t}Z_3, \end{aligned} \tag{5.1}$$

with Z_1, Z_2, Z_3 correlated standard normal distributed sample values and $Y^{df}(t) = \log\left(S^{df}(t)\right)$. The step size for the time interval $[0,T]$ equals $\Delta t = \frac{T}{N}$. The Monte Carlo scheme (5.1) can be written in the following form:

$$\begin{aligned} \begin{pmatrix} Y^{df}(t+\Delta t) \\ r_d(t+\Delta t) \\ r_f(t+\Delta t) \end{pmatrix} &= \begin{pmatrix} 1 & \Delta t & -\Delta t \\ 0 & 1-\lambda_d\Delta t & 0 \\ 0 & 0 & 1-\lambda_f\Delta t \end{pmatrix}\begin{pmatrix} Y^{df}(t) \\ r_d(t) \\ r_f(t) \end{pmatrix} \\ &+ \Delta t\begin{pmatrix} -\frac{1}{2}\sigma^2 \\ \lambda_d\theta_d(t) \\ \lambda_f\theta_f(t) - \rho_{S^{df}r_f}\sigma\sigma_f \end{pmatrix} + \sqrt{\Delta t}\begin{pmatrix} \sigma & 0 & 0 \\ 0 & \sigma_d & 0 \\ 0 & 0 & \sigma_f \end{pmatrix}\begin{pmatrix} Z_1 \\ Z_2 \\ Z_3 \end{pmatrix}. \end{aligned} \tag{5.2}$$

The Monte Carlo approximation of the time-zero price of the European-style FX option of type $k = 1, 2, 3$ (2.3) with a single underlying FX rate is given

by

$$\Pi_k^{MC}(0) = \frac{1}{M}\sum_{i=1}^{M} e^{-\Delta t\sum_{j=0}^{N-1} r_d^i(j\Delta t)} f_k\left(e^{Y^{df,i}(T)}\right). \tag{5.3}$$

Here M denotes the number of Monte Carlo estimates and $r_d^i(t)$ and $Y^{df,i}(t)$ denote the i-th Monte Carlo estimate of the domestic interest rate and log FX rate at time t, respectively. Note that the Euler scheme could also have been applied to the one-dimensional BSHW model (3.39) under the $\mathbb{Q}_T$-measure. In chapter 6 the consistency of the analytical expressions for European-style single FX options under the $\mathbb{Q}_T$-measure will be checked. This is done by comparing to numerical results obtained using the above Euler scheme for the BSHW model under the $\mathbb{Q}$-measure.

5.1.2 Monte Carlo for the M-BSHW model under the $\mathbb{Q}_T$-measure

The European-style FX basket option price (2.4) can be approximated by the Monte Carlo method applied to the BSHW model for log forward FX rates (3.36). Applying the Euler scheme to (3.39), while incorporating the specific Brownian motions as in (3.36) yields

$$\begin{pmatrix} \log\left(F^{d1}(t+\Delta t)\right) \\ \vdots \\ \log\left(F^{dN_{FX}}(t+\Delta t)\right) \end{pmatrix} = -\frac{1}{2}\Delta t \begin{pmatrix} \omega_{11}(t,T) \\ \vdots \\ \omega_{N_{FX}N_{FX}}(t,T) \end{pmatrix} + \sqrt{\Delta t}$$
$$\times \begin{pmatrix} \sigma_1 & & 0 & -\sigma_d A_d(t,T) & \sigma_{f,1}A_{f,1}(t,T) & & 0 \\ & \ddots & & \vdots & & \ddots & \\ 0 & & \sigma_{N_{FX}} & -\sigma_d A_d(t,T) & 0 & & \sigma_{f,N_{FX}}A_{f,N_{FX}}(t,T) \end{pmatrix}$$
$$\times \begin{pmatrix} Z_{S^{d1}} \\ \vdots \\ Z_{S^{dN_{FX}}} \\ Z_{r_d} \\ Z_{r_{f,1}} \\ \vdots \\ Z_{r_{f,N_{FX}}} \end{pmatrix}, \tag{5.4}$$

with $Z_{S^{d1}}, \ldots, Z_{S^{dN_{FX}}}, Z_{r_d}, Z_{r_{f,1}}, \ldots, Z_{r_{f,N_{FX}}}$ correlated standard normal distributed sample values. The Monte Carlo approximation of the time-zero

price (2.4) of the FX basket option of type $k = 1, 2$ (2.2) equals

$$\Pi_k^{MC}(0) = P_d(0,T)\frac{1}{M}\sum_{j=1}^{M} f_k\left(\left(F^{di,j}(T)\right)_{i\leq N_{FX}}\right),$$

with M denoting the number of Monte Carlo estimates and $F^{di,j}(T)$ denoting the j-th Monte Carlo estimate of the i-th forward FX rate at time T.

5.2 Finite differences

The principal components-based reduced European-style FX basket option pricing problem (4.18) can be solved by finite differences. The finite difference grid is taken as $[0,T] \times \left[z_{\alpha(1)}^{\min}, z_{\alpha(1)}^{\max}\right]$ for 1 spatial dimension and $[0,T] \times \left[z_{\alpha(1)}^{\min}, z_{\alpha(1)}^{\max}\right] \times \left[z_{\alpha(2)}^{\min}, z_{\alpha(2)}^{\max}\right]$ for 2 spatial dimensions. Furthermore

$$\begin{aligned}\frac{T}{N} &= \Delta t,\\ \frac{z_{\alpha(1)}^{\max} - z_{\alpha(1)}^{\min}}{M_{\alpha(1)}} &= \Delta z_{\alpha(1)},\\ \frac{z_{\alpha(2)}^{\max} - z_{\alpha(2)}^{\min}}{M_{\alpha(2)}} &= \Delta z_{\alpha(2)}.\end{aligned}$$

The grid boundaries are chosen as

$$\left[z_{\alpha(i)}^{\min}, z_{\alpha(i)}^{\max}\right] = \left[\overline{z}_{\alpha(i)} - \kappa\sigma_{z_{\alpha(i)}}, \overline{z}_{\alpha(i)} + \kappa\sigma_{z_{\alpha(i)}}\right], \qquad i \leq N_{FX},$$

with the bar in $\overline{z}_{\alpha(i)}$ indicating the average value[1]. Furthermore from (4.9) one has $\sigma_{z_{\alpha(i)}} = \sqrt{\lambda_i}$. In this research I use $\kappa = 10$ in order to ensure convergence of the PCA method. As λ_i is time-dependent, the maximum over the interval $[0,T]$ is chosen.

In order to discretize (4.18) for 1 and 2 spatial dimensions the derivatives of the eigenvector coefficients of the covariance matrix, $\frac{\partial q_{ml}(T-\tau)}{\partial \tau}$ for $m, l \leq N_{FX}$

[1]The problem is that one has to deal with the time-dependence of the expectation of the principal components. Therefore I use a more efficient and adapted version of the principal components $\mathbf{Z}$ (4.7): $\mathbf{Z}' = \mathbf{Z} - \mathbb{E}[\mathbf{Z}]$. As $\mathbb{E}[\mathbf{Z}] = \mathbf{Q}^\top \mathbb{E}[\mathbf{Y}]$, the change from $\mathbf{Z}$ to $\mathbf{Z}'$ implies a change of the function $\mathbf{B}$.

and $\tau \in [0, T]$, have to be discretized. This is done as follows:

$$\left(\frac{\partial q_{ij}(T-\tau)}{\partial \tau}\right)^n = \frac{q_{ij}(T - n\Delta t) - q_{ij}(T - (n-1)\Delta t)}{\Delta t}, \qquad i, j \leq N_{FX}, \tag{5.5}$$

with the superscript at the left hand side of (5.5) denoting the discretization at time $T - n\Delta t$, $1 \leq n \leq N$. Using (5.5), the following discretizations of

(4.18) for 1 and 2 spatial dimensions[2] are used:

$$
\begin{aligned}
&\frac{v_i^n - v_i^{n-1}}{\Delta t} \\
&= \frac{1}{2}\lambda_{\alpha(1)}(T-n\Delta t)\frac{v_{i+1}^n - 2v_i^n + v_{i-1}^n}{\left(\Delta z_{\alpha(1)}\right)^2} + \frac{v_{i+1}^n - v_i^n}{\Delta z_{\alpha(1)}} \\
&\times \sum_{m=1}^{N_{FX}} \frac{q_{m\alpha(1)}(T-(n-1)\Delta t) - q_{m\alpha(1)}(T-n\Delta t)}{\Delta t} \\
&\times \left[\sum_{j\in\alpha} q_{mj}(T-n\Delta t)z_{j,i} + \sum_{j\notin\alpha} q_{mj}(T-n\Delta t)\mathbb{E}\left[Z_j(T-n\Delta t)\right]\right], \\
&\frac{v_{i,j}^n - v_{i,j}^{n-1}}{\Delta t} \\
&= \frac{1}{2}\lambda_{\alpha(1)}(T-n\Delta t)\frac{v_{(j-1)(M_{\alpha(1)}+1)+i+1}^n - 2v_{(j-1)(M_{\alpha(1)}+1)+i}^n + v_{(j-1)(M_{\alpha(1)}+1)+i-1}^n}{\left(\Delta z_{\alpha(1)}\right)^2} \\
&+ \frac{v_{(j-1)(M_{\alpha(1)}+1)+i+1}^n - v_{(j-1)(M_{\alpha(1)}+1)+i}^n}{\Delta z_{\alpha(1)}} \\
&\times \sum_{m=1}^{N_{FX}} \frac{q_{m\alpha(1)}(T-(n-1)\Delta t) - q_{m\alpha(1)}(T-n\Delta t)}{\Delta t} \\
&\times \left[\sum_{k\in\alpha} q_{mk}(T-n\Delta t)z_{k,(j-1)(M_{\alpha(1)}+1)+i} + \sum_{k\notin\alpha} q_{mk}(T-n\Delta t)\mathbb{E}\left[Z_k(T-n\Delta t)\right]\right] \\
&+ \frac{1}{2}\lambda_{\alpha(2)}(T-n\Delta t)\frac{v_{j(M_{\alpha(1)}+1)+i}^n - 2v_{(j-1)(M_{\alpha(1)}+1)+i}^n + v_{(j-2)(M_{\alpha(1)}+1)+i}^n}{\left(\Delta z_{\alpha(2)}\right)^2} \\
&+ \frac{v_{j(M_{\alpha(1)}+1)+i}^n - v_{(j-1)(M_{\alpha(1)}+1)+i}^n}{\Delta z_{\alpha(2)}} \\
&\times \sum_{m=1}^{N_{FX}} \frac{q_{m\alpha(2)}(T-(n-1)\Delta t) - q_{m\alpha(2)}(T-n\Delta t)}{\Delta t} \\
&\times \left[\sum_{k\in\alpha} q_{mk}(T-n\Delta t)z_{k,(j-1)(M_{\alpha(1)}+1)+i} + \sum_{k\notin\alpha} q_{mk}(T-n\Delta t)\mathbb{E}\left[Z_k(T-n\Delta t)\right]\right].
\end{aligned}
\tag{5.6}
$$

[2]In order to accomplish efficiency in the finite difference method, I consider an adapted version of the principal components $\mathbf{Z}$ (4.7): $\mathbf{Z}' = \mathbf{Z} - \mathbb{E}[\mathbf{Z}]$. As $\mathbb{E}[\mathbf{Z}] = \mathbf{Q}^T\mathbb{E}[\mathbf{Y}]$, the change from $\mathbf{Z}$ to $\mathbf{Z}'$ implies a change of the function $\mathbf{B}$.

These discretizations are backward in time and centered in space, and $n = 1, \ldots, N$, $i = 1, \ldots, M_{\alpha(1)} + 1$ and $j = 1, \ldots, M_{\alpha(2)} + 1$. For the case of 2 spatial dimensions a lexicographic ordering is used[3]. As a boundary condition, the second derivatives in spatial direction are set equal to zero on the grid boundaries. Three implemented finite difference schemes are discussed below.

5.2.1 The BTCS scheme

Writing (5.6) in matrix form, the backward time centered space (BTCS) scheme becomes

$$\frac{\mathbf{v}^n - \mathbf{v}^{n-1}}{\Delta t} = F\left(t_n, \mathbf{v}^n\right) = \mathbf{B}(t_n)\mathbf{v}^n. \tag{5.7}$$

In the case of 2 spatial dimensions, $F = F_1 + F_2$ with correspondingly $\mathbf{B} = \mathbf{B}_1 + \mathbf{B}_2$. Here the subscripts indicate the dimension.

5.2.2 The Crank-Nicolson scheme

The Crank-Nicolson scheme is given by

$$\frac{\mathbf{v}^n - \mathbf{v}^{n-1}}{\Delta t} = \frac{1}{2}F\left(t_n, \mathbf{v}^n\right) + \frac{1}{2}F\left(t_{n-1}, \mathbf{v}^{n-1}\right). \tag{5.8}$$

5.2.3 The Hundsdorfer-Verwer scheme

The BTCS and Crank-Nicolson schemes are unconditionally stable for several PDEs. The disadvantage of the BTCS and Crank-Nicolson schemes is that it requires the calculation of an inverse matrix every time step, which can be very time costly. Therefore in this thesis I use the so-called Hundsdorfer-Verwer (HV) scheme, which is a splitting scheme of the alternating direction implicit (ADI) type. With the HV method, the splitting of the operator F into operators for each spatial dimension (see (5.7) and (5.8) for 2 spatial dimensions) is used to reduce the complexity of the calculation of the inverse. For extensive information on the HV scheme the reader is referred to e.g., In 't Hout and Foulon (2010).

[3]Lakoba (2016) was used as main source for the implementation of the 2-dimensional finite difference method.

Chapter 6

Numerical results

This chapter gives numerical results for the application of the PCA dimension reduction method for the M-BSHW model, as described in chapter 4, to FX basket option pricing. Three case studies are considered, with low correlation, moderate correlation and high correlation amongst the underlying currencies, respectively. Using market data from 31 August 2016, the BSHW model is calibrated for 27 currencies, including emerging market currencies[1], non-emerging market currencies and Asian and Middle Eastern currencies. The currency EUR is taken as the domestic currency. The foreign currencies for the three case studies are determined as follows:

- Case study 1: 5- and 10-dimensional FX basket option on the 5 and 10 most traded[2] currencies against the euro, respectively. The foreign currencies for the 5-dimensional FX basket option are CHF (Switzerland Franc), GBP (British Pound), JPY (Japan Yen), SEK (Sweden Krona) and USD (United States Dollar). For the 10-dimensional FX basket, additionally the currencies AUD (Australian Dollar), CAD (Canadian Dollar), DKK (Danisk Krone), NOK (Norwegian Krone) and PLN (Polish Zloty) are considered. The 10 currencies have a low correlation, with an average (absolute) correlation coefficient equal to 26.23% (see table 6.1.

- Case study 2: 5- and 10-dimensional FX basket option on emerging market currencies and Asian and Middle Eastern currencies. For the 5-dimensional FX basket option pricing, the foreign currencies IDR (Indonesia Rupiah), INR (Indian Rupee), KRW (South Korean Won),

[1]Emerging market currencies are currencies in emerging markets, developing countries that have some characteristics of a developed market, but where transitions in several dimensions take place. Examples of emerging markets are Brazil, Mexico and Turkey.

[2]Based on April 2016 turnover, see [1]

MYR (Malaysian Ringgit) and PHP (Philippine Peso) are included. For the 10-dimensional FX basket option pricing, additionally the currencies CNH (Chinese offshore Yuan), ILS (Israeli Shekel), MXN (Mexican Peso), TRY (Turkish Lira) and ZAR (South African Rand) are considered. The 10 currencies are moderately correlated, with an average (absolute) correlation coefficient equal to 60.63%, see table 6.1.

- Case study 3: 5- and 10-dimensional FX basket option on Asian and Middle Eastern currencies (both emerging and non-emerging market currencies). For the 5-dimensional FX basket, the foreign currencies AED (United Arab Emirates Dirham), CNH (Chinese offshore Yuan), CNY (Chinese Yuan), HKD (Hong Kong Dollar) and SAR (Saudi Arabian Riyal) are considered. For the 10-dimensional FX basket, additionally the currencies INR (India Rupee), PHP (Philippine Peso), SGD (Singapore Dollar), THB (Thai Baht) and TWD (Taiwan Dollar) are considered. The 10 currencies are highly correlated, with an average (absolute) correlation coefficient equal to 87.98%, see table 6.1.

	Case study 1	Case study 2	Case study 3
log FX rates	26.23%	60.63%	87.98%
log FX rate - short rate	14.46%	9.93%	11.42%
short rates	45.72%	17.81%	20.52%

Table 6.1: Average (absolute) correlation coefficient values for the 10-dimensional M-BSHW model components, for each of the three case studies.

In the sections below, the calibration scheme and calibration results are discussed, before numerical results for single FX option prices are briefly addressed. Furthermore the convergence of the PCA1 and PCA2 method is assessed on a 1- and 2-dimensional FX basket option, respectively. Finally the last sections are devoted to the performance and accuracy of the PCA1 and PCA2 method in 5- and 10-dimensional FX basket option pricing, for the three case studies introduced above.

6.1 Calibration of the M-BSHW model

6.1.1 Calibration scheme

Theoretically, all the parameters of the M-BSHW model could be calibrated to basket option market data at once. In this research however, I calibrate

each BSHW model separately and estimate the correlations between the risk factors, using real market data. A four-step procedure is used:

- Fit the widely-used Nelson-Siegel-Svensson model (see e.g., Gilli, Große & Schuman, 2010) to the yield curves of each of the currencies (including the domestic currency EUR). Analytical expressions can now be derived for the initial term-structure of interest rates and the mean-reversion function $\theta(t)$. The Nelson-Siegel-Svensson model for the yield curve is characterized by the parameters β_1, β_2, β_3, β_4, λ_1 and λ_2 and is a function of maturity. The model, with $R(0,T)$ the zero rate and T the time to maturity, is given by

$$R(0,T) = \beta_1 + \beta_2 \left[\frac{1 - e^{-\frac{T}{\lambda_1}}}{\frac{T}{\lambda_1}} \right] + \beta_3 \left[\frac{1 - e^{-\frac{T}{\lambda_1}}}{\frac{T}{\lambda_1}} - e^{-\frac{T}{\lambda_1}} \right] + \beta_4 \left[\frac{1 - e^{-\frac{T}{\lambda_2}}}{\frac{T}{\lambda_2}} - e^{-\frac{T}{\lambda_2}} \right]. \tag{6.1}$$

  Often the constraints $\lambda_1, \lambda_2 > 0$ and $\beta_1 > 0$ and $\beta_1 + \beta_2 > 0$ are imposed for the parameter estimation procedure [18]. Because the data does not support these constraints, they will not be included in the calibration scheme used in this research.

- Calibrate the Hull-White interest rate models using market swaption prices. ATM market quotes on implied volatility of swaptions can be converted to swaption prices using the Black'76 model, see for example Brigo and Mercurio (2006). For each Hull-White model, the volatility parameter (σ) and mean reversion parameter (λ) can be fitted to market prices by minimizing the sum of squared residuals (SSE):

$$SSE = \min_{\sigma,\lambda} \sum_i \left[\text{Swaption}_{\text{Market}}(T_i) - \text{Swaption}_{\text{HW}}(T_i, \sigma, \lambda) \right]^2.$$

  Here $\text{Swaption}_{\text{Market}}$ and $\text{Swaption}_{\text{HW}}$ are the market-quoted swaption price and the Hull-White theoretical swaption price, respectively.

- Use historial time series data to estimate the correlation between the FX rates, the correlation between the FX rates and the interest rates, and the correlation between the interest rates.

- For each of the FX rates of the M-BSHW model, fit the volatility parameter of the BSHW model to European call option market prices. Use the ordinary Black-Scholes model with deterministic interest rates

(3.2) to convert the ATM market quotes on implied volatility to market prices. The volatility parameters are fitted by minimizing the SSE:

$$SSE = \min_{\sigma} \sum_{i} \left[\text{Call}_{\text{Market}}(T_i) - \text{Call}_{\text{BSHW}}(T_i, \sigma) \right]^2 .$$

Here $\text{Call}_{\text{Market}}$ and $\text{Call}_{\text{BSHW}}$ are the market-quoted call option price and the BSHW theoretical call option price, respectively. The expression 3.15 can be used to calculate $\text{Call}_{\text{BSHW}}(T_i, \sigma)$, using the estimates of the other model parameters obtained at previous calibration steps.

6.1.2 M-BSHW calibration results for 27 currencies

Front office quants at ING Financial Markets delivered yield curve data, historical correlations, estimated Hull-White parameters and spot FX rates. Furthermore ATM-forward volatility quotes on European call options with a single FX rate underlying[3][4] were delivered. The reference date is 31 August 2016[5]. In line with the ATM-forward quotation convention, the strike equals the forward FX rate: $K(T) = S^{df}(0)\frac{P_f(0,T)}{P_d(0,T)}$. The historical correlations are based on 3 years of weekly history[6], and the Hull-White model parameters are calibrated to the leading diagonal of the ATM swaption matrix[7][8].

Appendix C shows the calibration results for each of the 27 currencies, separately shown for each of the three case studies. The three correlation tables, each shown in two separate sub-tables, are positive semi-definite[9],

[3]For several currencies, ATM-forward volatility quotes on European call options were delivered for the reverse currency pairs. However, from (3.24) it is clear that within the M-BSHW model framework, the volatility parameter values of the original currency pair and the reverse currency pair are equal.

[4]Note that ATM-forward volatility quotes are sufficient for the purpose of calibrating the M-BSHW model. Other quotes, such as RR or STR quotes would be needed for incorporation of the volatility smile.

[5]Most quotes at ING Financial Markets are sourced in through Bloomberg.

[6]The quotes from Friday end-of-day are picked. In case Friday is a holiday then the last working day of the week is picked.

[7]The ATM swaption matrix is a matrix with swaption price quotes for different expiries and maturities. The strike equals the ATM strike.

[8]Note that the Hull-White parameter estimates are derived using the yield curve as input. The yield curve used by ING in their parameter estimation procedure might be slightly different from the yield curves I use in this research. The impact of this deviation, however, can be assumed to be negligible.

[9]A symmetric and real $m \times m$-matrix M is positive semi-definite if and only if $x^T M x \geq 0$ for every non-zero column vector $x \in \mathbb{R}^n$.

which excludes the possibility of negative variances. Furthermore, the average of the absolute value of the correlation coefficients between the FX rates increases per case study, as shwon in table 6.1. The Hull-White mean reversion level λ is between 0.01 and 0.08 for all FX rates, and the Hull-White volatility parameters vary between 0.366% and 4.274%, with most parameter values around 1%. For most FX rates, the BSHW volatility parameters are around 10%, with 3 outliers for the emerging market currencies MYR (13.527%), MXN (13.993%) and ZAR (18.922%). Concerning the Nelson-Siegel-Svensson model for the yield curves[10], using the relation $f(0,t) = -\frac{\partial \log P(0,t)}{\partial t}$ the expression for the forward rate yields:

$$f(0,T) = \beta_1 + \beta_2 e^{-\frac{T}{\lambda_1}} + \beta_3 \frac{T}{\lambda_1} e^{-\frac{T}{\lambda_1}} + \beta_4 \frac{T}{\lambda_2} e^{-\frac{T}{\lambda_2}}. \tag{6.2}$$

From $r(0) = f(0,0) = \beta_1 + \beta_2$ one can conclude that the initial short rate value is equal to the sum of the first two coefficients of the Nelson-Siegel-Svensson model. To prevent negative short rates, the conditions $\beta_1 > 0$ and $\beta_1 + \beta_2 > 0$ are often imposed for the estimation of the Nelson-Siegel-Svensson model. However, from the market data it is not trivial that there are non-negative short rates, therefore the above conditions are not taken into account in the estimation procedure. Indeed, from Appendix C it is clear that for CHF, DKK, EUR and SEK the time-zero short rates are slightly negative (all above -0.8%).

Figure 6.1 shows the yield curves and the fitted yield curves using the Nelson-Siegel-Svensson model[11], for the currencies in each of the three cases studies. Note that, except for the Chinese Yuan, yields are available up to 50 years, while single FX options are typically liquid for maturities up to 5 years. Although the fit of the Nelson-Siegel-Svensson model is not perfect, the stylized facts are well-captured, which is sufficient for the research purposes of this thesis.
Figure 6.1 also shows the calibrated probability density functions of the log-normal distributed forward FX rates, for each of the three case studies. The forward FX rates are normalized with respect to their initial value, so they are all centered around 1.

[10]The Nelson-Siegel-Svensson model for the yield curves was fitted using the R-function *Svensson*.

[11]For the Saudi Arabian Riyal (SAR) no yields were available, therefore the yields and corresponding Nelson-Siegel-Svensson model parameters for the United Arab Emirates Dirham (AED) were used.

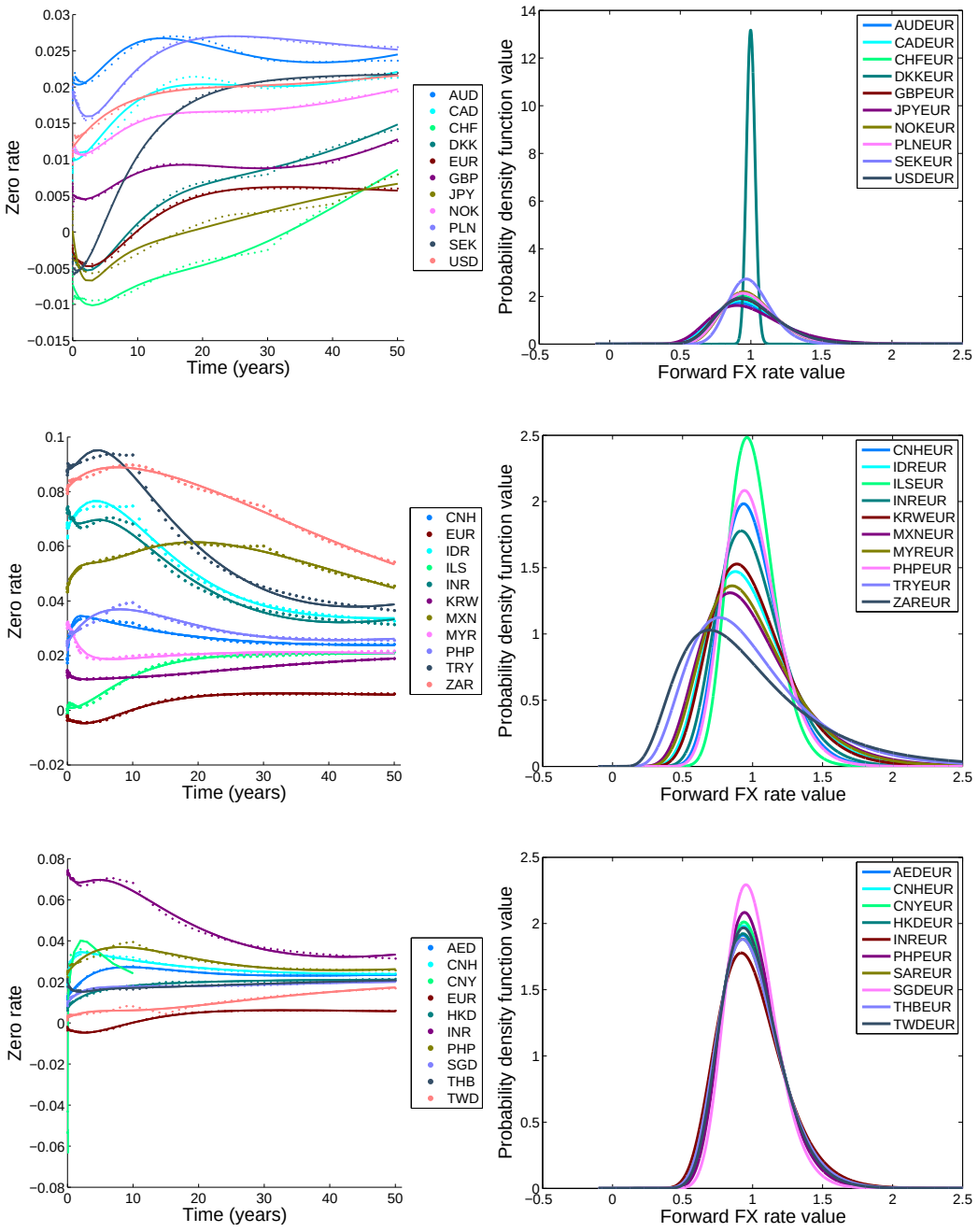

Figure 6.1: Calibrated market yield curves (left figures, dotted) and NSS model estimates (left figures, lines) and probability density functions of the forward FX rates (right figures) for the three case studies. In the right figures, the forward FX rates have been normalized with respect to their spot rate. Maturity is equal to 5 year. The reference date is August 31, 2016.

6.2 Numerical results for single FX options

In section 3.2.4 analytical formulas were derived for time-zero prices of call options and digital call options with a single FX rate underlying, under the BSHW model. These formulas were obtained by switching from the $\mathbb{Q}$- to the $\mathbb{Q}_T$-measure in the BSHW model. In this section the consistency of the analytical formulas (3.15) and (3.16) for the time-zero prices of single FX rate call and digital call options, respectively, under the BSHW model is investigated. Analytical values are compared to the prices calculated using formula (5.3) which uses the Monte Carlo scheme (5.2) for the BSHW model under the $\mathbb{Q}$-measure.

Table 6.2 shows time-zero prices for single FX rate call and digital call options approximated by the Monte Carlo scheme (5.2). These prices are compared to the prices derived using the analytical formulas (3.15) and (3.16). The calibrated parameter values are taken as input. The 10 most traded currencies against the euro are taken as foreign currency, and the strike is taken equal to the forward FX rate. Prices are shown for maturities equal to 6 months and 1, 3 and 5 years. For the Monte Carlo approach, 1.000.000 simulations and $100 \cdot T$ time steps were used.

Table 6.2 shows that the time-zero prices of the call options increase with maturity and that the time-zero prices of the digital call options decrease with maturity. The call option price increases with maturity as the FX rate value is more volatile for longer maturities. The digital call option price decreases with maturity as the forward FX rate has a (slightly) negative drift component (see (3.13)) and the option payoff is binary. The only exception is the digital call option on the DKKEUR rate, here the option price increases with maturity. This is because the discounting factor $P_d(0,T)$ is larger than 1 and increases with maturity, as the euro short rates can be negative. The fact that the discount factor increases with maturity outweighs the slightly negative drift component for the forward DKKEUR rate.

As to the Monte Carlo prices, for both the call and digital call option, and for all maturities and FX rates, the Monte Carlo prices are around the analytical price. For all cases, the analytical price is within a couple of standard deviations away from the Monte Carlo estimate. The standard error of the Monte Carlo estimate increases with maturity, especially for the call option prices. The call option prices, however, also increase with maturity, which largely offsets the increase in the Monte Carlo standard error. Obviously, more accurate and converging Monte Carlo estimates can be obtained by in-

creasing the number of time grid points in the Euler method and increasing the number of simulations.

		Maturity: 6M		Maturity: 1Y		Maturity: 3Y		Maturity: 5Y	
		Analytical price	Monte Carlo price (st. dev.)	Analytical price	Monte Carlo price (st. dev.)	Analytical price	Monte Carlo price (st. dev.)	Analytical price	Monte Carlo price (st. dev.)
Single FX call option	AUDEUR	0.021589	0.021532 (3.306486E-5)	0.030013	0.030013 (4.699730E-5)	0.048573	0.048627 (7.985513E-5)	0.058505	0.058467 (9.941042E-5)
	CADEUR	0.021196	0.021207 (3.250184E-5)	0.029553	0.029619 (4.624774E-5)	0.048261	0.048327 (7.906956E-5)	0.058465	0.058526 (9.845717E-5)
	CHFEUR	0.021773	0.021783 (3.302595E-5)	0.031248	0.031200 (4.804145E-5)	0.057600	0.057626 (9.260932E-5)	0.078958	0.078734 (1.308344E-4)
	DKKEUR	0.000339	0.000338 (4.975332E-7)	0.000493	0.000493 (7.250799E-7)	0.001032	0.001031 (1.516922E-6)	0.001656	0.001653 (2.430850E-6)
	GBPEUR	0.035053	0.035157 (5.371743E-5)	0.048938	0.048907 (7.623786E-5)	0.080840	0.080960 (1.316306E-4)	0.099820	0.099947 (1.674991E-4)
	JPYEUR	0.000296	0.000295 (4.558303E-7)	0.000418	0.000418 (6.585574E-7)	0.000726	0.000724 (1.209421E-6)	0.000936	0.000933 (1.625133E-6)
	NOKEUR	0.002744	0.002743 (4.172889E-6)	0.003825	0.003825 (5.902320E-6)	0.006256	0.006261 (1.002572E-5)	0.007623	0.007634 (1.251290E-5)
	PLNEUR	0.004826	0.004813 (7.271950E-6)	0.006855	0.006850 (1.048919E-5)	0.012219	0.012240 (1.942060E-5)	0.016273	0.016268 (2.655035E-5)
	SEKEUR	0.002061	0.002058 (3.102892E-6)	0.002906	0.002903 (4.426385E-6)	0.004950	0.004959 (7.747506E-6)	0.006213	0.006209 (9.854844E-6)
	USDEUR	0.025805	0.025804 (3.945866E-5)	0.035927	0.035975 (5.596835E-5)	0.058429	0.058355 (9.505163E-5)	0.070948	0.071241 (1.194991E-4)
Single FX digital call option	AUDEUR	0.484708	0.484505 (5.006414E-4)	0.479290	0.479737 (5.016237E-4)	0.468246	0.469187 (5.058582E-4)	0.460010	0.459307 (5.072564E-4)
	CADEUR	0.485323	0.485816 (5.007070E-4)	0.480200	0.481269 (5.017544E-4)	0.470148	0.470204 (5.063325E-4)	0.462967	0.463167 (5.085105E-4)
	CHFEUR	0.488992	0.489150 (5.008108E-4)	0.485038	0.484695 (5.019239E-4)	0.476104	0.475397 (5.067436E-4)	0.467564	0.467548 (5.088542E-4)
	DKKEUR	0.499629	0.499159 (5.008455E-4)	0.500236	0.499925 (5.018726E-4)	0.503311	0.503208 (5.052614E-4)	0.503404	0.502011 (5.053284E-4)
	GBPEUR	0.485970	0.485448 (5.006916E-4)	0.481143	0.481044 (5.017481E-4)	0.471893	0.471690 (5.065853E-4)	0.465206	0.465090 (5.092282E-4)
	JPYEUR	0.483860	0.483527 (5.007609E-4)	0.478035	0.477679 (5.019628E-4)	0.465657	0.464651 (5.076309E-4)	0.456132	0.455752 (5.112141E-4)
	NOKEUR	0.488069	0.488446 (5.007453E-4)	0.484064	0.483708 (5.017565E-4)	0.476713	0.477051 (5.062527E-4)	0.471234	0.471373 (5.081327E-4)
	PLNEUR	0.490259	0.490777 (5.007472E-4)	0.486813	0.485266 (5.016534E-4)	0.478811	0.479017 (5.054245E-4)	0.470122	0.469520 (5.057802E-4)
	SEKEUR	0.491094	0.490526 (5.007250E-4)	0.488265	0.488734 (5.017171E-4)	0.483460	0.483929 (5.055030E-4)	0.479237	0.478943 (5.061518E-4)
	USDEUR	0.486405	0.486141 (5.007636E-4)	0.481720	0.482082 (5.019280E-4)	0.472653	0.471883 (5.072612E-4)	0.465912	0.465307 (5.105240E-4)

Table 6.2: Single FX call option and single FX digital call option prices for maturities equal to 6 months, 1 year, 3 year and 5 year. The strike is taken equal to the forward FX rate. For the Monte Carlo price, 1.000.000 simulations and $100 \cdot T$ time steps were used.

6.3 Convergence of the PCA method

The convergence of the PCA1 and PCA2 method is assessed on a 5Y USD-EUR call option and a 5Y basket option on the currencies USD and GBP[12], each with weight $\frac{1}{2}$[13], respectively[14]. For both options the strike equals the forward FX (basket) rate. For the two options no truncation of the equation (4.18) is involved, the PCA method only involves a transformation of variables. To investigate convergence for the PCA1 method, the initial number of finite difference points in time- and space direction was set equal to 75 and 25, respectively. The absolute value of the relative error of the PCA1 method was calculated for 9 different step sizes for both time- and space direction, with a difference factor 2.

For the PCA2 method two spatial dimensions have to be discretized for finite differences, therefore compution time increases fastly with the number of finite difference points in spatial directions. Because the running time of the PCA2 method is much higher than the running time of the PCA1 method, less finite difference points were used to assess convergence of the PCA2 method. The following number of finite difference points in time- and space directions were used:

- for time direction: 20, 28, 40, 54, 76, 108, 150 (approximate difference factor: 1.4)[15].
- For space direction: 20, 26, 34, 44, 58, 74, 96 (approximate difference factor: 1.3)[15].

For the 5Y USD call option an analytical reference price (3.15) is available, which equals 0.070948. For the 5Y GBP USD basket call option the Monte Carlo method (5.4) is used to obtain a reference price. Using 10.000.000 simulations and 500 grid points in time direction, the Monte Carlo estimate equals 0.070758, with a standard error equal to $3.5983E-5$. The 99.7% confidence interval for the 5Y GBP USD basket option therefore equals $[0.070650, 0.070866]$.

[12]USD and GBP are the two most traded currencies against the euro, based on April 2016 turnover. See [1].

[13]Both FX rates are also normalized with respect to their spot rate.

[14]Most of the methods used to assess the convergence of the PCA1 and PCA2 method are based on methods used in Runborg (2012)

[15]Rounded to the nearest even number. Odd numbers are avoided because of interpolation errors in determining the time-zero price.

6.3.1 PCA1 convergence

Table 6.3 shows the absolute value of the relative errors of the PCA1 method for the 5Y USDEUR call option price, in percentages. The relative error is defined as the difference between the PCA1 solution and the analytical solution, divided by the analytical solution. From the results it is immediate that, compared to the time direction, much less finite difference grid points for the space direction are needed to ensure convergence at 1E-5 relative error margin. The tables in appendix D show that the PCA1 method has a rate of convergence 2 in time direction. Convergence rates are calculated using the formula $\left|\frac{\hat{v}_{2n}-\hat{v}_n}{\hat{v}_{4n}-\hat{v}_{2n}}\right|$, with $\hat{v}$ the PCA1 solution and n the number of grid points in either the time or space direction. The convergence rate in space direction is less trivial to derive due to the oscillating behavior. This is very likely because of the presence of the derivative with respect to time of the eigenvectors of the covariance matrix in the PDE equation (4.18). This derivative is approximated by a discrete derivative using the eigenvector coefficients at the finite difference time grid, which causes the oscillating convergence behavior. The oscillating behavior is almost identical for all grid step sizes for the time direction.

$n_t = 19200$	1.875466%	0.007047%	0.064626%	0.008106%	0.000825%	0.002417%	0.001298%	0.001066%	0.001032%
$n_t = 9600$	1.874471%	0.006023%	0.065652%	0.009131%	0.001849%	0.003441%	0.002322%	0.002090%	0.002056%
$n_t = 4800$	1.872482%	0.003975%	0.067702%	0.011179%	0.003897%	0.005489%	0.004370%	0.004138%	0.004104%
$n_t = 2400$	1.868503%	0.000120%	0.071804%	0.015275%	0.007993%	0.009584%	0.008466%	0.008234%	0.008200%
$n_t = 1200$	1.860547%	0.008310%	0.080007%	0.023467%	0.016183%	0.017775%	0.016657%	0.016424%	0.016390%
$n_t = 600$	1.844638%	0.024687%	0.096408%	0.039848%	0.032561%	0.034153%	0.033034%	0.032802%	0.032768%
$n_t = 300$	1.812835%	0.057427%	0.129198%	0.072595%	0.065303%	0.066897%	0.065777%	0.065544%	0.065510%
$n_t = 150$	1.749287%	0.122855%	0.194726%	0.138038%	0.130735%	0.132331%	0.131209%	0.130976%	0.130942%
$n_t = 75$	1.622424%	0.253499%	0.325572%	0.268713%	0.261387%	0.262988%	0.261863%	0.261629%	0.261595%
	$n_z = 25$	$n_z = 50$	$n_z = 100$	$n_z = 200$	$n_z = 400$	$n_z = 800$	$n_z = 1600$	$n_z = 3200$	$n_z = 6400$

Table 6.3: Absolute value of the relative error of the PCA1 method for a 5Y USDEUR call price, in percentages. The strike of the option equals the forward FX rate. The relative errors are calculated for different number of grid points in time and space direction for finite differences. The analytical solution is calculated using formula (3.15) and equals 0.070948.

6.3.2 PCA2 convergence

Table 6.4 shows the 5Y GBP USD basket call option prices estimated by the PCA2 method. Different number of grid points for the finite difference method are taken in time and spatial directions. Green-marked values are within the 99.7% confidence interval[16] of the option price. Except for the

[16]This corresponds to three standard deviations from the mean.

cases where the number of finite difference grid points is very small, many option prices estimated with the PCA2 method are within the 99.7% confidence interval. Note however that, although 10.000.000 Monte Carlo simulations were used, the confidence interval is still quite wide.

The results in table 6.4*a* and 6.4*b* show that the number of grid points for the first principal component (n_{z_1}) is very dominant in the convergence behavior of the PCA2 solution. From table 6.4*a* it is clear that only for $n_{z_1} = 74$ and $n_{z_1} = 96$ the PCA2 solution is within the 99.7% confidence interval generated by Monte Carlo simulations, independent of the choice for n_t. Furthermore table 6.4*b* shows that for n_{z_1} fixed and equal to 100, all PCA2 solutions are within the 99.7% confidence interval, for any choice of n_t and n_{z_2}. The only outliers are the solutions where $n_{z_2} = 74$. Finally, table 6.4*c* shows that only for values of n_{z_1} that are greater than or equal to 34, PCA2 solutions are within the 99.7% confidence interval. Although the value of n_{z_2} has impact on the PCA2 solution, for all values of n_{z_2} there are PCA2 solutions that are within the 99.7% confidence interval.

Tables $E.1a$ to $E.3b$ show the convergence rates for the PCA2 solution in time and space directions. Convergence rates are calculated using the formula $\frac{\hat{v}_{2n}-\hat{v}_n}{\hat{v}_{4n}-\hat{v}_{2n}}$, with $\hat{v}$ the PCA2 solution and n the number of grid points in either the time or one of the spatial directions. Table $E.1$ shows that, apart from some (very large) outliers for certain numbers of grid points, the convergence rate is around or slightly above 2. Tables $E.2a$ to $E.3b$ show very oscillating convergence rates in the direction of both principal components. Tables $E.2a$ and $E.3a$ show that the convergence rates in the direction of both principal components is almost insensitive to the number of grid points for time.

The observation that the number of grid points for the first principal component is very dominant in the convergence behavior of the PCA2 solution can be explained by the fact that the first principal component captures relatively a larger part of the total variable variance. The oscillating convergence behavior in the directions of both principal components is presumably caused by the presence of the derivative with respect to time of the eigenvectors of the covariance matrix in the PDE equation (4.18). This derivative is approximated by a discrete derivative using the eigenvector coefficients at the finite difference time grid, which causes the oscillating convergence behavior.

$n_t = 150$	0.069974	0.070411	0.070311	0.069256	0.069821	0.070676	0.070741
$n_t = 108$	0.069974	0.070411	0.070311	0.069256	0.069821	0.070676	0.070741
$n_t = 76$	0.069974	0.070411	0.070311	0.069257	0.069821	0.070676	0.070741
$n_t = 54$	0.069975	0.070412	0.070312	0.069258	0.069822	0.070676	0.070741
$n_t = 40$	0.069976	0.070412	0.070312	0.069260	0.069823	0.070677	0.070742
$n_t = 28$	0.069978	0.070415	0.070315	0.069264	0.069825	0.070680	0.070745
$n_t = 20$	0.069984	0.070420	0.070320	0.069270	0.069831	0.070685	0.070750
	$n_{z_1} = 20$	$n_{z_1} = 26$	$n_{z_1} = 34$	$n_{z_1} = 44$	$n_{z_1} = 58$	$n_{z_1} = 74$	$n_{z_1} = 96$

(a) $n_{z_2} = 100$.

$n_t = 150$	0.070777	0.070751	0.070763	0.070719	0.070684	0.070375	0.070749
$n_t = 108$	0.070777	0.070751	0.070763	0.070719	0.070684	0.070374	0.070749
$n_t = 76$	0.070777	0.070752	0.070763	0.070719	0.070684	0.070375	0.070749
$n_t = 54$	0.070777	0.070752	0.070764	0.070719	0.070684	0.070375	0.070749
$n_t = 40$	0.070778	0.070753	0.070765	0.070720	0.070685	0.070376	0.070750
$n_t = 28$	0.070781	0.070755	0.070767	0.070722	0.070688	0.070378	0.070753
$n_t = 20$	0.070786	0.070760	0.070773	0.070728	0.070693	0.070383	0.070758
	$n_{z_2} = 20$	$n_{z_2} = 26$	$n_{z_2} = 34$	$n_{z_2} = 44$	$n_{z_2} = 58$	$n_{z_2} = 74$	$n_{z_2} = 96$

(b) $n_{z_1} = 100$.

$n_{z_1} = 96$	0.070517	0.070238	0.070744	0.070747	0.070435	0.070617	0.070741
$n_{z_1} = 74$	0.070124	0.070727	0.070725	0.070541	0.070641	0.070715	0.070697
$n_{z_1} = 58$	0.070774	0.070758	0.070652	0.070558	0.070749	0.070737	0.070100
$n_{z_1} = 44$	0.070777	0.070632	0.070648	0.070759	0.070736	0.070041	0.069027
$n_{z_1} = 34$	0.070604	0.070558	0.070703	0.070687	0.069931	0.068919	0.070201
$n_{z_1} = 26$	0.070387	0.070506	0.070483	0.069842	0.068798	0.069994	0.070390
$n_{z_1} = 20$	0.070029	0.070008	0.069400	0.068182	0.069528	0.069895	0.069970
	$n_{z_2} = 20$	$n_{z_2} = 26$	$n_{z_2} = 34$	$n_{z_2} = 44$	$n_{z_2} = 58$	$n_{z_2} = 74$	$n_{z_2} = 96$

(c) $n_t = 100$.

Table 6.4: 5Y GBP USD basket call option prices, for different number of grid points for time and space directions for finite differences, calculated using the PCA2 method. The strike equals the basket forward rate. The reference solution is calculated using 10.000.000 Monte Carlo simulations and 500 grid points in time direction. The 99.7% confidence interval for the 5Y GBP USD basket option equals $[0.070650, 0.070866]$. Green-marked values are within this 99.7% confidence interval.

6.4 5-dimensional FX basket call option

Figure 6.2 shows the percentage of total variance captured by each of the principal components under the calibrated 5-dimensional M-BSHW model for log forward rates, for each of the three case studies. The results are very similar in case of $T = 1$ and $T = 3$ and therefore only results for $T = 5$ are included. Additionally, table 6.5 gives an overview of the cumulative percentage of variance captured by the principal components specifically at $t = 0, 2.5, 5$ for the $T = 5$ European-style FX basket option.

The figures show that the part of total variance captured by the principal components significantly depends on the correlation structure between the log FX rates. For case study 1, the first principal component captures slightly below 48% of total variance, while the first two principal components together capture around 70% of total variance. For case study 3 the first principal component captures approximately 80% ($t = 0$) to more than 95% ($t = 5$) of total variance. The four remaining principal components all capture less than 10% of total variance.

The large difference in variance captured by the first or first two principal components between the case studies is the direct consequence of the different correlation structure. Average correlation between the log FX rates equals 26.23%, 60.63% and 87.98% for case study 1, 2 and 3, respectively, see table 6.1. The correlations between the FX rates and Hull-White interest rates, and the correlations between the interest rates have a much smaller impact on the variance captured by the principal components. This is because the Hull-White volatility parameter values are very small compared to the BSHW volatility paramter values, see tables $C.3$, $C.6$ and $C.9$.

	t = 0			**t = 2.5**			**t = 5**		
# PC	**Case study 1**	**Case study 2**	**Case study 3**	**Case study 1**	**Case study 2**	**Case study 3**	**Case study 1**	**Case study 2**	**Case study 3**
1	47.28 %	71.94 %	80.46 %	47.24 %	75.09 %	91.67 %	47.92 %	76.89 %	97.07 %
2	67.78 %	81.45 %	87.82 %	68.41 %	83.73 %	95.62 %	70.99 %	86.33 %	99.55 %
3	85.00 %	89.45 %	94.25 %	84.14 %	92.16 %	97.73 %	83.57 %	93.79 %	99.96 %
4	93.07 %	95.92 %	97.48 %	92.58 %	97.74 %	99.01 %	92.18 %	98.76 %	100.00 %
5	100.00 %	100.00 %	100.00 %	10.000 %	100.00 %	100.00 %	100.00 %	100.00 %	100.00 %

Table 6.5: Cumulative percentage of variance captured by principal components, for the 5-dimensional FX basket option pricing problem, $T = 5$.

Figure 6.3 depicts the coefficient values of the five log forward rates for

the first two principal components, for each of the three case studies. The ordering in absolute coefficient size for the first principal component is, with one or two exceptions, in line with the ordering in BSHW volatility, see tables $C.3$, $C.6$ and $C.9$. FX rates with a higher BSHW volatility parameter value have a higher (absolute value of the) coefficient value. The coefficient values of the second principal components have not a direct relation with the BSHW model parameter values, but in general the coefficient values fluctuate more over time. This behaviour can be generalized: the coefficient values of higher principal components (i.e. principal components with a small variance compared to other principal components) fluctuate more over time. For some principal components there are even significant jumps in coefficient value, for a certain point in time. This makes it difficult to ensure convergence for PCA2 solutions based on these principal components. A large number of time points are needed to approximate the discretization (5.5) accurately for these particular points in time.

Table 6.6 shows the option price estimates obtained by the PCA1 method, the PCA2(1,2) method and the asymptotic expansion method for case studies 1,2 and 3, respectively. For the PCA1 method, 5.000 grid points for time direction and 5.000 grid points for space direction are taken. For the PCA2(1,2) method, 300 grid points for time direction and 75 grid points for space directions are taken[17]. An exception is case study 1, here 100 grid points are used for both time and space directions. This is chosen because the coefficients values of the principal components fluctuate much more over time for case studies 2 and 3. More grid points in time direction will ensure better approximations of the derivative of the coefficient values of the principal components in (4.18).

The reference solution is given by the Monte Carlo method (5.4), with 10.000.000 simulations and $100 \cdot T$ time points. The relative error of the PCA methods with respect to the reference solution is given in parantheses. For case study 3, the coefficient values of a few higher-order principal components are oscillating over time. Therefore many time points in the finite difference method for the scheme (5.6) are needed in order to approximate the derivative of the principal component coefficient value with respect to time. For the number of time points I used, the finite difference method yields inaccurate results, therefore the asymptotic expansion values for case study 3 are not included in the overview.

[17]For case study 3, 76 grid points for space directions were taken because it was discovered that for an even number of grid points interpolation errors could occur.

Table 6.6 shows that for the three case studies, FX basket call option prices are higher for higher correlations and higher volatility parameters. The FX basket call option prices shown in table 6.6 are lowest for case study 1 and highest for case study 2. This can be explained as, although average correlation is lowest for case study 1 and highest for case study 3, the average BSHW volatility parameter value is highest for case study 2 and lowest for case study 1.
Furthermore the results show that the option prices increase with maturity. This is because the underlying is more volatile for longer maturities.

The results in table 6.6 show three clear trends. The first is that the relative error of the PCA1 and PCA2(1,2) solution is largest for case study 1 and smallest for case study 3. This is directly attributable to the average correlation value between the FX rates, which is lowest for case study 1 and highest for case study 3, see table 6.1. The relative errors are larger for higher maturities, this is because the FX basket option underlying is more volatile for higher maturities.

The second trend is that the relative error of the PCA2(1,2) solution is almost always lower than the relative error of the PCA1 solution. This is in line with expectations as the PCA2(1,2) method includes the second principal component in the FX basket option pricing problem. By including the second principal component in the FX basket option pricing problem, a larger part of the total variance captured by all variables is included in the pricing problem.

The third trend is that the asymptotic solution does not always give more accurate results than the PCA2(1,2) solution. For case study 1, the asymptotic solution yields very accurate results. For all maturities, the relative error is below or slightly above 1%, and increases with maturity, as expected. For the other two case studies, the asymptotic solution yields less accurate results. For case study 2, the relative error of the asymptotic expansion solution is largest for the short maturity ($T = 1$), which is not in line with expectations. For case study 3, for the number of grid points I used, no converging results were obtained. The less accurate results for the asymptotic expansion for case studies 2 and 3 is due to the oscillating behavior and/or the sudden jumps of the coefficient values of the principal components. As a consequence, many time points in the finite difference method for the scheme (5.6) are needed in order to accurately approximate the derivative of the principal component coefficient value with respect to the time. Recommendations for future research concerning this finding are reported in chapter 7.

	Case study	MC price (standard deviation)	PCA1 (relative error)	PCA2(1,2) (relative error)	Asymptotic expansion (relative error)
T=1	Case study 1	0.025244 (1.212308E-5)	0.023338 (-7.5514%)	0.023921 (-5.2439%)	0.025104 (-0.5565%)
	Case study 2	0.038409 (1.883081E-5)	0.037615 (-2.0656%)	0.038247 (-0.4201%)	0.039667 (3.2769%)
	Case study 3	0.037181 (1.812875E-5)	0.037083 (-0.2640%)	0.037013 (-0.4520%)	- (-%)
T=3	Case study 1	0.043124 (2.110405E-5)	0.038056 (-11.7513%)	0.039547 (-8.2946%)	0.042855 (-0.6232%)
	Case study 2	0.062234 (3.168524E-5)	0.059704 (-4.0652%)	0.060359 (-3.0123%)	0.062147 (-0.1409%)
	Case study 3	0.059390 (2.985934E-5)	0.058991 (-0.6722%)	0.059204 (-0.3135%)	- (-%)
T=5	Case study 1	0.054898 (2.730942E-5)	0.046873 (-14.6179%)	0.049032 (-10.6851%)	0.054327 (-1.0397%)
	Case study 2	0.075515 (3.971716E-5)	0.071331 (-5.5408%)	0.071992 (-4.6652%)	0.074509 (-1.3317%)
	Case study 3	0.071508 (3.673465E-5)	0.070456 (-1.4708%)	0.070785 (-1.0112%)	- (-%)

Table 6.6: 5-dimensional FX basket call option price estimates for case studies 1, 2 and 3. The absolute values of the relative error of the PCA1 and PCA2(1,2) method are given. The basket weights are equal to $\frac{1}{5}$ and, furthermore, the FX rates have been normalized with respect to their spot rate. The strike equals the forward FX basket rate. Computation time equals approximately 20, 60 and 90 minutes for the Monte Carlo estimate, for $T = 1$, $T = 3$ and $T = 5$, respectively. Computation time equals approximately 20 minutes for the PCA1 and approximately 20 minutes for the PCA2 estimate.

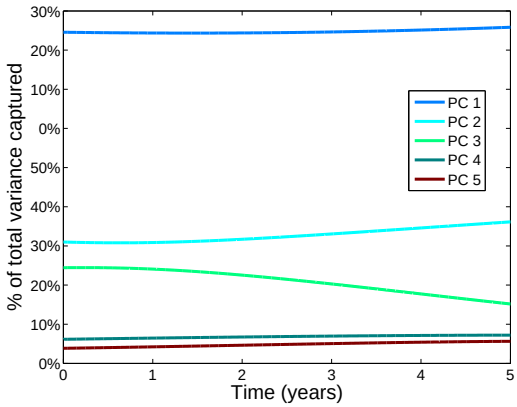

(a) Case study 1.

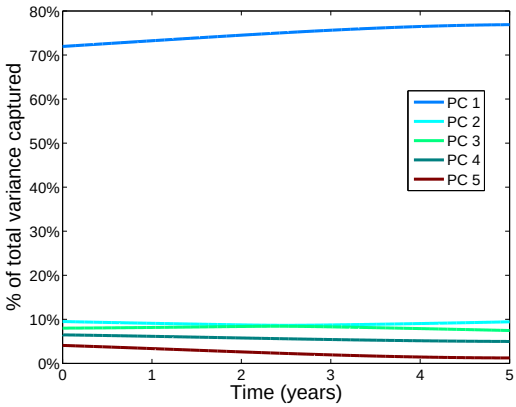

(b) Case study 2.

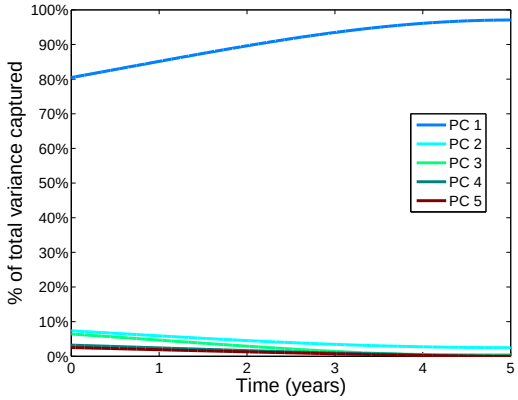

(c) Case study 3.

Figure 6.2: Part of total variable variance explained by each of the principle components of the 5-dimensional M-BSHW model, for each of the three case studies. The foreign currencies are CHF, GBP, JPY, SEK and USD for case study 1, IDR, INR, KRW, MYR and PHP for case study 2 and AED, CNH, CNY, HKD and SAR for case study 3. Maturity equals $T = 5$.

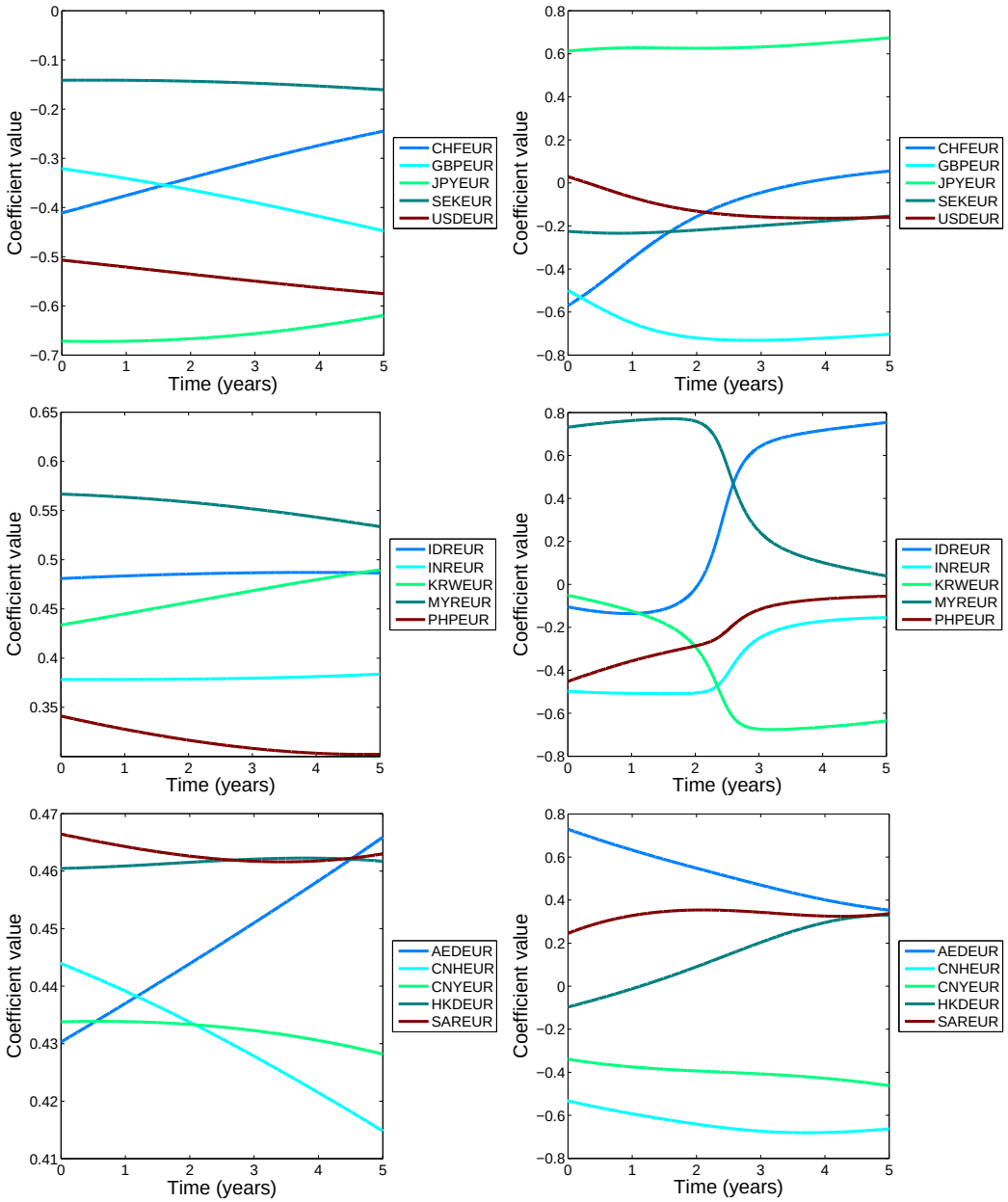

Figure 6.3: Coefficient values of the first (left figures) and second principal components (right figures) of the 5-dimensional M-BSHW model. Case study 1 figures are shown at the top, case study 2 figures on the middle and case study 3 figures on the bottom. The FX rates for each case study are shown in the legends. Maturity equals $T = 5$.

6.5 10-dimensional FX basket call option

Figure 6.4 shows the percentage of total variance captured by each of the principal components under the calibrated 10-dimensional M-BSHW model for log forward rates, for each of the three case studies. The results are very similar in case of $T = 1$ and $T = 3$ and are therefore not included. Additionally, table 6.7 gives an overview of the cumulative percentage of variance captured by the principal components at $t = 0, 2.5, 5$ for the $T = 5$ European-style FX basket option.

Similar to the case of the 5-dimensional FX basket call option, the part of total variance captured by the principal components depends on the correlation values between the log FX rates. For case study 1, the first principal component captures around 40% of total variance, depending on time t. The first two principal components together capture around 60% of total variance. For case study 3 the first principal component captures between approximately 70% ($t = 0$) and 90% ($t = 5$) of total variance. The four remaining principal components all capture less than 10% of total variance. The large difference in variance captured by the first or first two principal components between the case studies is, similarly to previous section, the direct consequence of the different correlation structure. Average correlation between the log FX rates equals 26.23%, 60.63% and 87.98% for case study 1, 2 and 3, respectively, see table 6.1. The correlations between the FX rates and Hull-White interest rates, and the correlations between the interest rates have a much smaller impact on the variance captured by the principal components.

	t = 0			**t = 2.5**			**t = 5**		
# PC	**Case study 1**	**Case study 2**	**Case study 3**	**Case study 1**	**Case study 2**	**Case study 3**	**Case study 1**	**Case study 2**	**Case study 3**
1	38.98 %	56.4 %	72.55 %	41.38 %	59.47 %	82.9 %	44.12 %	64.29 %	89.82 %
2	57.02 %	72.75 %	80.38 %	58.67 %	74.74 %	88.58 %	60.66 %	78.25 %	93.47 %
3	68.00 %	83.63 %	85.19 %	68.38 %	83.57 %	91.67 %	70.32 %	83.44 %	95.60 %
4	78.47 %	88.66 %	88.93 %	77.67 %	88.31 %	94.08 %	77.94 %	87.42 %	97.29 %
5	85.64 %	91.96 %	92.27 %	84.71 %	91.81 %	95.86 %	84.24 %	91.06 %	98.31 %
6	90.16 %	94.30 %	95.14 %	89.56 %	94.73 %	97.17 %	89.21 %	94.44 %	99.07 %
7	94.04 %	96.42 %	96.76 %	93.66 %	96.84 %	98.18 %	93.34 %	96.85 %	99.77 %
8	97.35 %	97.87 %	98.14 %	97.32 %	98.1 %	99.03 %	97.18 %	98.55 %	99.98 %
9	99.57 %	98.96 %	99.11 %	99.81 %	99.18 %	99.61 %	99.92 %	99.54 %	100.00 %
10	100.00 %	100.00 %	100.00 %	100.00 %	100.00 %	100.00 %	100.00 %	100.00 %	100.00 %

Table 6.7: Cumulative percentage of variance captured by the principal components for the 10-dimensional FX basket option pricing problem, $T = 5$.

Figure 6.5 depicts the coefficient values of the ten log forward rates for the first two principal components, for each of the three case studies. The ordering in absolute coefficient size for the first principal component is, with a few exceptions, in line with the ordering in variance, see appendix C. In general, the coefficient values of higher principal components (i.e. principal components with a small variance compared to other principal components) fluctuate more over time. For some principal components there are even significant jumps in coefficient value, for a certain point in time. This makes it difficult to ensure convergence for PCA2 solutions based on these principal components. A large number of time points are needed to approximate the discretization (5.5) accurately for these particular points in time.

Table 6.8 shows the option price estimates obtained by the PCA1 method, the PCA2(1,2) method and the asymptotic expansion method for case studies 1,2 and 3, respectively. For the PCA1 method, PCA2 method and the Monte Carlo method, the same number of grid points and the same settings were used as with the 5-dimensional FX basket call option (see section 6.4). For case study 3, the coefficient values of a few higher-order principal components are oscillating over time. Because of this many time points in the finite difference method for the scheme (5.6) are needed in order to approximate the derivative of the principal component coefficient value with respect to the time. For the number of time points I used, the finite difference method yields inaccurate results, therefore the asymptotic expansion values for case study 3 are not included in the overview.

Similarly to the results for the 5-dimensional FX basket call option, FX basket call option prices are higher for higher correlations and higher volatility parameters. The 10-dimensional FX basket call option prices shown in table 6.8 are lowest for case study 1 and highest for case study 2. This can be explained as, although average correlation is lowest for case study 1 and highest for case study 3, the average BSHW volatility parameter value is highest for case study 2 and lowest for case study 1.
Furthermore the results show that the call option prices increase with maturity, this is again because the FX basket underlying is more volatile for higher maturities.

The results for the 10-dimensional FX basket call option price in table 6.8 show the same trends as for the 5-dimensional FX basket call option. First, the relative error of the PCA1 and PCA2(1,2) solution is largest for case study 1 and smallest for case study 3. Second, the relative error of the PCA2(1,2) solution is almost always smaller than the relative error of the

PCA1 solution. Third, the asymptotic solution does not always give more accurate results than the PCA2(1,2) solution. The difference with the 5-dimensional FX basket call option is that the PCA1 and PCA2 method are less accurate for the 10-dimensional FX basket call option, i.e. the relative errors are larger. This is because the part of total variance captured by the first or first two principal components is smaller for the 10-dimensional FX basket call option.

For case study 1, the asymptotic solution yields results that are in line with expectations. The relative error of the asymptotic expansion is smaller than the relative error of the PCA1 and PCA2(1,2) solutions, and it increases for higher maturities. For the other two case studies, similarly to the case of the 5-dimensional FX basket call option, the asymptotic solution yields less accurate results. For case study 2, the relative error of the asymptotic expansion solution is smallest for maturity equal to 3 years, which is not in line with expectations. For case study 3, for the number of grid points I used, no converging results were obtained. The less accurate results for the asymptotic expansion for case studies 2 and 3 is due to the oscillating behavior and/or the sudden jumps of the coefficient values of the principal components. As a consequence, many time points in the finite difference method for the scheme (5.6) are needed in order to accurately approximate the derivative of the principal component coefficient value with respect to the time. Recommendations for future research concerning this finding are reported in chapter 7.

	Case study	MC price (standard deviation)	PCA1 (relative error)	PCA2(1,2) (relative error)	Asymptotic expansion (relative error)
T=1	Case study 1	0.021449 (1.029481E-5)	0.019847 (-7.4683%)	0.020200 (-5.8258%)	0.021243 (-0.9607%)
	Case study 2	0.036204 (1.773062E-5)	0.034689 (-4.1852%)	0.035563 (-1.7723%)	0.038187 (5.4747%)
	Case study 3	0.034227 (1.663634E-5)	0.033983 (-0.7135%)	0.034396 (0.4943%)	- (-%)
T=3	Case study 1	0.035872 (1.751071E-5)	0.031320 (-12.6900%)	0.032379 (-9.7369%)	0.035069 (-2.2367%)
	Case study 2	0.057870 (2.947712E-5)	0.053997 (-6.6916%)	0.055112 (-4.7658%)	0.057787 (-0.1427%)
	Case study 3	0.055169 (2.755008E-5)	0.054208 (-1.7416%)	0.054654 (-0.9328%)	- (-%)
T=5	Case study 1	0.044863 (2.218491E-5)	0.037279 (-16.9042%)	0.039038 (-12.9837%)	0.042896 (-4.3839%)
	Case study 2	0.069518 (3.664816E-5)	0.063892 (-8.0929%)	0.064706 (-6.9216%)	0.063371 (-8.8415%)
	Case study 3	0.066813 (3.409622E-5)	0.064921 (-2.8329%)	0.065739 (-1.6087%)	- (-%)

Table 6.8: 10-dimensional FX basket call option price estimates for case studies 1, 2 and 3. The absolute values of the relative error of the PCA1 and PCA2 method are given. The basket weights are equal to $\frac{1}{10}$ and, furthermore, the FX rates have been normalized with respect to their spot rate. The strike equals the forward FX basket rate. Computation time equals approximately 30, 100 and 160 minutes for the Monte Carlo estimate, for $T = 1$, $T = 3$ and $T = 5$, respectively. Computation time equals approximately 20 minutes for the PCA1 estimate and approximately 20 minutes for the PCA2 estimate.

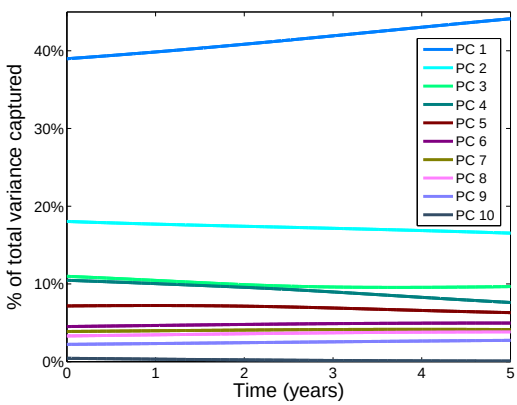

(a) Case study 1.

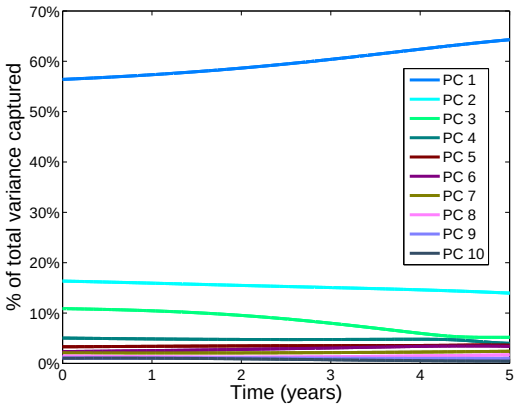

(b) Case study 2.

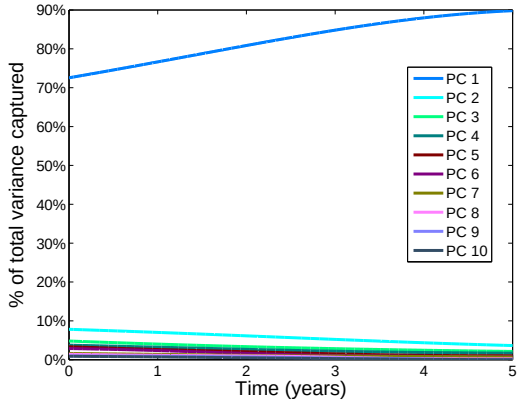

(c) Case study 3.

Figure 6.4: Part of total variable variance explained by each of the principle components of the 10-dimensional M-BSHW model, for each of the three case studies. Maturity equals $T = 5$.

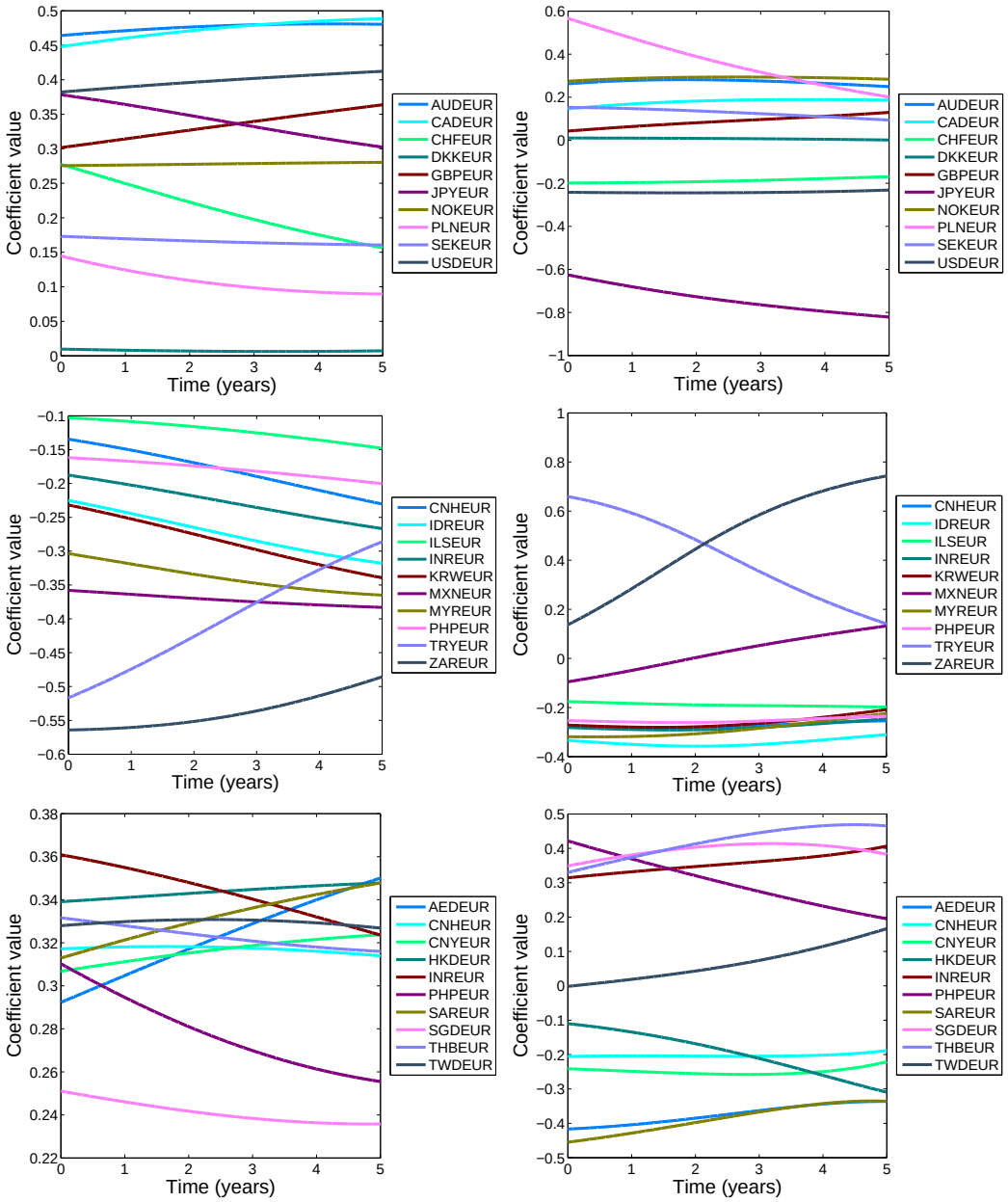

Figure 6.5: Coefficient values of the first (left figures) and second principal components (right figures) of the 10-dimensional M-BSHW model. Case study 1 figures are shown at the top, case study 2 figures on the middle and case study 3 figures on the bottom. The FX rates for each case study are shown in the legends. Maturity equals $T = 5$.

Chapter 7

Conclusion

Because of the large demand for financial derivatives to hedge the risks of multiple assets simultaneously, dimension reduction for high-dimensional option pricing is extensively studied in literature. Most of the academic literature addresses dimension reduction for Quasi-Monte Carlo methods by approximating low effective dimensions by their low-order ANOVA terms. Reisinger (2004) introduced a principal components-based dimension reduction to option pricing under the multi-dimensional Black-Scholes model with constant volatilities. By transforming the original variables to the principal components of the model, the pricing PDE is transformed to the heat equation. The dimension of the pricing problem is then reduced by truncating the heat equation to a couple of principal components that have relatively high variance.

The research conducted in this master thesis applies a time-dependent principal components-based dimension reduction to European-style FX basket option pricing. The underlying FX rates are modeled by the multi-dimensional Black-Scholes-Hull-White model with stochastic interest rates. The coefficients of the principal components are time-dependent as the coefficients of the eigenvectors of the covariance matrix are time-dependent as well. This thesis therefore directly contributes to the literature on dimension reduction in high dimensional derivative pricing.

By switching from the domestic spot risk-neutral measure to the domestic forward risk-neutral measure, the $(2N_{FX}+1)$-dimensional Black-Scholes-Hull-White model can be reduced to a N_{FX}-dimensional Black-Scholes model with time-dependent volatility. The FX basket option pricing problem is then transformed in terms of the principal components. The coefficients of the principal components are time-dependent as the coefficients of the

eigenvectors of the covariance matrix are time-dependent. The relative variances of the principal components depend on the covariations between the FX rates and interest rates. For high correlations and similar variances one or two principal components usually capture a large part of total variance. The dimension of the FX basket option pricing problem is then reduced by substituting all time-dependent principal components, except for the first or first two principal components with largest variance, by their time-zero expectation.

The performance and accuracy of this dimension reduction method was assessed based on three case studies. In these case studies, 5 and 10 low, moderately and highly correlated currencies were considered as underlyings for the FX basket option, respectively. The low correlated currencies are the most traded currencies against the domestic currency euro, the moderately and highly correlated currencies are both emerging and non-emerging market currencies, and Asian and Middle Eastern currencies. The clear overall trend is that the accuracy of the PCA1 and PCA2(1,2) method increases when either the average correlation between the FX rates increases or maturity decreases. Furtermore, the relative error of the PCA2(1,2) solution is, except for one case, always smaller than the relative error of the PCA1 solution. This is because the PCA2(1,2) method includes the second principal component in the FX basket call option pricing problem. Finally, the PCA1 and PCA2(1,2) method are trivially more accurate for the 5-dimensional FX basket call option compared to the 10-dimensional FX basket call option. This is because for the 10-dimensional FX basket call option more principal components are substituted by their time-zero expected value.

The accuracy of the PCA1 and PCA2(1,2) methods is one-to-one related with the part of total variance captured by the first and first two principal components, respectively. For the $5Y$ 5-dimensional FX basket call option price, the first principal component captures at least 47%, 71% and 80% of total variance for the low, moderately and highly correlated currencies, respectively. For the first two principal components, these percentages equal 67%, 81% and 87%. The accuracy of the PCA1 and PCA2(1,2) methods increases significantly: the relative error equals 14.62%, 5.54% and 1.47% for the PCA1 solution. For the PCA2(1,2) solution, these errors are equal to 10.69%, 4.67% and 1.01%, respectively.

For the $5Y$ 10-dimensional FX basket call option price, the first principal component captures at least 38%, 56% and 72% of total variance for the low, moderately and highly correlated currencies, respectively. For the first

two principal components, these percentages equal 57%, 72% and 80%. The accuracy of the PCA1 and PCA2(1,2) methods increases significantly: the relative error equals 16.90%, 8.09% and 2.83% for PCA1, and 12.98%, 6.92% and 1.61% for PCA2(1,2), respectively.

The research results showed that the asymptotic solution does not always give more accurate results than the PCA2(1,2) solution, which is not in line with expectations. The less accurate results for the asymptotic expansion are due to the oscillating behavior and/or the sudden jumps of the coefficient values of the principal components. Therefore many time points in the finite difference scheme are needed to get converging results.

Recommendations for future research concern both the enhancement of the calculation of the asymptotic expansion solution and applications to other stochastic multi-dimensional models. Especially for highly correlated FX rates, coefficients of the higher-order principal component can show oscillating behavior, making the finite difference solutions significantly less stable. Future work can address this problem by implementing time-dependent grid distances. Here one could use smaller grid distances for the time direction in areas where principal component coefficients show oscillating behavior.

As an extension to the research in this master thesis, the performance and accuracy of the time-dependent principle components-based dimension reduction method can be assessed in the calculation of the Greeks for the FX basket option price. The Greeks measure the sensitivity of derivative prices to several underlying parameter values. It is expected that the accuracy of the dimension reduction technique of this thesis applied to the calculation of Greeks is similar to the accuracy reported in this thesis.

Finally, future research could be devoted to apply the time-dependent principal component-based dimension reduction to local volatility and/or stochastic volatility models. The general principle used in this master thesis research was the application of a principle components transformation to the multi-dimensional Black-Scholes-Hull-White model. Subsequently, in the FX basket option pricing the low-variance principal components were substituted by their expectation. This principle can be adapted and applied to models that are able to capture the volatility smile.

Bibliography

[1] Bank for International Settlements (2016). *Triennial Central Bank Survey: Foreign exchange turnover in April 2016.*

[2] Bank for International Settlements (2016). *Triennial Central Bank Survey: Global foreign exchange market turnover in 2016.*

[3] Beneder, R., & Elkenbracht-Huizing, M. (2003). Foreign exchange options and the volatility smile. *Medium Econometrische Toepassingen*, 2, 30-36.

[4] Björk, T. (2009). *Arbitrage theory in continuous time.* Oxford university press.

[5] Boshuizen, F., Van der Vaart, A., Van Zanten, H., Banachewicz, K., Zareba, P., & Belitser, E. (2014). Lecture notes for course Stochastic Processes for Finance.

[6] Brigo, D., & Mercurio, F. (2007). *Interest rate models-theory and practice: with smile, inflation and credit.* Springer Science & Business Media.

[7] Broadie, M., & Glasserman, P. (2004). A stochastic mesh method for pricing high-dimensional American options.*Journal of Computational Finance, 7*, 35-72.

[8] Castagna, A. (2010).*Fx options and smile risk.* John Wiley & Sons.

[9] Clark, I. J. (2011). *Foreign exchange option pricing: a practitioner's guide.* John Wiley & Sons.

[10] Dang, D. M., Christara, C. C., Jackson, K. R., & Lakhany, A. (2010). A PDE pricing framework for cross-currency interest rate derivatives. *Procedia Computer Science, 1*(1), 2371-2380.

[11] De Col, A., Gnoatto, A., & Grasselli, M. (2013). Smiles all around: FX joint calibration in a multi-Heston model. *Journal of Banking & Finance, 37*(10), 3799-3818.

[12] Deelstra, G., & Rayée, G. (2013). Local volatility pricing models for long-dated FX derivatives. *Applied Mathematical Finance, 20*(4), 380-402.

[13] Doust, P. (2012). The stochastic intrinsic currency volatility model: a consistent framework for multiple fx rates and their volatilities. *Applied Mathematical Finance, 19*(5), 381-445.

[14] Downarowicz, A. (2010). The First Fundamental Theorem of Asset Pricing. *Revista de Economía Financiera, 2*, 23-35.

[15] Ekedahl, E., Hansander, E., & Lehto, E. (2007). Dimension reduction for the black-scholes equation. *Department of Information Technology, Uppsala University.*

[16] Filipović, D. (2009). *Term-Structure Models.* Springer, Berlin.

[17] Garman, M. B., & Kohlhagen, S. W. (1983). Foreign currency option values. *Journal of international Money and Finance, 2*(3), 231-237.

[18] Gilli, M., Große, S., & Schumann, E. (2010). Calibrating the nelson-siegel-svensson model. *Available at SSRN 1676747.*

[19] Girsanov, I. V. (1960). On transforming a certain class of stochastic processes by absolutely continuous substitution of measures. *Theory of Probability & Its Applications, 5*(3), 285-301.

[20] Grzelak, L. A., & Oosterlee, C. W. (2012). On cross-currency models with stochastic volatility and correlated interest rates. *Applied Mathematical Finance, 19*(1), 1-35.

[21] Grzelak, L. A., Oosterlee, C. W., & Van Weeren, S. (2012). Extension of stochastic volatility equity models with the Hull–White interest rate process. *Quantitative Finance, 12*(1), 89-105.

[22] Hakala, J., & Wystup, U. (2008). *FX basket options* (No. 14). Frankfurt School of Finance and Management, Centre for Practical Quantitative Finance (CPQF).

[23] Heston, S. L. (1993). A closed-form solution for options with stochastic volatility with applications to bond and currency options. *Review of financial studies, 6*(2), 327-343.

[24] Hull, J., & White, A. (1990). Pricing interest-rate-derivative securities. *Review of financial studies, 3*(4), 573-592.

[25] Imai, J., & Tan, K. S. (2006). A general dimension reduction technique for derivative pricing. *Journal of Computational Finance, 10*(2), 129.

[26] In't Hout, K. J., & Foulon, S. (2010). ADI finite difference schemes for option pricing in the Heston model with correlation. *Int. J. Numer. Anal. Model, 7*(2), 303-320.

[27] Jolliffe, I. (2002). *Principal component analysis*. John Wiley & Sons, Ltd.

[28] Joy, C., Boyle, P. P., & Tan, K. S. (1996). Quasi-Monte Carlo methods in numerical finance. *Management Science, 42*(6), 926-938.

[29] Lakoba, T. I. (2016). The Heat equation in 2 and 3 spatial dimensions. *Lecture Notes*. Retrieved from
`http://www.cems.uvm.edu/~tlakoba/math337/`

[30] Lee, R. W. (2005). Implied volatility: Statics, dynamics, and probabilistic interpretation. In *Recent Advances in Applied Probability* (pp. 241-268). Springer US.

[31] Leippold, M., Slee, J., Suisse, C., & Hasler, U. (2006). FX Basket Options.

[32] Kohler, M., Krzyżak, A., & Todorovic, N. (2010). Pricing of high dimensional american options by neural networks. *Mathematical Finance, 20*(3), 383-410.

[33] Norgaard, J. (2011). Pricing and hedging of fx plain vanilla options. *Aarhus School of Business*.

[34] Pettersson, U., Larsson, E., Marcusson, G., & Persson, J. (2008). Improved radial basis function methods for multi-dimensional option pricing. *Journal of Computational and Applied Mathematics, 222*(1), 82-93.

[35] Reisinger, C. (2004). Numerische Methoden für hochdimensionale parabolische Gleichungen am Beispiel von Optionspreisaufgaben.

[36] Reisinger, C., & Wissmann, R. (2015). Error analysis of truncated expansion solutions to high-dimensional parabolic PDEs. arXiv preprint arXiv:1505.04639.

[37] Reisinger, C., & Wittum, G. (2007). Efficient hierarchical approximation of high-dimensional option pricing problems. *SIAM Journal on Scientific Computing, 29*(1), 440-458.

[38] Reiswich, D., & Wystup, U. (2012). FX volatility smile construction. *Wilmott, 2012*(60), 58-69.

[39] Runborg, O. (2012). Verifying Numercial Convergence Rates. *Lecture Notes*. Retrieved from `https://www.kth.se/social/upload/52ea4f1ff2765454c236fe79/ConvRate.pdf`

[40] Sabino, P. (2007). Monte Carlo methods and path-generation techniques for pricing multi-asset path-dependent options. *Available at SSRN 1020151*.

[41] Shcherbakov, V., & Larsson, E. (2016). Radial basis function partition of unity methods for pricing vanilla basket options. Computers & Mathematics with Applications, 71(1), 185-200.

[42] Shreve, S. E. (2004). *Stochastic calculus for finance II: Continuous-time models* (Vol. 11). Springer Science & Business Media.

[43] Simaitis, S. (2014). *Stochastic interest rate and volatility implications for the exposure of FX options* (MSc Thesis, University of Amsterdam).

[44] Simaitis, S., de Graaf, C. S. L., Hari, N., & Kandhai, D. (2016). Smile and default: the role of stochastic volatility and interest rates in counterparty credit risk. *Quantitative Finance*, 1-16.

[45] Van Haastrecht, A., Lord, R., Pelsser, A., & Schrager, D. (2009). Pricing long-maturity equity and FX derivatives with stochastic interest rates and stochastic volatility. *Insurance: Mathematics and Economics, 45*(3).

[46] Wang, X., & Sloan, I. H. (2011). Quasi-Monte Carlo methods in financial engineering: An equivalence principle and dimension reduction. *Operations Research, 59*(1), 80-95.

Appendix A

Derivation of the BSHW model dynamics under the $\mathbb{Q}_T$-measure

Under the domestic risk neutral measure $\mathbb{Q}$ one has from (3.3) and (3.8), using definition (3.11),

$$\begin{aligned} dS^{df}(t) &= (r_d(t) - r_f(t))\, S^{df}(t)dt + \sigma S^{df}(t)dW^{\mathbb{Q}}_{S^{df}}(t), \\ dP_d(t,T) &= r_d(t)P_d(t,T)dt + P_d(t,T)\sigma_d A_d(t,T)dW^{\mathbb{Q}}_d(t), \\ dP_f(t,T) &= \left[r_f(t) - \rho_{S^{df}r_f}\sigma\sigma_f A_f(t,T)P_f(t,T)\right]dt \\ &\quad + P_f(t,T)\sigma_f A_f(t,T)dW^{\mathbb{Q}}_f(t). \end{aligned}$$

Then by Itô one has

$$\begin{aligned} & d\frac{P_F(t,T)}{P_D(t,T)} \\ &= \frac{1}{P_d(t,t)}dP_f(t,T) - \frac{P_f(t,tT)}{P_d(t,T)^2}dP_d(t,T) + \frac{P_f(t,T)}{P_d(t,T)^3}P_d(t,T)^2 \\ &\quad \times \sigma_d^2 A_d^2(t,T)dt - \frac{1}{P_d(t,T)^2}\rho_{r_f r_d}P_f(t,T)P_d(t,T)\sigma_f\sigma_d A_f(t,T)A_d(t,T)dt \\ &= \left[r_f(t) - r_d(t) - \rho_{S^{df}r_f}\sigma\sigma_f A_f(t,T) + \sigma_d^2 A_d^2(t,T)\right. \\ &\quad \left.-\rho_{r_f r_d}\sigma_f\sigma_d A_f(t,T)A_d(t,T)\right]\frac{P_f(t,T)}{P_d(t,T)}dt - \sigma_d A_d(t,T)\frac{P_f(t,T)}{P_d(t,T)}dW^{\mathbb{Q}}_d(t) \\ &\quad + \sigma_f A_f(t,T)\frac{P_f(t,T)}{P_d(t,T)}dW^{\mathbb{Q}}_f(t). \end{aligned}$$

Again by using Itô one has

$$
\begin{aligned}
&dF^{df}(t) := dS^{df}(t)\frac{P_f(t,T)}{P_d(t,T)} \\
&= (r_d(t) - r_f(t))\, S^{df}(t)\frac{P_f(t,T)}{P_d(t,T)}dt + \sigma S^{df}(t)\frac{P_f(t,T)}{P_d(t,T)}dW^{\mathbb{Q}}_{S^{df}}(t) \\
&\quad + S^{df}(t)d\frac{P_f(t,T)}{P_d(t,T)} - \rho_{S^{df}r_d}\sigma S^{df}(t)\sigma_d A_d(t,T)\frac{P_f(t,T)}{P_d(t,T)}dt \\
&\quad + \rho_{S^{df}r_f}\sigma S^{df}(t)\sigma_f A_f(t,T)\frac{P_f(t,T)}{P_d(t,T)}dt \\
&= \left[\sigma_d^2 A_d^2(t,T) - \rho_{r_f r_d}\sigma_f\sigma_d A_f(t,T)A_d(t,T) - \rho_{S^{df}r_d}\sigma\sigma_d A_d(t,T)\right] \\
&\quad \times S^{df}(t)\frac{P_f(t,T)}{P_d(t,T)}dt + \sigma S^{df}(t)\frac{P_f(t,T)}{P_d(t,T)}dW^{\mathbb{Q}}_{S^{df}}(t) \\
&\quad - \sigma_d A_d(t,T)S^{df}(t)\frac{P_f(t,T)}{P_d(t,T)}dW^{\mathbb{Q}}_d(t) + \sigma_f A_f(t,T)S^{df}(t)\frac{P_f(t,T)}{P_d(t,T)}dW^{\mathbb{Q}}_f(t) \\
&:= \left[\sigma_d^2 A_d^2(t,T) - \rho_{r_f r_d}\sigma_f\sigma_d A_f(t,T)A_d(t,T) - \rho_{S^{df}r_d}\sigma\sigma_d A_d(t,T)\right] F^{df}(t)dt \\
&\quad + \sigma F^{df}(t)dW^{\mathbb{Q}}_{S^{df}}(t) - \sigma_d A_d(t,T)F^{df}(t)dW^{\mathbb{Q}}_d(t) + \sigma_f A_f(t,T)F^{df}(t)dW^{\mathbb{Q}}_f(t).
\end{aligned}
$$

Now using Girsanov's first fundamental theorem (Girsanov, 1960), one has that the processes

$$
\begin{aligned}
W^{\mathbb{Q}_T}_{S^{df}}(t) &:= W^{\mathbb{Q}}_{S^{df}}(t) + \int_0^t \theta_1(s)ds, \\
W^{\mathbb{Q}_T}_{d}(t) &:= W^{\mathbb{Q}}_{d}(t) + \int_0^t \theta_2(s)ds, \\
W^{\mathbb{Q}_T}_{f}(t) &:= W^{\mathbb{Q}}_{f}(t) + \int_0^t \theta_3(s)ds,
\end{aligned}
$$

are Brownian motions under the domestic forward risk-neutral measure $\mathbb{Q}_T$. The choices

$$
\begin{aligned}
\theta_1(t) &= -\rho_{S^{df}r_d}\sigma_d A_d(t,T), \\
\theta_2(t) &= -\sigma_d A_d(t,T), \\
\theta_3(t) &= -\rho_{r_f r_d}\sigma_d A_d(t,T),
\end{aligned}
$$

make the process $F^{df}(t)$ a martingale under the domestic forward risk-neutral measure $\mathbb{Q}_T$. Then the process $F^{df}(t)$ has the $\mathbb{Q}_T$-dynamics given by

$$
\begin{aligned}
&dF^{df}(t) \\
&= \sigma F^{df}(t)dW^{\mathbb{Q}_T}_{S^{df}}(t) + \sigma_f A_f(t,T)F^{df}(t)dW^{\mathbb{Q}_T}_f(t) - \sigma_d A_d(t,T)F^{df}(t)dW^{\mathbb{Q}_T}_d(t).
\end{aligned}
$$

Appendix B

Principal components-based dimension reduction for the multi-dimensional Black-Scholes model

Under the real-world measure $\mathbb{P}$, the N-dimensional Black-Scholes model with μ_i and σ_i the drift- and volatility parameters ($i \in \{1, \ldots, N\}$), respectively, is given by:

$$dS_i(t) = \mu_i S_i(t)dt + \sigma_i S_i(t)dW_i^{\mathbb{P}}(t), \qquad i = 1, \ldots, N,$$

with stochastic covariation process given by $d\left[W_i^{\mathbb{P}}, W_j^{\mathbb{P}}\right](t) = \rho_{ij}dt$ for $i, j \leq N$. Consider the problem of pricing a derivative with underlying the stochastic processes $\mathbf{S}(t) = (S_1(t), \ldots, S_N(t))^\top$ for $t \geq 0$. Let $u(\mathbf{S}, t)$ denote the derivative price at time t. Using the Feynman-Kac theorem the Black-Scholes PDE for u equals

$$\frac{\partial u}{\partial t} + \sum_{i=1}^{N} \mu_i S_i \frac{\partial u}{\partial S_i} + \frac{1}{2}\sum_{i=1}^{N}\sum_{j=1}^{N} \sigma_i \sigma_j \rho_{ij} S_i S_j \frac{\partial^2 u}{\partial S_i \partial S_j} - ru = 0, \tag{B.1}$$

with $u = u(\mathbf{S}, t)$ the option price at time t, depending on the underlying at time t. The initial condition is given by $u(\mathbf{S}, T) = f(\mathbf{S})$.

Now let $\mathbf{\Sigma}$ denote the covariance matrix of the stochastic variables $\mathbf{S}$, then one has $\Sigma_{ij} = \sigma_i \sigma_j \rho_{ij}$. Let $\mathbf{Q} := (q_{ij})_{i,j\in\{1,\ldots,N\}}$ denote the matrix with the eigenvectors of the covariance matrix as columns. Here $\mathbf{Q} = (\mathbf{q}_1, \mathbf{q}_2, \ldots, \mathbf{q}_N)$ with $\mathbf{q}_1, \mathbf{q}_2, \ldots, \mathbf{q}_N$ the eigenvectors corresponding to the largest to smallest eigenvalues. Let $\{\lambda_i\}_{i\in\{1,\ldots,N\}}$ denote the eigenvalues, and define $\boldsymbol{\lambda} =$

$(\lambda_1, \ldots, \lambda_N)^\top$.

Applying the principal component transformation $\mathbf{Z} := \mathbf{Q}^\top \mathbf{S}$ to the multi-dimensional Black-Scholes PDE (B.1) yields an inefficient equation. Instead one can apply the transformation

$$\mathbf{Z} := \mathbf{Q}^\top \ln \mathbf{S}. \tag{B.2}$$

Here $\mathbf{Z} = (Z_1, \ldots, Z_N)^\top$. Let v denote the derivative value process corresponding to the principal components $\mathbf{Z}$, then one has, using $u(\mathbf{S}, t) = v(\mathbf{Z}, t)$:

$$\begin{aligned} \frac{\partial u}{\partial S_i} &= \sum_{k=1}^{N} \frac{\partial v}{\partial Z_k} \frac{1}{S_i} q_{ik}, \\ \frac{\partial^2 u}{\partial S_i \partial S_j} &= \sum_{k=1}^{N} \frac{\partial^2 v}{\partial Z_k^2} \frac{1}{S_i} \frac{1}{S_j} q_{ik} q_{jk} - \sum_{k=1}^{N} \frac{\partial v}{\partial Z_k} \frac{1}{S_i^2} q_{ik} 1_{\{i=j\}}. \end{aligned} \tag{B.3}$$

From $\mathbf{q}_i^\top \mathbf{\Sigma} \mathbf{q}_i = \lambda_i$ we get $\lambda_i = \sum_{k=1}^{N} \sum_{j=1}^{N} q_{ki} q_{ji} \sigma_k \sigma_j \rho_{jk}$, for $i \leq N$. Applying (B.3) to the Black-Scholes PDE (B.1) then yields

$$\frac{\partial v}{\partial t} + \sum_{i=1}^{N} \sum_{k=1}^{N} q_{ik} \frac{\partial v}{\partial Z_k} \left[\mu_i - \frac{1}{2} \sigma_i^2 \right] + \frac{1}{2} \sum_{k=1}^{N} \lambda_k \frac{\partial^2 v}{\partial Z_k^2} - rv = 0, \tag{B.4}$$

with $v(\mathbf{Z}, T) = f\left(\left(e^{\sum_{j=1}^{N} q_{ij} Z_j(T)} \right)_{i \leq N}, T \right)$.

One can add a time translation to (B.2) to remove the first-order term from (B.4). Transformation (B.2) then becomes

$$\mathbf{Z} = \mathbf{Q}^\top \left[\ln \mathbf{S} - \mathbf{B}(t) \right], \tag{B.5}$$

with $B_i(t) = \mu_i - \frac{1}{2}\sigma_i^2$. Using that

$$\frac{\partial Z_k}{\partial t} = -\sum_{j=1}^{N} q_{jk} \left(\mu_j - \frac{1}{2} \sigma_j^2 \right), \qquad k = 1, \ldots, N,$$

the PDE (B.4) transforms into

$$\frac{\partial v}{\partial t} + \frac{1}{2} \sum_{k=1}^{N} \lambda_k \frac{\partial^2 v}{\partial Z_k^2} - rv = 0, \tag{B.6}$$

with $v(\mathbf{Z},T) = f\left(\left(e^{\sum_{j=1}^{N} q_{ij}Z_j(T)+B_i(T)}\right)_{i\leq N}, T\right)$. Optionally, the rV-term in the PDE above can be eliminated by the substitution $Y(t) = e^{rt}Z(t)$, yielding the heat equation [35]. Reversing time using $\tau = T - t$ yields for the associated value process $w(\mathbf{Z},\tau) = v(\mathbf{Z},T-\tau)$:

$$\frac{\partial w}{\partial \tau} = \frac{1}{2}\sum_{k=1}^{N} \lambda_k \frac{\partial^2 w}{\partial Z_k^2} - rv, \tag{B.7}$$

with initial condition $w(\mathbf{Z},0) = f\left(\left(e^{\sum_{j=1}^{N} q_{ij}Z_j(T)+B_i(T)}\right)_{i\leq N}, 0\right)$.

Appendix C

Calibration results

	AUDEUR	CADEUR	CHFEUR	DKKEUR	GBPEUR	JPYEUR	NOKEUR	PLNEUR	SEKEUR	USDEUR
AUDEUR	1	0,70998	0,21425	0,09220	0,42902	0,22618	0,51225	0.28270	0,34357	0,50564
CADEUR	0,70998	1	0,22067	0,21423	0,51868	0,25187	0,56067	0,15199	0,33063	0,61109
CHFEUR	0,21425	0,22067	1	0,15852	0,21162	0,29807	0,23606	-0,09269	0,17665	0,22626
DKKEUR	0,09220	0,21423	0,15852	1	0,09516	0,02698	0,13059	-0,14679	0,05202	0,12634
GBPEUR	0,42902	0,51868	0,21162	0,09516	1	0,14691	0,28786	0,11387	0,28008	0,52649
JPYEUR	0,22618	0,25187	0,29807	0,02698	0,14691	1	0,09373	-0,03290	0,12973	0,49604
NOKEUR	0,51225	0,56067	0,23606	0,13059	0,28786	0,093736	1	0,30297	0,42093	0,24012
PLNEUR	0,28270	0,15199	-0,09269	-0,14679	0,11387	-0,03290	0,30297	1	0,21987	0,09395
SEKEUR	0,34357	0,33063	0,17665	0,05202	0,28008	0,12973	0,42093	0,21987	1	0,26402
USDEUR	0,50564	0,61109	0,22626	0,12634	0,52649	0,49604	0,24012	0,09395	0,26402	1
r_{AUD}	0,36823	0,18858	-0,05218	0,01802	0,17602	-0,23181	0,17581	0,10432	0,16216	0,12147
r_{CAD}	0,29168	0,44867	-0,10163	0,27408	0,17482	-0,28677	0,19545	-0,00269	0,1117	0,14944
r_{CHF}	-0,10996	-0,10824	-0,56621	0,21752	-0,13643	-0,38434	-0,13346	0,06547	-0,02536	-0,25356
r_{DKK}	-0,03896	-0,07888	-0,12723	-0,01280	-0,09943	-0,31591	-0,06199	0,00604	0,12240	-0,19140
r_{EUR}	-0,05858	-0,10148	-0,13692	0,01537	-0,08734	-0,35615	-0,03700	0,05609	0,09369	-0,18862
r_{GBP}	0,20581	0,26149	-0,06254	0,09915	0,40359	-0,30421	0,15338	0,09192	0,14075	0,12821
r_{JPY}	0,03697	0,01095	-0,04614	0,06364	0,08017	-0,04189	0,00554	-0,07516	0,09318	0,02658
r_{NOK}	0,14910	0,18523	-0,13733	0,07467	0,06494	-0,27831	0,44767	0,07157	0,21012	-0,05184
r_{PLN}	-0,05304	0,00154	-0,06459	0,17042	0,06348	-0,03182	-0,16298	-0,26333	-0,07840	0,05659
r_{SEK}	0,10736	0,05196	-0,11944	-0,00334	0,10066	-0,2043	0,07790	0,09275	0,3875	0,01569
r_{USD}	0,23185	0,28669	-0,14296	0,03944	0,31281	-0,31959	0,15943	0,10266	0,102	0,27683

Table C.1: Historical correlations for case study 1 currencies and associated interest rates, part 1.

	r_{AUD}	r_{CAD}	r_{CHF}	r_{DKK}	r_{EUR}	r_{GBP}	r_{JPY}	r_{NOK}	r_{PLN}	r_{SEK}	r_{USD}
AUDEUR	0,36823	0,29168	-0,10996	-0,03896	-0,05858	0,20581	0,03697	0,14910	-0,05304	0,10736	0,23185
CADEUR	0,18858	0,44867	-0,10824	-0,07888	-0,10148	0,26149	0,01095	0,18523	0,00154	0,05196	0,28669
CHFEUR	-0,05218	-0,10163	-0,56621	-0,12723	-0,13692	-0,06254	-0,04614	-0,13733	-0,06459	-0,11944	-0,14296
DKKEUR	0,01802	0,27408	0,21752	-0,01280	0,01537	0,09915	0,06364	0,07467	0,17042	-0,00334	0,03944
GBPEUR	0,17602	0,17482	-0,13643	-0,09943	-0,08734	0,40359	0,08017	0,06494	0,06348	0,10066	0,31281
JPYEUR	-0,23181	-0,28677	-0,38434	-0,31591	-0,35615	-0,30421	-0,04189	-0,27831	-0,03182	-0,2043	-0,31959
NOKEUR	0,17581	0,19545	-0,13346	-0,06199	-0,03700	0,15338	0,00554	0,44767	-0,16298	0,07790	0,15943
PLNEUR	0,10432	-0,00269	0,06547	0,00604	-0,05609	0,09192	-0,07516	0,07157	-0,26333	0,09275	0,10266
SEKEUR	0,16216	0,1117	-0,02536	0,12240	0,09369	0,14075	0,09318	0,21012	-0,07840	0,3875	0,102
USDEUR	0,12147	0,14944	-0,25356	-0,19140	-0,18862	0,12821	0,02658	-0,05184	0,05659	0,01569	0,27683
r_{AUD}	1	0,53915	0,21261	0,34027	0,41902	0,5049	0,27895	0,44894	0,23143	0,45044	0,57465
r_{CAD}	0,53915	1	0,47925	0,51021	0,54418	0,73243	0,26705	0,62061	0,33968	0,55349	0,77883
r_{CHF}	0,21261	0,47925	1	0,58014	0,521	0,42558	0,23139	0,48958	0,24339	0,46768	0,37741
r_{DKK}	0,34027	0,51021	0,58014	1	0,86870	0,51493	0,25171	0,57218	0,24869	0,66560	0,44523
r_{EUR}	0,41902	0,54418	0,521	0,86870	1	0,61096	0,30404	0,60802	0,29969	0,6956	0,55418
r_{GBP}	0,5049	0,73243	0,42558	0,51493	0,61096	1	0,23619	0,60398	0,34617	0,60269	0,81015
r_{JPY}	0,27895	0,26705	0,23139	0,25171	0,30404	0,23619	1	0,30019	0,20340	0,3087	0,28308
r_{NOK}	0,44894	0,62061	0,48958	0,57218	0,60802	0,60398	0,30019	1	0,24670	0,61860	0,57678
r_{PLN}	0,23143	0,33968	0,24339	0,24869	0,29969	0,34617	0,20340	0,24670	1	0,31867	0,34140
r_{SEK}	0,45044	0,55349	0,46768	0,66560	0,6956	0,60269	0,3087	0,61860	0,31867	1	0,54512
r_{USD}	0,57465	0,77883	0,37741	0,44523	0,55418	0,81015	0,28308	0,57678	0,34140	0,54512	1

Table C.2: Historical correlations for case study 1 currencies and associated interest rates, part 2.

	Nelson-Siegel-Svensson parameters							Hull-White parameters		BSHW parameters (EUR as domestic CCY)		
CCY	β_1	β_2	β_3	β_4	λ_1	λ_2	max. maturity (years)	λ	σ	Spot rate	σ_{BSHW}	max. maturity (years)
AUD	0.08526	-0.06458	-0.04825	-0.17839	3.34737	27.33338	50.03836	0.01187	0.00795	0.67512	0.11537	5.00274
CAD	0.08176	-0.07191	-0.04758	-0.16869	3.90499	27.33032	50.03288	0.01399	0.00735	0.68542	0.11119	5.00274
CHF	0.06118	-0.06844	-0.05327	-0.16395	3.34737	17.29590	50.03836	0.04318	0.00740	0.91284	0.08340	5.00274
DKK	0.08268	-0.08573	-0.07376	-0.18737	3.90499	23.98754	50.03836	0.01	0.00653	0.13434	0.00881	10.00548
EUR	0.00316	-0.00591	-0.03503	0.03292	3.90499	8.93135	50.03836	0.04138	0.00740	-	-	-
GBP	0.10640	-0.10118	-0.06487	-0.26433	4.46263	26.49386	50.03288	0.08	0.01030	1.17961	0.10679	5.00274
JPY	0.01562	-0.01545	-0.03659	-0.03595	1.67444	10.60274	50.03562	0.04138	0.00740	0.00869	0.12111	5.00274
NOK	0.05622	-0.04497	-0.03596	-0.10571	3.34737	23.15109	50.03836	0.01	0.00725	0.10781	0.09161	2
PLN	0.02056	-0.00110	-0.03286	0.03727	2.78972	8.93135	50.03836	0.01	0.01022	0.22943	0.07441	2
SEK	0.02177	-0.02668	-0.04032	0.02104	2.78972	8.93135	50.03836	0.01	0.00643	0.10513	0.06977	2
USD	0.04662	-0.03499	0.00967	-0.06863	8.92370	27.33338	50.03836	0.02049	0.00895	0.89783	0.10348	5.00274

Table C.3: Estimates on Hull-White model parameters and BSHW model parameters for case study 1 currencies.

	CNHEUR	IDREUR	ILSEUR	INREUR	KRWEUR	MXNEUR	MYREUR	PHPEUR	TRYEUR	ZAREUR
CNHEUR	1	0.67624	0.62106	0.83315	0.69245	0.60219	0.63872	0.85299	0.49079	0.41016
IDREUR	0.67624	1	0.50964	0.67948	0.61949	0.52737	0.70272	0.71473	0.49593	0.44912
ILSEUR	0.62106	0.50964	1	0.62394	0.55165	0.5191	0.57285	0.6591	0.36836	0.27575
INREUR	0.83315	0.67948	0.62394	1	0.74061	0.66158	0.67253	0.87616	0.57648	0.45855
KRWEUR	0.69245	0.61949	0.55165	0.74061	1	0.62992	0.717	0.741	0.55517	0.53131
MXNEUR	0.60219	0.52737	0.5191	0.66158	0.62992	1	0.63079	0.59675	0.67678	0.68828
MYREUR	0.63872	0.70272	0.57285	0.67253	0.717	0.63079	1	0.74667	0.57143	0.53865
PHPEUR	0.85299	0.71473	0.6591	0.87616	0.741	0.59675	0.74667	1	0.53882	0.40842
TRYEUR	0.49079	0.49593	0.36836	0.57648	0.55517	0.67678	0.57143	0.53882	1	0.64049
ZAREUR	0.41016	0.44912	0.27575	0.45855	0.53131	0.68828	0.53865	0.40842	0.64049	1
r_{EUR}	-0.1429	-0.08957	-0.0797	-0.16283	-0.10019	-0.07037	-0.07725	-0.17561	-0.05432	-0.01136
r_{CNH}	0.05209	0.02704	0.08582	0.00888	0.01444	-0.08538	0.02609	0.03244	0.03469	-0.1193
r_{IDR}	0.00381	-0.02478	0.00199	-0.08224	-0.12211	-0.06944	-0.1093	-0.10008	-0.03813	-0.03138
r_{ILS}	0.08215	-0.00184	0.20446	-0.00434	0.01672	-0.04101	-0.06492	0.0367	0.0194	-0.11865
r_{INR}	-0.0292	-0.17128	-0.03831	-0.15117	-0.00735	0.04942	-0.14657	-0.14915	-0.05918	-0.08178
r_{KRW}	0.073	-0.01337	0.04357	0.06327	0.09135	0.03966	0.05731	0.06182	0.08091	-0.01497
r_{MXN}	0.15173	0.03629	0.03341	-0.03045	-0.03122	-0.13167	-0.07358	0.0416	-0.11516	-0.17867
r_{MYR}	0.03262	-0.23811	0.01051	-0.02601	-0.15517	-0.13953	-0.33382	-0.02418	-0.16701	-0.30125
r_{PHP}	0.01036	-0.09502	-0.0731	-0.08672	-0.07494	-0.12424	-0.13554	-0.12014	-0.1166	-0.09933
r_{TRY}	0.08634	-0.14704	0.0975	-0.05024	-0.13802	-0.23514	-0.14848	-0.00674	-0.53278	-0.33074
r_{ZAR}	0.01993	-0.13759	0.04263	-0.09234	-0.12044	-0.31461	-0.16401	-0.01747	-0.33693	-0.66813

Table C.4: Historical correlations for case study 2 currencies and associated interest rates, part 1.

	r_{EUR}	r_{CNH}	r_{IDR}	r_{ILS}	r_{INR}	r_{KRW}	r_{MXN}	r_{MYR}	r_{PHP}	r_{TRY}	r_{ZAR}
CNHEUR	-0.1429	0.05209	0.00381	0.08215	-0.0292	0.073	0.15173	0.03262	0.01036	0.08634	0.01993
IDREUR	-0.08957	0.02704	-0.02478	-0.00184	-0.17128	-0.01337	0.03629	-0.23811	-0.09502	-0.14704	-0.13759
ILSEUR	-0.0797	0.08582	0.00199	0.20446	-0.03831	0.04357	0.03341	0.01051	-0.0731	0.0975	0.04263
INREUR	-0.16283	0.00888	-0.08224	-0.00434	-0.15117	0.06327	-0.03045	-0.02601	-0.08672	-0.05024	-0.09234
KRWEUR	-0.10019	0.01444	-0.12211	0.01672	-0.00735	0.09135	-0.03122	-0.15517	-0.07494	-0.13802	-0.12044
MXNEUR	-0.07037	-0.08538	-0.06944	-0.04101	0.04942	0.03966	-0.13167	-0.13953	-0.12424	-0.23514	-0.31461
MYREUR	-0.07725	0.02609	-0.1093	-0.06492	-0.14657	0.05731	-0.07358	-0.33382	-0.13554	-0.14848	-0.16401
PHPEUR	-0.17561	0.03244	-0.10008	0.0367	-0.14915	0.06182	0.0416	-0.02418	-0.12014	-0.00674	-0.01747
TRYEUR	-0.05432	0.03469	-0.03813	0.0194	-0.05918	0.08091	-0.11516	-0.16701	-0.1166	-0.53278	-0.33693
ZAREUR	-0.01136	-0.1193	-0.03138	-0.11865	-0.08178	-0.01497	-0.17867	-0.30125	-0.09933	-0.33074	-0.66813
r_{EUR}	1	0.02801	-0.06617	0.3933	0.08045	0.24297	0.06035	-0.02777	-0.02111	0.08322	-0.02659
r_{CNH}	0.02801	1	0.15302	0.02535	-0.00598	-0.05334	0.04523	-0.09211	-0.01149	0.0017	0.05884
r_{IDR}	-0.06617	0.15302	1	-0.02941	-0.0722	-0.06216	-0.04709	0.02284	0.09961	0.00843	-0.07548
r_{ILS}	0.3933	0.02535	-0.02941	1	0.20579	0.49093	0.45258	0.36717	0.23638	0.24983	0.34366
r_{INR}	0.08045	-0.00598	-0.0722	0.20579	1	0.18097	0.18003	0.32214	0.29857	0.14134	0.17875
r_{KRW}	0.24297	-0.05334	-0.06216	0.49093	0.18097	1	0.32377	0.35757	0.18941	0.20565	0.21571
r_{MXN}	0.06035	0.04523	-0.04709	0.45258	0.18003	0.32377	1	0.38701	0.23791	0.30041	0.39389
r_{MYR}	-0.02777	-0.09211	0.02284	0.36717	0.32214	0.35757	0.38701	1	0.17918	0.34026	0.37294
r_{PHP}	-0.02111	-0.01149	0.09961	0.23638	0.29857	0.18941	0.23791	0.17918	1	0.18461	0.09475
r_{TRY}	0.08322	0.0017	0.00843	0.24983	0.14134	0.20565	0.30041	0.34026	0.18461	1	0.46962
r_{ZAR}	-0.02659	0.05884	-0.07548	0.34366	0.17875	0.21571	0.39389	0.37294	0.09475	0.46962	1

Table C.5: Historical correlations for case study 2 currencies and associated interest rates, part 2.

	Nelson-Siegel-Svensson parameters							Hull-White parameters		BSHW parameters (EUR as domestic CCY)		
CCY	β_1	β_2	β_3	β_4	λ_1	λ_2	max. maturity (years)	λ	σ	Spot rate	σ_{BSHW}	max. maturity (years)
EUR	0.00316	-0.00591	-0.03503	0.03292	3.90499	8.93135	50.03836	0.04138	0.0074	-	-	-
CNH	0.03667	-0.01743	0.01662	-0.04302	0.55915	27.60912	50.03562	0.08	0.00846	0.1342	0.0931	2
IDR	0.04115	0.0253	134.8589	-134.8401	8.36606	8.37221	50.03836	0.08	0.00997	0.00007	0.12923	2
ILS	0.01972	-0.01866	-0.03319	0.02685	3.34736	8.37221	50.03836	0.01	0.00933	0.23686	0.0754	1
INR	0.13835	-0.06467	-0.06918	-0.33849	1.67442	25.10129	50.03836	0.08	0.00997	0.0134	0.10118	2
KRW	0.02495	-0.01141	-0.01287	-0.03157	1.67442	8.37221	50.03836	0.08	0.00668	0.00081	0.12757	2
MXN	-0.00599	0.05018	0.0573	0.19854	1.67442	13.39092	50.03836	0.01	0.01712	0.04776	0.13993	2
MYR	0.01166	0.01961	0.01813	0.03021	0.55915	20.919	50.03836	0.08	0.01059	0.22166	0.13527	10.00548
PHP	0.03959	-0.01501	0.19381	-0.19707	8.36606	11.71646	50.03562	0.01	0.01314	0.01927	0.07745	5.00274
TRY	0.18114	-0.09292	-0.065	-0.46032	1.67442	2593775	50.03836	0.08	0.04274	0.30349	0.11582	2
ZAR	-0.00368	0.08495	0.04358	0.2067	3.90499	12.55447	50.03836	0.01	0.01702	0.06183	0.18922	2

Table C.6: Estimates on Hull-White model parameters and BSHW model parameters for case study 2 currencies.

	AEDEUR	CNHEUR	CNYEUR	HKDEUR	INREUR	PHPEUR	SAREUR	SGDEUR	THBEUR	TWDEUR
AEDEUR	1	0.92885	0.95011	0.999	0.84212	0.88852	0.9997	0.79412	0.85089	0.90585
CNHEUR	0.92885	1	0.97524	0.92977	0.83315	0.85299	0.93047	0.83519	0.82575	0.89851
CNYEUR	0.95011	0.97524	1	0.95318	0.84244	0.87332	0.95108	0.82643	0.83856	0.91175
HKDEUR	0.999	0.92977	0.95318	1	0.84856	0.89334	0.99834	0.80042	0.85475	0.91234
INREUR	0.84212	0.83315	0.84244	0.84856	1	0.87616	0.84159	0.79085	0.8285	0.86174
PHPEUR	0.88852	0.85299	0.87332	0.89334	0.87616	1	0.88711	0.82698	0.87661	0.90009
SAREUR	0.9997	0.93047	0.95108	0.99834	0.84159	0.88711	1	0.79486	0.851	0.9055
SGDEUR	0.79412	0.83519	0.82643	0.80042	0.79085	0.82698	0.79486	1	0.85767	0.8719
THBEUR	0.85089	0.82575	0.83856	0.85475	0.8285	0.87661	0.851	0.85767	1	0.87616
TWDEUR	0.90585	0.89851	0.91175	0.91234	0.86174	0.90009	0.9055	0.8719	0.87616	1
r_{EUR}	-0.18849	-0.1429	-0.17776	-0.18672	-0.16283	-0.17561	-0.1881	-0.16878	-0.17897	-0.1688
r_{AED}	0.23285	0.20619	0.21853	0.23546	0.19517	0.19896	0.22493	0.23007	0.1577	0.2232
r_{CNH}	0.11595	0.05209	0.05643	0.11214	0.00888	0.03244	0.11369	-0.02691	0.0652	-0.00243
r_{CNY}	0.16601	0.16119	0.17478	0.16914	0.16787	0.17976	0.16451	0.1401	0.12921	0.14211
r_{HKD}	0.18482	0.10661	0.12737	0.18064	0.02694	0.03735	0.18223	-0.02054	0.00989	0.06908
r_{INR}	-0.01116	-0.0292	-0.02222	-0.01415	-0.15117	-0.14915	-0.00949	-0.06529	-0.15041	-0.03969
r_{PHP}	0.02112	0.01036	0.01902	0.01659	-0.08672	-0.12014	0.02232	-0.05065	-0.07808	-0.03422
r_{SAR}	0.16037	0.08544	0.09251	0.15599	0.09485	0.12648	0.15583	0.04901	0.12054	0.13175
r_{SGD}	0.18233	0.12051	0.15821	0.18092	-0.00025	-0.00282	0.1822	-0.07729	-0.06172	0.03874
r_{THB}	0.18246	0.14763	0.14427	0.17968	0.04959	0.02694	0.18323	-0.01009	0.00378	0.08758
r_{TWD}	0.16203	0.18732	0.18016	0.15916	0.05832	0.11499	0.16236	0.06219	0.03722	0.15764

Table C.7: Historical correlations for case study 3 currencies and associated interest rates, part 1.

	r_{EUR}	r_{AED}	r_{CNH}	r_{CNY}	r_{HKD}	r_{INR}	r_{PHP}	r_{SAR}	r_{SGD}	r_{THB}	r_{TWD}
AEDEUR	-0.18849	0.23285	0.11595	0.16601	0.18482	-0.01116	0.02112	0.16037	0.18233	0.18246	0.16203
CNHEUR	-0.1429	0.20619	0.05209	0.16119	0.10661	-0.0292	0.01036	0.08544	0.12051	0.14763	0.18732
CNYEUR	-0.17776	0.21853	0.05643	0.17478	0.12737	-0.02222	0.01902	0.09251	0.15821	0.14427	0.18016
HKDEUR	-0.18672	0.23546	0.11214	0.16914	0.18064	-0.01415	0.01659	0.15599	0.18092	0.17968	0.15916
INREUR	-0.16283	0.19517	0.00888	0.16787	0.02694	-0.15117	-0.08672	0.09485	-0.00025	0.04959	0.05832
PHPEUR	-0.17561	0.19896	0.03244	0.17976	0.03735	-0.14915	-0.12014	0.12648	-0.00282	0.02694	0.11499
SAREUR	-0.1881	0.22493	0.11369	0.16451	0.18223	-0.00949	0.02232	0.15583	0.1822	0.18323	0.16236
SGDEUR	-0.16878	0.23007	-0.02691	0.1401	-0.02054	-0.06529	-0.05065	0.04901	-0.07729	-0.01009	0.06219
THBEUR	-0.17897	0.1577	0.0652	0.12921	0.00989	-0.15041	-0.07808	0.12054	-0.06172	0.00378	0.03722
TWDEUR	-0.1688	0.2232	-0.00243	0.14211	0.06908	-0.03969	-0.03422	0.13175	0.03874	0.08758	0.15764
r_{EUR}	1	0.22188	0.02801	0.04649	0.26997	0.08045	-0.02111	0.33684	0.25192	0.13693	0.17674
r_{AED}	0.22188	1	-0.03478	0.07356	0.14489	-0.0144	0.09878	0.2404	0.14582	0.18077	0.07537
r_{CNH}	0.02801	-0.03478	1	-0.02558	0.20036	-0.00598	-0.01149	0.13809	0.10099	0.14981	0.10886
r_{CNY}	0.04649	0.07356	-0.02558	1	0.22442	0.05841	0.03402	0.05488	0.1763	0.2099	0.20784
r_{HKD}	0.26997	0.14489	0.20036	0.22442	1	0.2735	0.28879	0.46373	0.73827	0.50786	0.51716
r_{INR}	0.08045	-0.0144	-0.00598	0.05841	0.2735	1	0.29857	0.00764	0.31644	0.28208	0.25776
r_{PHP}	-0.02111	0.09878	-0.01149	0.03402	0.28879	0.29857	1	0.14361	0.21145	0.21372	0.20191
r_{SAR}	0.33684	0.2404	0.13809	0.05488	0.46373	0.00764	0.14361	1	0.27546	0.25238	0.25891
r_{THB}	0.25192	0.14582	0.10099	0.1763	0.73827	0.31644	0.21145	0.27546	1	0.61801	0.46628
r_{TWD}	0.13693	0.18077	0.14981	0.2099	0.50786	0.28208	0.21372	0.25238	0.61801	1	0.40693
r_{SGD}	0.17674	0.07537	0.10886	0.20784	0.51716	0.25776	0.20191	0.25891	0.46628	0.40693	1

Table C.8: Historical correlations for case study 3 currencies and associated interest rates, part 2.

	Nelson-Siegel-Svensson parameters							Hull-White parameters		BSHW parameters (EUR as domestic CCY)		
CCY	β_1	β_2	β_3	β_4	λ_1	λ_2	max. maturity (years)	λ	σ	Spot rate	σ_{BSHW}	max. maturity (years)
EUR	0.00316	-0.00591	-0.03503	0.03292	3.90499	8.93135	50.03836	0.04138	0.0074	-	-	-
AED	0.02684	-0.01438	0.11474	-0.09509	6.13553	8.37221	50.03836	0.08	0.01503	0.24443	0.10162	5.00274
CNH	0.03667	-0.01743	0.01662	-0.04302	0.55915	27.60912	50.03562	0.08	0.00846	0.1342	0.0931	2
CNY	0.01239	0.2176	-0.55466	0.0943	0.00153	1.25888	10.01096	0.08	0.00846	0.13443	0.0947	2
HKD	0.01866	-0.01131	0.00024	0.00936	1.67442	27.61065	50.03836	0.01	0.00952	0.11574	0.10067	5.00274
INR	0.13835	-0.06467	-0.06918	-0.33849	1.67442	25.10129	50.03836	0.08	0.00997	0.0134	0.10118	2
PHP	0.03959	-0.01501	0.19381	-0.19707	8.36606	11.71646	50.03562	0.01	0.01314	0.01927	0.07745	5.00274
SAR	0.02684	-0.01438	0.11474	-0.09509	6.13553	8.37221	50.03836	0.08	0.01629	0.23939	0.10096	5.00274
SGD	0.0232	-0.01371	-0.00126	-0.01471	1.1168	10.0451	50.03836	0.08	0.01059	0.6584	0.07618	2
THB	0.02428	-0.00467	-0.01813	-0.01697	1.1168	9.20863	50.03836	0.08	0.01059	0.02592	0.09808	10.00548
TWD	0.02777	-0.02519	-0.00931	-0.05658	1.67442	8.37221	50.03836	0.08	0.00366	0.0283	0.09689	2

Table C.9: Estimates on Hull-White model parameters and BSHW model parameters for case study 3 currencies.

Appendix D

Convergence rates for the PCA1 method

$n_t = 4800$	2.00	2.00	2.00	2.00	2.00	2.00	2.00	2.00	2.00
$n_t = 2400$	2.00	2.00	2.00	2.00	2.00	2.00	2.00	2.00	2.00
$n_t = 1200$	2.00	2.00	2.00	2.00	2.00	2.00	2.00	2.00	2.00
$n_t = 600$	2.00	2.00	2.00	2.00	2.00	2.00	2.00	2.00	2.00
$n_t = 300$	2.00	2.00	2.00	2.00	2.00	2.00	2.00	2.00	2.00
$n_t = 150$	2.00	2.00	2.00	2.00	2.00	2.00	2.00	2.00	2.00
$n_t = 75$	2.00	2.00	2.00	2.00	2.00	2.00	2.00	2.00	2.00
	$n_z = 25$	$n_z = 50$	$n_z = 100$	$n_z = 200$	$n_z = 400$	$n_z = 800$	$n_z = 1600$	$n_z = 3200$	$n_z = 6400$

(a) Convergence rates in time direction.

$n_t = 19200$	26.07	1.27	7.76	4.58	1.42	4.82	6.76
$n_t = 9600$	26.07	1.27	7.76	4.58	1.42	4.82	6.76
$n_t = 4800$	26.07	1.27	7.76	4.58	1.42	4.82	6.76
$n_t = 2400$	26.07	1.27	7.76	4.58	1.42	4.82	6.76
$n_t = 1200$	26.07	1.27	7.76	4.58	1.42	4.82	6.76
$n_t = 600$	26.06	1.27	7.76	4.58	1.42	4.82	6.76
$n_t = 300$	26.06	1.27	7.76	4.58	1.42	4.82	6.76
$n_t = 150$	26.05	1.27	7.76	4.58	1.42	4.82	6.76
$n_t = 75$	26.03	1.27	7.76	4.58	1.42	4.82	6.76
	$n_z = 25$	$n_z = 50$	$n_z = 100$	$n_z = 200$	$n_z = 400$	$n_z = 800$	$n_z = 1600$

(b) Convergence rates in space direction.

Table D.1: Convergence rates for the PCA1 method, in time and space direction. Assessed on 5Y USDEUR call option price, with strike equal to the forward FX rate. The analytical solution is calculated using formula (3.15) and equals 0.070948. Convergence rates are calculated by $\left|\frac{\hat{v}_{2n}-\hat{v}_n}{\hat{v}_{4n}-\hat{v}_{2n}}\right|$, with $\hat{v}_n$ the price calculated using the PCA1 method with n grid points in the concerning direction.

Appendix E

Convergence rates for the PCA2 method

$n_t = 76$	4.9	38.17	1.08	1.93	15.88	11.2	81.85
$n_t = 54$	2.73	3.26	6.07	1.81	3.15	3.6	3.3
$n_t = 40$	1.98	2.1	2.4	1.58	2.08	2.16	2.11
$n_t = 28$	2.58	2.67	2.84	2.22	2.66	2.71	2.68
$n_t = 20$	2.03	2.07	2.14	1.83	2.06	2.09	2.13
	$n_{z_1} = 20$	$n_{z_1} = 26$	$n_{z_1} = 34$	$n_{z_1} = 44$	$n_{z_1} = 58$	$n_{z_1} = 74$	$n_{z_1} = 96$

(a) Convergence rates in time direction, $n_{z_2} = 100$.

$n_t = 76$	160.34	14.63	82.95	6.79	3.74	0.41	134.95
$n_t = 54$	3.32	3.54	3.3	3.77	4.12	10.53	3.31
$n_t = 40$	2.11	2.15	2.11	2.19	2.24	2.55	2.11
$n_t = 28$	2.68	2.7	2.68	2.73	2.76	2.91	2.68
$n_t = 20$	2.17	2.18	2.17	2.19	2.2	2.27	2.17
	$n_{z_2} = 20$	$n_{z_2} = 26$	$n_{z_2} = 34$	$n_{z_2} = 44$	$n_{z_2} = 58$	$n_{z_2} = 74$	$n_{z_2} = 96$

(b) Convergence rates in time direction, $n_{z_1} = 100$.

Table E.1: Convergence rates for the PCA2 method, in time direction. Assessed on a 5Y GBP USD basket call option price, with strike equal to the forward basket rate. The basket weights are equal to $\frac{1}{2}$ and, furthermore, the FX rates have been normalized with respect to their spot rate. Convergence rates are calculated by $\left|\frac{\hat{v}_{2n}-\hat{v}_n}{\hat{v}_{4n}-\hat{v}_{2n}}\right|$, with $\hat{v}_n$ the price calculated using the PCA2 method with n grid points in the time direction.

$n_t = 150$	4.38	0.09	1.87	0.66	13.18
$n_t = 108$	4.38	0.09	1.87	0.66	13.17
$n_t = 76$	4.38	0.09	1.87	0.66	13.17
$n_t = 54$	4.37	0.09	1.87	0.66	13.16
$n_t = 40$	4.37	0.1	1.87	0.66	13.16
$n_t = 28$	4.36	0.1	1.87	0.66	13.15
$n_t = 20$	4.35	0.1	1.87	0.66	13.11
	$n_{z_1} = 20$	$n_{z_1} = 26$	$n_{z_1} = 34$	$n_{z_1} = 44$	$n_{z_1} = 58$

(a) Convergence rates in z_1 direction, $n_{z_2} = 100$.

$n_{z_1} = 58$	1.65	0.06	3.77	0.08	0.53	0.23	13.68
$n_{z_1} = 44$	0	4.02	0.06	11.84	0.12	31.5	1.79
$n_{z_1} = 34$	67.94	0.58	12.03	0.36	61.68	1.61	1.1
$n_{z_1} = 26$	1.26	0.71	3.99	11.66	1.41	0.96	0.16
$n_{z_1} = 20$	1.64	9.53	4.94	1.96	0.64	0.09	2.23
	$n_{z_2} = 20$	$n_{z_2} = 26$	$n_{z_2} = 34$	$n_{z_2} = 44$	$n_{z_2} = 58$	$n_{z_2} = 74$	$n_{z_2} = 96$

(b) Convergence rates in z_1 direction, $n_t = 100$.

Table E.2: Convergence rates for the PCA2 method, in z_1 direction. Assessed on a 5Y GBP USD basket call option price, with strike equal to the forward basket rate. The basket weights are equal to $\frac{1}{2}$ and, furthermore, the FX rates have been normalized with respect to their spot rate. Convergence rates are calculated by $\left|\frac{\hat{v}_{2n}-\hat{v}_n}{\hat{v}_{4n}-\hat{v}_{2n}}\right|$, with $\hat{v}_n$ the price calculated using the PCA2 method with n grid points in the z_1 direction.

$n_t = 150$	2.14	0.27	1.28	0.11	0.83
$n_t = 108$	2.14	0.27	1.28	0.11	0.83
$n_t = 76$	2.13	0.27	1.28	0.11	0.83
$n_t = 54$	2.13	0.27	1.28	0.11	0.83
$n_t = 40$	2.13	0.27	1.28	0.11	0.83
$n_t = 28$	2.12	0.27	1.28	0.11	0.83
$n_t = 20$	2.12	0.27	1.29	0.11	0.83
	$n_{z_2} = 20$	$n_{z_2} = 26$	$n_{z_2} = 34$	$n_{z_2} = 44$	$n_{z_2} = 58$

(a) Convergence rates in z_2 direction, $n_{z_1} = 100$.

$n_{z_1} = 96$	0.55	156.64	0.01	1.72	1.46
$n_{z_1} = 74$	263.92	0.01	1.84	1.34	4.22
$n_{z_1} = 58$	0.15	1.12	0.49	15.44	0.02
$n_{z_1} = 44$	9.13	0.14	4.89	0.03	0.69
$n_{z_1} = 34$	0.32	8.92	0.02	0.75	0.79
$n_{z_1} = 26$	5.27	0.04	0.61	0.87	3.02
$n_{z_1} = 20$	0.03	0.5	0.91	3.66	4.88
	$n_{z_2} = 20$	$n_{z_2} = 26$	$n_{z_2} = 34$	$n_{z_2} = 44$	$n_{z_2} = 58$

(b) Convergence rates in z_2 direction, $n_t = 100$.

Table E.3: Convergence rates for the PCA2 method, in z_2 direction. Assessed on a 5Y GBP USD basket call option price, with strike equal to the forward basket rate. The basket weights are equal to $\frac{1}{2}$ and, furthermore, the FX rates have been normalized with respect to their spot rate. Convergence rates are calculated by $\left|\frac{\hat{v}_{2n}-\hat{v}_n}{\hat{v}_{4n}-\hat{v}_{2n}}\right|$, with $\hat{v}_n$ the price calculated using the PCA2 method with n grid points in the z_2 direction.